University of São Paulo
"Luiz de Queiroz" College of Agriculture

Creating optimized machine working patterns on agricultural fields

Mark Spekken

Thesis presented to obtain the degree of Doctor in Science. Area: Agricultural Systems Engineering

Piracicaba
2015

Mark Spekken
Agronomist

Creating optimized machine working patterns on agricultural fields

Versão revisada de acordo com a resolução CoPGr 6018 de 2011

Advisor:
Prof. Dr. **JOSÉ PAULO MOLIN**

Thesis presented to obtain the degree of Doctor in Science. Area: Agricultural Systems Engineering

Piracicaba
2015

Dados Internacionais de Catalogação na Publicação
DIVISÃO DE BIBLIOTECA - DIBD/ESALQ/USP

Spekken, Mark
Creating optimized machine working patterns on agricultural fields / Mark Spekken. - - versão revisada de acordo com a resolução CoPGr 6018 de 2011. - - Piracicaba, 2015.
122 p. : il.

Tese (Doutorado) - - Escola Superior de Agricultura “Luiz de Queiroz”.

1. Planejamento de percursos 2. Improdutividade de operações 3. Erosão hídrica de solo 4. Simulação virtual de trajetos 5. Balanço econômico de áreas agrícolas 6. Agricultura de precisão I. Título

CDD 631.3
S742c

I DEDICATE

Prologue of the Gospel of John

"In the beginning was the Logos, and the Logos was with God, and the Logos was God. He was with God in the beginning. Through him all things were made; without him nothing was made that has been made. In him was life, and that life was the light of all mankind. The light shines in the darkness, and the darkness has not understood it."

For a reader familiar with this quoting, the term "Logos" (from the original author's text in Greek) was inappropriately translated to the word "Verb". "Logos" has several translations within the scope of logic, reason, intelligence, calculation, knowledge. For the grounds in which I believe, the current trend to dissociate God from science, or even to antagonize them, is wrong.

Ironically, many of us run after mystical experiences, ancient healing practices, bargains with the divine, magical rituals or substances, mysterious prophecies, positive thinking on energies… many hopes that overrule science (if not the very common sense)… sometimes even claiming it will bring them closer to God.

The very author of the quoting above points to God as the truth, and even an intelligent person like Steve Jobs believed he could ignore the truth of his cancer by using alternative means.

Science reveals God; from the organization of atomic particles to the complex structures of a single cell and its fantastic DNA governance, not to mention the interaction of these cells into tissues, organs, systems, and the full body. The perfection of our environmental organization was made possible by a unique setting of our planet in the solar system. Some scientists argue that "God may be improbable, but the existence of life is even more."

Much of my work during this PhD was on computer programming, trying to make an algorithm to reproduce a limited part of a person's intelligence… making a tool to serve others. In some analogy, we are God's algorithm… scientists, doctors, engineers, professors, farmers, mechanics, technicians… continuously serving one another using Logos.

We cannot deny Logos… we are all subject to it... even when we don't understand.

To Him who always showed me that He was right… and I, wrong

ACKNOWLEDGEMENTS

- For the physical means to develop this work.

To the University of São Paulo and the Agricultural College “Luiz de Queiroz”, for accepting me in the post-graduate program and providing me all the infrastructure needed.
To CAPES and FAPESP to provide me the financial funds needed during this time.
To the free-Pascal initiative group, for the free programming platform Lazarus; ACPA (Australian Centre for Precision Agriculture), for the free application Vesper 2.0; and Quantum GIS - free GIS foundation group.
To São Martinho group, that provided me data to be used in case studies.

- For the academic orientation needed on the course of this work.

To professor José Paulo Molin, my good advisor and supervisor for over a decade.
To professor Sytze de Bruin, for his great insight in modelling and scientific writing in the algorithm and manuscripts written.
To two good friends and academic colleagues (from Piracicaba and Gothenburg), who were of essential help in two of the manuscripts in this thesis.

- For the support, friendship and love

To Guljamal Jumamuratova, my wife and (great) editor of this work, for all the help and meaning she gives to my daily life.
To all of my friends and colleagues from LAP: André Freitas Colaço, Lucas Cortinove, Matheus Tonini Eitelwein, Lucas Rios do Amaral, Adriano Anselmi, Fernanda Cristina de Souza e Gustavo Portz. Among you guys there were many talks and laughs, besides your help in many tasks.
To my parents Simon and Carolina Spekken, for helping to guide my way until here.

There are still many not mentioned here, from Brazil and abroad, that had closer or distant help in this work and in my academic life.

My thankfulness and best wishes to all of you

CONTENTS

RESUMO

Criando padrões de trabalho otimizado para máquinas em talhões agrícolas

No contexto agrícola atual, improdutividade de máquinas agrícolas em campo e seus impactos sobre o solo ao longo de suas vias são inevitáveis. Estas máquinas têm custos diretos e indiretos associados ao seu trabalho no campo, como tempo improdutivo gasto em manobras quando estes atingem os limites do talhão. Também nestes limites, há uma dupla aplicação de insumos agrícolas quando as máquinas estão cobrindo cabeceiras. Ambas as questões se agravam em talhões de geometria irregular. Além disso, o tempo improdutivo também pode aparecer em operações de carga / descarga do reservatório da máquina com insumos / bens colhidos, o que pode aumentar com um uso indevido do reservatório da máquina devido ao comprimento inadequado do percurso em campo. Ainda, superfícies irregulares e íngremes apresentam um problema para o estabelecimento de culturas em fileira e caminhos de máquinas contra declive. Apesar de operações em nível serem uma prática comum para reduzir o escoamento e aumentar a infiltração de água, curvas de nível nunca são paralelas, enquanto operações agrícolas são sempre paralelas. Muitas destas questões foram alvo de otimização computacional para planejamento de percursos de para máquinas agrícolas, onde a ineficiência foi, em geral, minimizada e tentativas de redução da perda de solo estabelecimento de percursos mais adequados também produziu resultados. Esta tese reuniu estas questões em uma abordagem de planejamento de percurso quantificando e direcionando custos de perda de solo e improdutividade de máquinas para sua devida localização. Métodos foram propostos e modificados, como: criar e replicar trajetos transitáveis de máquinas; encontrar referências ideais para a cobertura do trajeto em superfícies irregulares (curvas ou retas); quantificação dos impactos da perda de solo por um determinado padrão de percursos; identificar espacialmente o fluxo da água e sua concentração; definir geometricamente diferentes tipos de manobras e calcular o seu tempo, espaço e energia demandada; obter a área sobreposta de aplicação de insumos; e quantificar custo de reposição da máquina em relação à subutilização de seu reservatório para seguir trajetos de comprimento inadequado. Um aplicativo-algoritmo foi obtido capaz de simular um grande número de cenários de padrões de percurso, e exibindo aqueles que foram otimizados por critérios definidos pelo usuário. A cultura da cana, em condições brasileiras, foi a principal cultura de estudo nesta tese devido ao seu alto custo de mecanização (assim como custos operacionais improdutivos), alta suscetibilidade à erosão do solo na sua fase de plantio, e ocupando predominantemente áreas de superfície irregular. Os estudos de caso foram sujeitos ao algoritmo que obteve resultados coerentes e impactos minimizados. Os resultados do algoritmo mostram potencial para que os métodos avaliados sejam utilizados por tomadores de decisão da área agrícola.

Palavras-chave: Planejamento de percursos; Improdutividade de operações; Erosão hídrica de solo; Simulação virtual de trajetos; Balanço econômico de áreas agrícolas; Agricultura de precisão

ABSTRACT

Creating optimized machine working patterns on agricultural fields

In the current agricultural context, agricultural machine unproductivity on fields and their impacts on soil along pathways are unavoidable. These machines have direct and indirect costs associated to their work in field, with non-productive time spent in manoeuvres when these are reaching field borders; likewise, there is a double application of product when machines are covering headlands while adding farm inputs. Both issues aggravate under irregular field geometry. Moreover, unproductive time can also appear in operations of loading/offloading the machine's reservoir with inputs/harvested-goods, which can increase with an improper use of the reservoir due to the inadequate machine path length. On the other hand, irregular steep surfaces present a problem for establishment of row crops and machine paths towards erosion. Though contouring (i.e., performing field operations perpendicular to slope direction) is a common practice to reduce runoff and increase water infiltration, still elevation contours are never parallel, while machine operations always are. Many of these issues were target for optimization in computer path planning for agricultural machines, where unproductivity was overall minimized and attempts of soil loss reduction by more proper path establishment also yielded results. This thesis gathered these issues in a combined path planning approach making possible to address soil loss and unproductive costs to their proper location. A number of methods was proposed and modified: creating and replicating steerable machine track; finding more optimal references for path coverage on irregular surfaces (curved or straight); quantifying the impacts of soil loss for a given path pattern; identifying spatially the water flow and concentration; defining geometrically different manoeuvre types and calculate its time, space and energy demands; obtain the overlapped area of input application; and quantifying the machine replenishment cost in relation to underuse of its reservoir for following tracks of inadequate length. An algorithm-application was achieved, which is capable of simulating a large number of path coverage scenarios and to display optimized ones based on a user defined criteria. Sugarcane crop, grown in Brazilian conditions, was the main object of study in this thesis because of its high in-field mechanization costs (along with unproductive operational costs), high susceptibility of soil erosion in its planting phase, and for occupying an area of predominant rolling surface. Case studies were subject to this algorithm that provided suitable outputs with minimized impacts. The outputs of the algorithm were comprehensive and showed potential for the methods to be used by agricultural decision makers.

Keywords: Path-planning; Unproductivity of agricultural operations; Soil erosion by water; Virtual simulation of tracks; Economic balance of agricultural plots; Precision agriculture

1 INTRODUCTION

For centuries, the animal and machine work on agricultural fields followed (and still keeps following) a similar pattern of coverage. This pattern is known as boustrophedon paths, i.e. parallel passes with alternate directions (JIN; TANG, 2010), which is the most efficient method for full field coverage within actual in-field machine traffic limits.

As this practice remains unchanged, it faces two main practical issues: irregular geometry of fields and irregular field surfaces. Although these issues may exist simultaneously, they have distinct consequences in farm operations.

Irregular shaped fields have been studied for some decades for inefficiency concerns towards production scale (WITNEY, 1988). Indices were attributed to machine efficiency for distinct field shapes with and without the presence of obstacles (STURROCK et al., 1977). However, the results and suggestions were limited and applicable to only a few field geometry cases. The more recent availability of computational processing made possible more accurate studies for quantifying field geometry (OKSANEN; VISALA, 2007); as well as simulating virtual trajectories of machines on field representations, originating the scope of agricultural path planning.

This path-planning development was strongly pushed by the adoption of GNSS (Global Navigation Satellite System) within machine guidance, which is increasing in adoption by farmers (HOLLAND et al., 2013). The technology available allows complete routes to be inserted in the interface of the equipment, freeing the operator and also enabling robots to work in fields.

Computer path-planning algorithms were developed to overcome issues of reducing machine unproductive time (JIN; TANG, 2006; OKSANEN; VISALA, 2009; BOCHTIS et al., 2010; SPEKKEN; DE BRUIN, 2013); minimizing overlap coverage of applied inputs (PALMER et al., 2003; DE BRUIN et al., 2009); aiding in the movement of auxiliary units in harvesting procedures (BOCHTIS et al., 2010).

In Brazilian sugarcane production system, efforts are being carried to reduce the prohibitive mechanization costs, especially because of the mechanized harvesting. These efforts are being undertaken by redesigning the machine paths in longer tracks to minimize manoeuvring time and to improve field logistics. Commercial tools were developed in Computer Aided Design (CAD) environment to speed the drawing of pre-planned tracks by human intuition. This procedure is colloquially known as “sistematização”.

Still, despite the claim of high mechanization costs by the sugarcane growers, and the energy being spent in redrawing the paths, the exact costs of the manoeuvres are unknown.
Also, most of the growing areas that are subject to this redesign (of paths and crop rows) are located in irregular steep surfaces, and decision makers speculate about the removal of the counter-erosion-terraces to lengthen the machine paths. This happens because terraces follow non-uniform contours and are not crossable by machines resulting in many inefficient sub-fields with short machine paths. By removing terraces, decision makers must allocate the crop rows in patterns that decrease water runoff to a minimum. Methods to find this pattern and quantify its soil-conservation capability are not available yet.
Seldom path planning works were developed for minimizing the soil loss by water erosion (JIN; TANG, 2011), which are limited in path design and unable to give a comprehensive view of the soil loss impact distribution, i.e. providing distinct soil erosion intensities over the field. This same remark is true for the other works carried so far in path-planning, because despite they succeeded in reducing overall costs, these costs are still an average for the whole field. Common sense shows that short field-tracks have equivalent manoeuvring costs as long ones, so the distribution of the manoeuvre cost along its respective track is not constant. This implies that operational costs vary over the field. Nonetheless, no studies addressed this distribution.
This thesis presents three chapters given as complete manuscripts that respond for the issues presented above:
- a comprehensive study on manoeuvring costs, using sugarcane as a study subject (Chapter 2).
- an agricultural path planning model to quantify and minimize soil loss in regard to the pattern of establishment of machine paths and crop rows on field (Chapter 3).
- a method to merge operational and soil conservation costs in regard to path definition, and identifying the intensity of these costs spatially on the field (Chapter 4).

Hypothesis

The development of a computational model for machine coverage simulation on fields can, by recovering the impacts of each simulation, select routes that minimize financial and environmental costs as well as allowing distinct operational costs to be retrieved on different parts of the field.

References

BOCHTIS, D.D.; SØRENSEN, C.G.; VOUGIOUKAS, S.G. Path planning for in-field navigation-aiding of service units. **Computers and Electronics in Agriculture,** Amsterdam, v. 74, n. 1, p. 80-90, 2010.

BOCHTIS, D.D.; SØRENSEN, C.G.; BUSATO, P.; HAMEED, I.A.; RODIAS, E., GREEN, O.; PAPADAKIS, G. Tramline establishment in controlled traffic farming based on operational machinery cost. **Biosystems Engineering,** London, v. 107, n. 3, p. 221-231, 2010.

DE BRUIN, S.; LERINK, P.; KLOMPE, A.; VAN DER WAL, T.; HEIJTING, S. Spatial optimization of cropped swaths and field margins using GIS. **Computers and Electronics in Agriculture,** Amsterdam, v. 68, n. 2, p. 185-190, 2009.

HOLLAND, J.K.; ERICKSON, B.; WIDMAR, D.A. Precision agricultural services dealership survey results. West Lafayette: Purdue University, Dept. of Agricultural Economics, 2013. 68 p.

JIN, J.; TANG, L. Optimal path planning for arable farming. In: ASABE ANNUAL INTERNATIONAL MEETING, 2006, Portland. **Proceedings…** St. Joseph: American Society of Agricultural Engineers, 2006. p. 304-312.

_____. Optimal coverage path planning for arable farming on 2D surfaces. **Transactions of the ASABE,** St. Joseph, v. 53, n. 1, p. 283, 2010.

_____. Coverage path planning on three-dimensional terrain for arable farming**. Journal of Field Robotics,** Hoboken, v. 28, n. 3, p. 424-440, 2011.

OKSANEN, T.; VISALA, A. **Path planning algorithms for agricultural machines.** 2007. 112 p. Thesis (PhD) - Automation Technology Laboratory, Helsinki University of Technology, Espoo, 2007. (Series A. Research Reports, 31).

_____. Coverage path planning algorithms for agricultural field machines. **Journal of Field Robotics,** Hoboken, v. 26, n. 8, p. 651-668, 2009.

PALMER, R.J.; WILD, D.; RUNTZ, K. Improving the efficiency of field operations. **Biosystems Egineering,** London, v. 84, n. 3, p. 283-288, 2003.

SPEKKEN, M.; DE BRUIN, S. Optimized routing on agricultural fields by minimizing maneuvering and servicing time. **Precision Agriculture,** Dordrecht, v. 14, n. 2, p. 224-244, 2013.

STURROCK, F.G.; CATHIE, J.; PAYNE, T.A. **Economies of scale in farm mechanization.** Cambridge: Cambridge University, Department of Land Economy, 1977. 15 p. (Ocas. Papers,. 22, Economics Unit).

WITNEY, B. **Choosing and using farm machines.** Burnt Mill: Longman Scientific & Technical, Longman Group UK, 412 p. 1988. 412 p.

2 COST OF BOUNDARY MANOEUVRES IN SUGARCANE PRODUCTION

Abstract

Machinery has direct and indirect costs associated to their work in field, and there is a non-productive time spent in manoeuvres when these are reaching field borders. Many works have been carried out in order to reduce the number of manoeuvres in complex field shapes and changing the type of manoeuvres in order to speed them. Biofuel producing crops like sugarcane (*Saccharum spp.*) demand, besides economic profitability, positive energy output in their production chain. The crop has narrow width of equipment and demand time-costly manoeuvres which may add significant input mainly on short rows. Using a method and calculations applicable for other crops, this study takes operational, spatial, economic, and energy factors into account to observe the impact of manoeuvring in the edge of a sugarcane crop row. Energy and economic costs were retrieved from hourly use of machines for four main field operations and their respective manoeuvring costs. Likewise crop parameters were retrieved with its data crossed towards the operational costs to see the dimensions of row-length benefits. The increase in row length and width has decreasing turning benefits that may collide with the logistics of the auxiliary units. The impacts of turning patterns were obtained, it suggests changes to minimize time and space for manoeuvring in planting and cultivating operations, and using wider roads and more steerable carriers in harvesting operations. In standard scenarios of production system it was found that row lengths up to 50 meters are unable to pay for the economic turning costs in its edge.

Keywords: *Saccharum spp.*; Energy; Path planning; Mechanization; Agricultural machinery

Nomenclature:

ARL	Average row length being cover by the operation (m)
CRME	Cost of manoeuvring in a row-edge (MJ or US$)
DBA	Distance between implement and front tractor axles (m)
DBT	Distance between turns within a U-turn (m)
D-MDS	Distance followed by the tractor parallel to the road to the manoeuvre dedicated space (m)
EFB_{area}	Energy or financial balance per area (MJ ha^{-1} or US$ ha^{-1})
$EFB_{metre\text{-}row}$	Energy or financial balance per metre-row (MJ m^{-1} or US$ m^{-1})
Eh	Hourly energy input (MJ h^{-1})
EMCRL	Equivalent manoeuvre cost in row length (m)
Emw	Energy given per unit weight (N kg^{-1})
F	Yearly frequency of occurrence of the operation
fv,rv	Forward and rearward velocities (m s^{-1})
h	Length of the overlapping zone (m)
ICMA	Input cost of manoeuvring per area (MJ ha^{-1} or US$ ha^{-1})

LT Hourly lifetime of the implement (h)

M Mass of implement (kg)

MDS Manoeuvre dedicated space, a wider width of the roads required for the P-turns.

NRC_{Oper} Number of rows covered by the operation

Oper Identifier of the field operation

Pm Average power output of the tractor during its lifetime (kW)

Pn Nominal power of the tractor (kW)

P-turn Manoeuvre type executed by an agricultural machine operating in a headland pattern. The machine moves into a region which allows a full loop turn.

q Angle between machine direction and a perpendicular field border (in radians)

qme Manufacturing and repair and maintenance energy per unit fuel consumption (MJ g^{-1})

qs Specific mean consumption (g kW^{-1} h^{-1})

r Turning radius (m)

RRM Ratio of repair and maintenance energy to manufacturing energy

RTM_{Oper} Relative time spent in maneuvering (%)

TCMRE Sum of manoeuvring operations costs in a headland (MJ or US$)

TC_{Oper} Time cost of a manoeuvre (MJ h-1 or US$ h-1)

Ti Hourly lifetime of the tractor (h)

TM_{Oper} Time spent in a manoeuvre for the operation (s)

T-turn Manoeuvre type executed by an agricultural machine operating in a headland pattern. Also known as reverse turn, the machine turns to one side and then reverses to be able to reach an adjacent machine track.

U-turn Manoeuvre type executed by an agricultural machine operating in a headland pattern. The steering does not exceed 180 ° for turning to reach a next machine track.

w Width of the operation (m)

WMS, UMS, TMS and *PMS* Respectively the W-turn, U-turn, T-turn and P-turn manoeuvring spaces required (equivalent to the road or headland width, in m)

WMT, UMT, TMT and *PMT* Respectively W-turn, U-turn, T-turn and P-turn manoeuvring time cost (s)

WPR Weight per Power Ratio (N kW^{-1})

WS Working speed of the operation (m s^{-1})

Ω-*turn* Manoeuvre type executed by an agricultural machine operating in a headland pattern. The steering exceeds 180 ° for turning in the shape of a lamp-bulb to reach a following machine track.

2.1 Introduction

There are environmental and economic costs associated with the work of machinery on agricultural fields. Soil compaction, overlap of worked area and also the acquisition and operation of the respective machinery are among the factors with negative impacts in the sustainability of the agricultural production.

Generally, agricultural machines do not spend its time on field fully doing the operation they were acquired to perform. Loading or offloading agricultural inputs and turning are the main non-working factors computed in the overall efficiency (WITNEY, 1988). Reducing these non-productive time reduces the production costs.

An increasing proportion of sugarcane production is shifting to fully mechanized operations. However, because of the high biomass harvested and the narrow width of machines, these are highly demanded per area leading mechanization to the first place in the list for cost production (40% of the cost according to MILAN, 2004).

In Brazil, ethanol for automotive fuel is derived from sugarcane and is used pure or blended with gasoline (from 18 to 25% of ethanol). This ethanol is basically produced in sugarcane mills and distilleries, and the crop covers close to 9 million hectares in the country (COMPANHIA NACIONAL DE ABASTECIMENTO - CONAB, 2013).

The energy balance of the sugarcane crop has been studied. As a bioenergy supplier it is expected that the energy produced by the crop to safely excel its inputs. Macedo (1998) found ratios of the output/input of sugarcane energy of 9.2 considering an input of 15.2 GJ ha^{-1}, while Oliveira et al. (2005) obtained a ratio of 3.7 and an input of 36 GJ ha^{-1}. These studies were carried out having a holistic approach focusing on the hectare as the research unit. Macedo et al. (2008) calculated the embodied energy (per Mg) of sugarcane, from field production to the stage of energy products (ethanol and electricity). This latter approach gives a more accurate estimate, once the logistic costs of the production and processing are more specifically related to product quantity than area.

Coelho (2009) pointed that mechanized harvest operation in sugarcane can amount from 30 to 35% of the production costs. The author studied efficiency issues from a system case

study and found that a sugarcane harvester spends only an average of 8.5 hours of effective work in continuous 24 hours (three shifts of 8 hours labor).

Sugarcane is a row-crop in which undesired machine traffic (across or upon rows) leads to damage on its ratoon from which the crop has to re-establish and grow again. A number of 5 to 6 crop re-establishments from the same ratoon is normally expected until a new implantation of the crop takes place, making the crop very responsive to controlled traffic farming (PAULA; MOLIN, 2012). Because of this control, the number of machine tracks is a multiple of the number of rows and headlands for machine turns are absent in order to avoid machine overrun.

Because of the high output of canes harvested per area, an intense logistic transport system is required on a net of primary and secondary roads, with widths of 8 and 5m respectively, occupying a significant fraction of the area (2.5 to 4% of the total field area, BENEDINI; CONDE, 2008). These roads are also used for turning the field machinery and the limits in their width will impact the manoeuvring time. Studies to find the optimal width for these roads considering such aspects are still lacking.

In order to reduce the considerable impact of sugarcane mechanization costs, recent increasing efforts have been spent in redesigning field features by relocating roads and erosion-control-terraces in order to establish planned crop rows (GUIMARÃES, 2004).

Simulating machine paths to cover a field in advance, also known as path planning, has already been studied by authors to minimize the number of turns (OKSAMEN; VISALA, 2009; JIN; TANG, 2006; TAIX, 2006) and to reduce the time for each turn (BOCHTIS; VOUGIOUKAS, 2008; SPEKKEN; DE BRUIN, 2013).

Although such approaches are capable of increasing field efficiency, machine working pattern is always parallel which contrasts with many fields that are not limited by parallel borders or obstacles. This results in short rows on field corners, for which the turning-costs may surpass its benefit (in economic or in energy parameters).

Despite methods for detecting such tracks in the path planning scope have already been proposed (SPEKKEN; MOLIN, 2012b), the economic and energy criteria that define the costs of a turning edge of a row have not yet been studied, including the related row-length cost/benefit.

Considering energy and economic criteria, the following research questions are posed:

- What is the cost of manoeuvres in sugarcane in time and inputs?
- What are the benefits for changing turning patterns on the edge of rows?
- What is the break-even length of a row with respect to manoeuvre cost?
- A method to find an optimized relation between turning time and width of the roads.

2.2 Methodology

The methods for obtaining and analyzing the data is described in four main sub-chapters: overview of sugarcane machine operations; modelling the manoeuvres; the time and spatial cost of manoeuvring and its balance; and scenarios for calculating the impact of the manoeuvre-types.

2.2.1 Overview of manoeuvring types and sugarcane machine operations

In general, in agricultural field operations, there are three main types of machine manoeuvres (Figure 2.1): Ω-turns, U-turns and T-turns (BOCHTIS; VOUGIOUKAS, 2008). The angle between the working direction and the field border also influences the manoeuvre behavior and the space required for it (JIN; TANG, 2010; SPEKKEN; DE BRUIN, 2013).

Ω-turns are the faster types of manoeuvres to turn back into an adjacent row, but it demands more manoeuvring space (CARIOU et al., 2010), which would demand wider roads for manoeuvres that would have to be taken from productive areas. U-turns are fast and require less space for manoeuvring; they are feasible when the implementing width is larger than diameter for turning or when rows are skipped (BOCHTIS; VOUGIOUKAS, 2008) as shown in Figure 2.1.

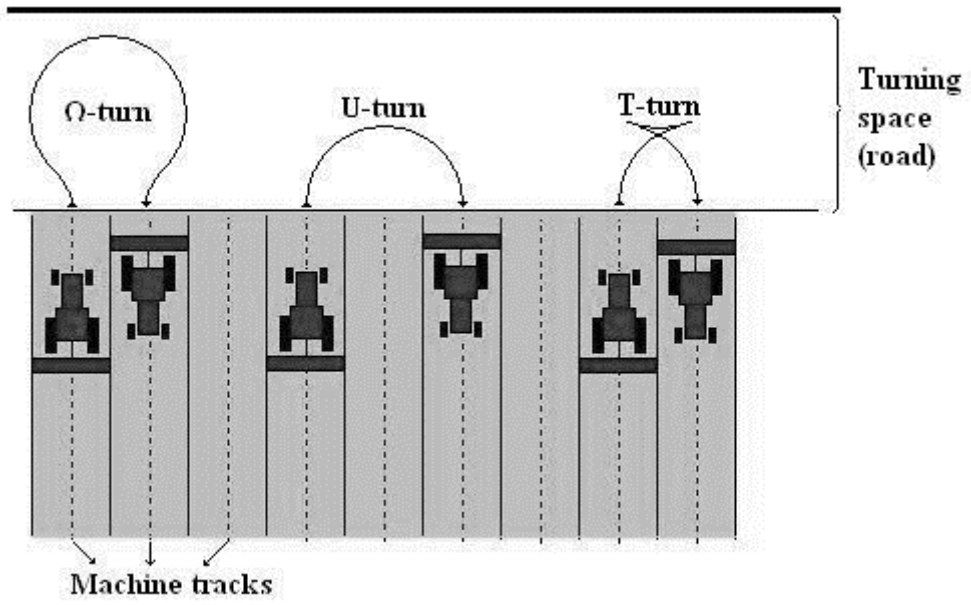

Figure 2.1 - Manoeuvring types common in field operations (SPEKKEN; DE BRUIN, 2013)

T-turns more commonly seen in sugarcane operations due to its low demand for manoeuvring space to reach and adjacent track within narrow roads. Shifting from T-turns into skipping rows is possible with the use of guidance systems, which assure parallelism in a correct skipping distance from a previous row.

In this work, four main field operations are considered for determining sugarcane manoeuvring costs: planting, cultivating, spraying, and harvesting. These can be seen respectively in Figure 2.2a, b, c and d.

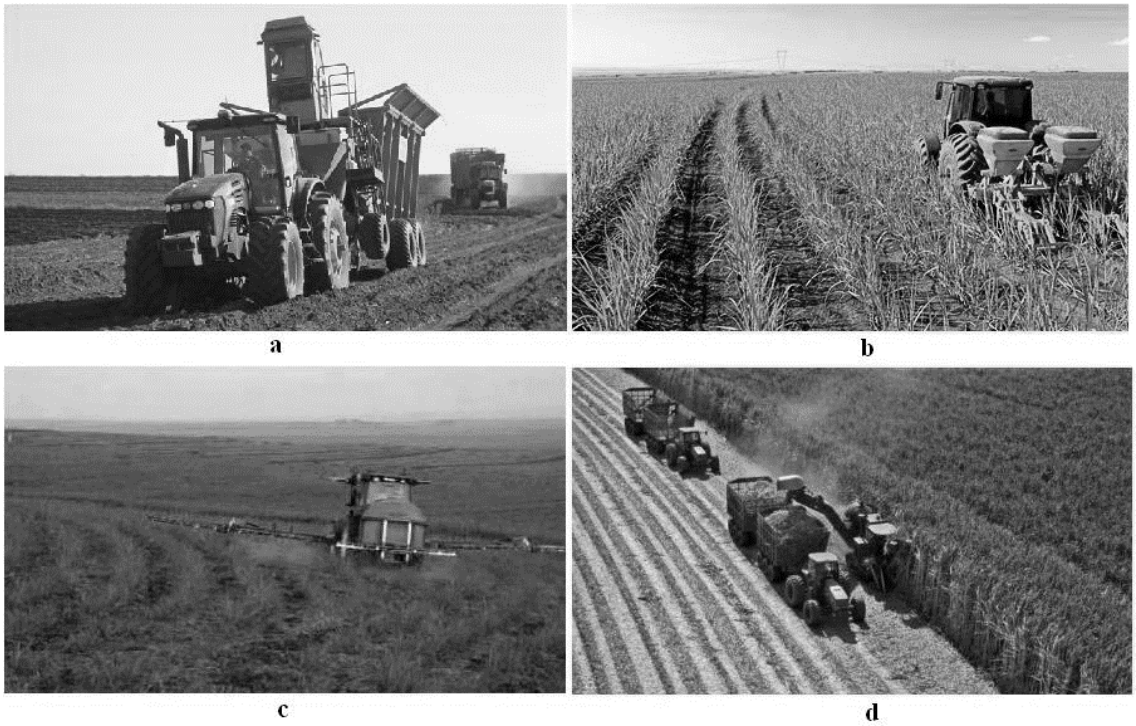

Figure 2.2 - View of four mechanical operations in sugarcane production: planting (a); cultivating (b); spraying (c); and harvesting (d)

Figure 2.2a shows a mechanized planting operation, which occurs usually every five years. It shows a standard sugarcane planter pulled by the tractor summing a 14 m long set which length limits considerably its turning capacity. In Figure 2.2b, a cultivator is attached to a tractor performing three simultaneous operations: cultivating, applying fertilizer and chisel-ploughing the soil; for which manoeuvres are only limited by the tractor steering capacity. Both planting and cultivating operations are limited to perform in only two crop rows for which the work width is smaller than the diameter of turning. Spraying operation (Figure 2.2c) is comparable to regular crops; its width easily surpasses its turning capacity. Figure 2.2d shows sugarcane harvesting, in which two wagon-carriers pulled in line by a tractor that receives the

billets while moving side-by-side to the harvester (similar to forage harvesting). The harvester generally covers a single row; nevertheless, recent machinery developments are increasing the harvesting width up to 2 rows.

Because of the large turning radius of the carrier, the non-existence of crop-covered headlands and the limited width of roads, the wagons are the main time-consumers in manoeuvres. Baio (2011) remarked that the sugarcane harvester is capable of performing U-turns at the ends of the rows faster than the cane wagon and that the latter affected the total operational field efficiency of the mechanized system.

Spraying operations regularly use of U-turns and its manoeuvre time is herein set in 20 s with its manoeuvring space fitting to the minimum existing road width.

Skipping rows are unsuitable in harvest since the machines cannot skip a row without overrunning and damaging a crop-row on the side. In many cases, a more elaborate manoeuvre is found, which leads the machine to travel a certain distance in order to reach a manoeuvre-dedicated-space (*MDS*) to turn and return parallel to the harvester. This manoeuvre is herein designated as P-turn, due to the "P" shape of the turn (Figure 2.3).

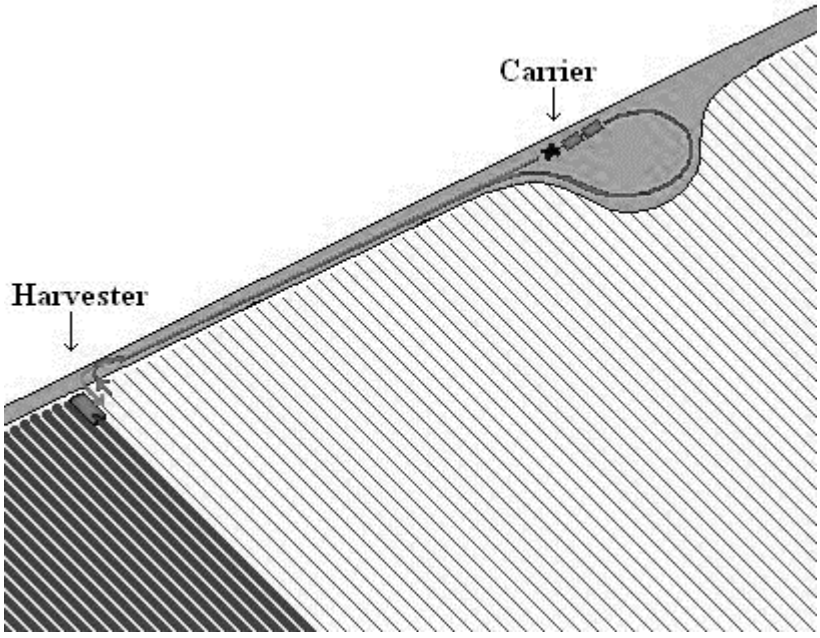

Figure 2.3 - Long manoeuvre of a double-wagon carrier for avoiding the overrun of the crop area

The tractor-double-wagon set (shown in Figures 2.2d and 2.3) has a 10.8-m turning radius. A single-wagon set with equal storage capacity (larger basket) has a turning radius of 7 m. Self-propelled carriers (trucks with baskets) have a turning radius of 5 m.

2.2.2 Modelling the manoeuvres

For sugarcane fields, both the space required for turning and the time spend in a turn determines the cost of manoeuvring. Regarding loop turns (Ω-turn and U-turn), a modified approach after Jin and Tang (2010) is herein used to obtain space (headland or road) and time demanded for manoeuvring.

Both T-turns and P-turns are time demanding, and the time spent in these is dependent on: operator skill, distance to the *MDS* (if it is the case) and the type of wagon-carrier (double-wagon carriers hardly use T-turns). Coelho (2009) suggests the time spent in harvesting manoeuvres for sugarcane to be of 50 s for a specific case study area, while Benedini and Conde (2008) consider the same manoeuvres to be of 1.5 to 2.0 minutes (for harvesting).

Herein, the modelling of a T-turn follows a modified U-turn which includes a rearwards motion, and one new approach is proposed to estimate the time spend in a P-turn. The three main variables that are required in the geometry of all the manoeuvres are: the width of the operation (w), the turning radius (r) and the angle in which the machine heads towards a perpendicular field border (θ). Figure 2.4 shows the elaboration and variable influence in the types of manoeuvres here studied.

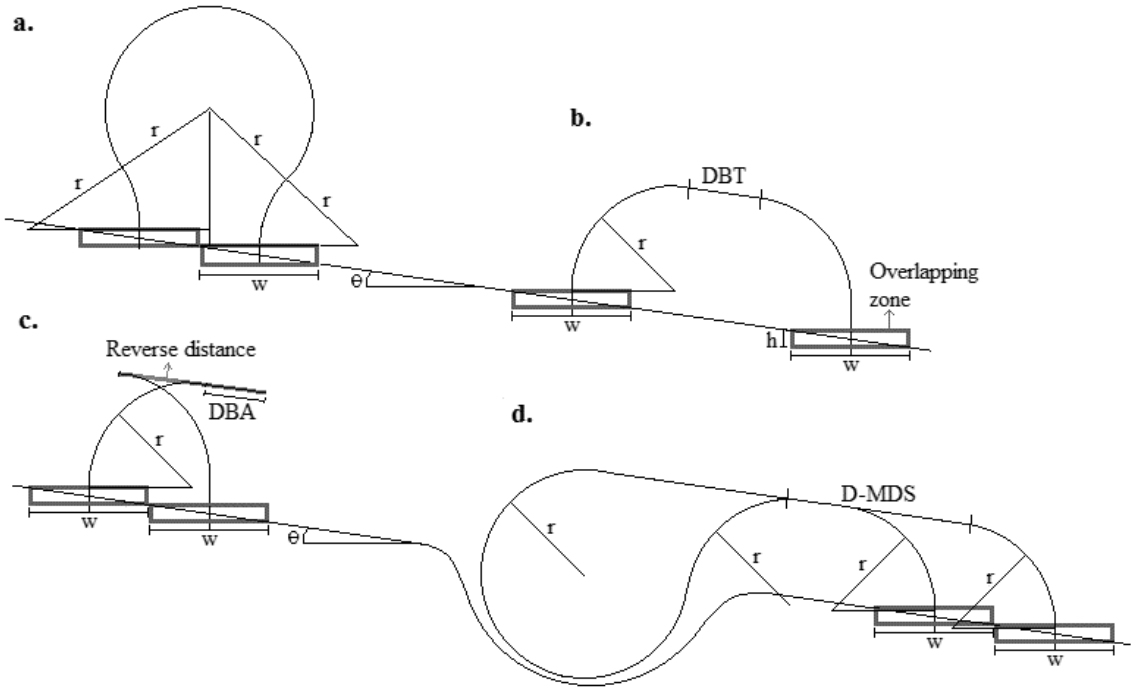

Figure 2.4 - Composition of the types of manoeuvres: Ω-turn (a), U-turn (b), T-turn (c) and P-turn (d)

The angle θ can vary along the fields, but in sugarcane often roads are designed in close perpendicularity to the crop rows (with exception to field corners). A general assumption is herein made for θ of 10 degrees as a general standard value for calculations. In Figure 2.4, *h* is the length of the overlapping zone, given by:

$$h = \frac{w}{\tan(90 - \theta)} \tag{2.1}$$

Sugarcane fields does not contain headlands (therefore no real overlap of pesticides and/or fertilizers), and also because of the small width of most operations, the *h* value is usually low. Its influence in the space required for manoeuvre is found in steeper values of θ.

The variable *DBT* is the straight distance between steering within a U-turn, and is the difference between the length of skipped rows and the turning diameter. *DBA* is distance between implement and front tractor axles (single axle trailed implement); and it is the minimum distance needed for a machine to become fully perpendicular to a field border, before starting to follow a reverse distance.

D-MDS is distance followed by the tractor parallel to the road to the manoeuvre dedicated space, accounted before/after leaving the field.

2.2.2.1 Space demand for manoeuvres

The space demand for manoeuvres is related to the width of road required for completing the manoeuvre, exception made to the P-turn because of its requirement for an *MDS*.

The minimum manoeuvring space required for the Ω-turn, U-turn and T-turn (*ΩMS, UMS* and *TMS*) are respectively given by Equations (2.2) and (2.3):

$$\Omega MS = r + \cos(\theta)\left\{\sin\left[2r.\arccos\left(\frac{r + {}^{w}\!/_{2} + h.\tan(\theta))}{2r}\right)\right] + h.\tan^{2}(\theta)\right\} + \frac{w}{2} \tag{2.2}$$

$$UMS = TMS = r.(\sin(\theta) + 1) + {}^{w}\!/_{2} \tag{2.3}$$

The manoeuvring space for T-turn is herein taken as geometrically equal as the space for a U-turn.

For the P-turn the space demand considering a space for manoeuvring and operating along the road (Road width) and the space of occupied by the *MDS* (MDS width), both of these can be seen in Figure 2.5 and used in the full space demand calculation.

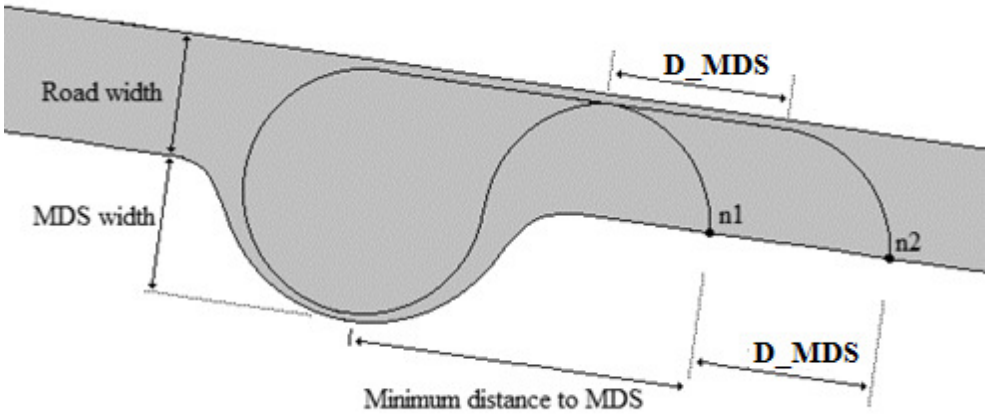

Figure 2.5 - Space requirements for a P-turn

In Figure 2.5, the node *n1* is located at minimum distance necessary, in length, for a machine to perform a P-turn (considering the location from the start of the steering in n1 to the center of the *MDS*), which is given by:

$$Minimum\ distance\ to\ MDS = 2r + r.\cos(\theta) \tag{2.4}$$

The *Road width* is obtained by:

$$Road\ width = r - r.\sin(\theta) + {}^{w}\!/_{2} \tag{2.5}$$

The *MDS* width is obtained by:

$$MDS\ width = 2r + w - Road\ \ width \tag{2.6}$$

Considering the node *n2* as the farthest point from which a machine would go for a specific *MDS*, a longer distance would lead the machine to use another *MDS* next to the field. The equivalent full width (manoeuvring space required for a P-turn: *PMS*), can be given by:

$$PMS = Road\ width + \frac{\left[\pi.(MDS\ width)^2 / 2\right]}{MDS\ width + Mininum\ Dis\tan ce\ to\ MDS + D\_MDS} \tag{2.7}$$

2.2.2.2 Time demand for manoeuvres

The time for manoeuvring is obtained by the ratio of length of the manoeuvres (modelled after their elaboration in Figure 2.4) and the velocity of the machine along this manoeuvring patterns. Agricultural machinery work in constant engine throttle, therefore the manoeuvring velocity is likely to keep the same for a selected manoeuvring in a specific gear. Fluctuations of speed may occur between gear shifting while (or before) entering/finishing the manoeuvre, but the value is here considered less significant.

The times spend for Ω-turn and U-turn are respectively given by Equations (2.8) and (2.9):

$$\Omega MT = \frac{r}{fv}.\left\{2.\left[\arccos\left(\frac{r + w/2 + h.\tan(\theta))}{2r}\right) + \arccos\left(\frac{r + w/2 - h.\tan(\theta))}{2r}\right)\right] + \pi\right\} \tag{2.8}$$

$$UMT = \frac{\left(\pi r + DBT + 2r.\tan(\theta)\right)}{fv} \tag{2.9}$$

Where *ΩMT*, *UMT* are the correspondent lengths followed by a machine in each manoeuvre. While for the loop turns the machine motion is in constant forward velocity, for the T-turn the time spent is a sum of: a forward steering time (before and after reversing), given by the ratio of forward distance by the forward velocity); a straight reversing time, given by the ratio of the reverse distance by rearward velocity; and two stopping times required to cease the machine movement and change the gears between reversing direction. As the stopping movement is not sudden for any moving machine, a simplification is considered in this work adding the deceleration time to the stopping time in the reversing direction steps. To obtain the

T-turn time (*TMT*), a composition of two distances separated in forward and rearward motions are summed:

$$TMT = \frac{Forward\_distance}{fv} + \frac{Reverse\_distance}{rv} + 2.Stop\_time \tag{2.10}$$

$$Forward\_distance = \pi r + 2r.\tan(\theta) + DBA \tag{2.11}$$

$$Reverse\_distance = DBA + 2(r - w) \tag{2.12}$$

In the P-turn herein, the time calculation is also fractioned in two distinct velocities, because it is considered that it contains a steering motion followed in a regular velocity (fv_1) and a significant longer straight motion driven in faster velocity (fv_2). Therefore, in this work, the manoeuvre time is decomposed in two different lengths rationed by two different velocities:

$$PMT = \frac{2r\left(3\pi/2 - \theta\right)}{fv_1} + \frac{2\left(r + D\_MDS\right) - w}{fv_2} \tag{2.13}$$

2.2.2.3 The choice of manoeuvre type

For some operations the choice of a manoeuvre could be just a matter of time spent when there are no issues in requirements for space. While for others, the choice for manoeuvres must consider a balance between loss of area (for a bigger manoeuvre space demand) and its time consumption.

Two costs are here considered for space and time consumption in manoeuvres: energy and financial.

2.2.3 The time and spatial cost of manoeuvring and its balance

2.2.3.1 Manoeuvring cost in time proportion

For any operation in a field plot, the fraction of time spent in a manoeuvre considering a full time work within it is given by the length of a row, the working speed of the machine and the time of manoeuvring. The relative time spent in manoeuvring is given by:

$$RTM_{Oper} = \frac{TM_{Oper}}{\left(ARL / WS\right) + TM_{Oper}} \quad (2.14)$$

Where:

RTM_{Oper} is the relative time spent in manoeuvring (in percentage);

TM_{Oper} is the time spent in a manoeuvre for the operation (s);

WS is the working speed of the operation (m s^{-1});

ARL is the average row(s) length being cover by the operation (m);

The variable RTM_{Oper} is the fraction of time spent by a machine in the manoeuvring operation, which is not dependent on the width of field coverage.

2.2.3.2 Calculating manoeuvre input costs

The input embodiment of sugarcane, or the input materials required in its production, is shown in Figure 2.6, with the diagram of material flow.

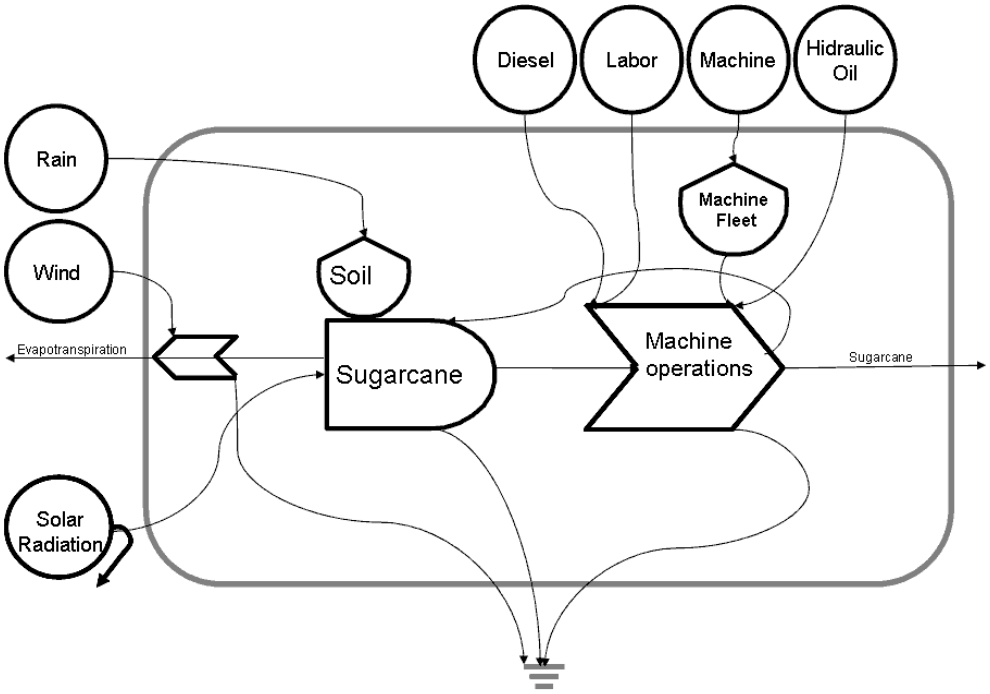

Figure 2.6 - Diagram of material flow in a mechanized sugarcane production system
Modified after Romanelli and Milan (2010)

In Figure 2.6, the inputs regarding machine operations are given by diesel, labour, machine and hydraulic oil. In this study, these are the inputs considered in the operational costs, which are calculated into the economic (R$) and energy variables (J).

The financial values found in literature were subject to currency conversion from real (R$) to dollar (US$). Considering the period from which the values were obtained, the ratio value of real/dollar was of 1.77 R$ US^{-1} in January 2008 to 2.37 R$ US^{-1} in January 2014. The average of the monthly ratio for this period (72 months) was of 1.97 R$ US^{-1}, which is the conversion value used.

The cost variable is finally obtained in units per time (MJ h^{-1} or US$ h^{-1}) for which all the operational decision-making costs are obtained.

2.2.3.3 The hourly energy input

The respective implements used in these operations are given in Table 2.1, being a single class of power tractor used for all the operations (Table 2.2). The operation of harvesting demands three machines: a tractor, a sugarcane carrier and the harvester.

To obtain the relation energy/time, the indirect and direct energy inputs required for a machine are calculated. Manufacture, and repair and maintenance (R&M) are the mechanization indirect inputs here considered.

To calculate the indirect energy input of the machines the approach of Mikkola and Ahokas (2010) is used. Equation 2.15 shows how the calculation is done for self-propelled agricultural machines.

$$qme = \frac{Emw \cdot WPR \cdot Pn}{qs \cdot Ti \cdot Pm} \tag{2.15}$$

Where:

qme is the manufacturing and R&M energy per unit fuel consumption (MJ g^{-1});

Emw is energy given per unit weight (MJ kg^{-1});

WPR is the Weight per Power Ratio (kg kW^{-1});

Pn is the nominal power of the tractor (kW);

qs is the specific mean consumption (g kW^{-1} h^{-1});

Ti is the hourly lifetime of the tractor (h);

Pm is the average power output of the tractor during its lifetime use (kW);

The calculation for hourly energy input of implements is shown in Equation 2.16 adapted after Mikkola and Ahokas (2010) to hourly energy demand.

$$Eh = \frac{Emw \cdot (1 + RRM) \cdot M}{LT} \tag{2.16}$$

Where:

Eh is the hourly energy input (MJ h^{-1});

RRM is the ratio of R&M energy to manufacturing energy;

M is the mass of the implement (kg);

LT is the hourly lifetime of the implement (h);

The manufacturing energy (*Emw*) was of 90 MJ kg^{-1}. The specific parameters of the machines and the respective indirect energy consumption are given in Tables 2.1 and 2.2.

Table 2.1 - Parameters and calculated hourly energy cost of the implements used in the sugarcane operations

Equipment	Mass (kg)[a]	Lifetime (h) [a]	Ratio of the lifetime R&M energy to	Energy for manufacturing + R&M, (MJ h^{-1})

			manufacturing energy [c]	
Sugarcane planter	6300	10000	0.55	87.89
Cultivator	1100	10000	0.55	15.35
Sprayer	1000	4000	0.37	30.83
Sugarcane transporter [b]	10900	21000	0.3	60.73

[a] The mass, lifetime and width are typical for the type and size of the machine in Brazilian market in 2013.
[b] Lifetime, width and velocity in same pace as the sugarcane harvester
[c] Coefficients are presented by Bowers (1992)

Table 2.2 - Hourly energy cost and parameters for indirect and fuel energy input of the self-propelled equipment used in the sugarcane operations

Equipments	Energy for manufacturing + R&M (MJ h^{-1})	Output power (kW)	Specific fuel consumption (g kW^{-1} h^{-1})	Hourly intake (L h^{-1})[c]	Fuel energy input (MJ h^{-1})[d]
Sugarcane harvester	159.9[a]	180	260	57.07	2185.9
Tractor	41.51[b]	80	280	27.32	1046.24

[a] Mantoam et al. (2014).
[b] considering power of 132 kW, mass of 9000 kg and lifetime of 16000 h.
[c] density for diesel fuel of 0.82 kg L^{-1}.
[d] energy output of diesel of 38.3 MJ L^{-1}.

2.2.3.4 The economic input and final hourly costs

Studies of hourly economic inputs in sugarcane machine operations are more widely available. In full work efficiency, Zacharias et al. (2011) found a cost of 45.70 US$ h^{-1} for mechanized sugarcane planting. Baio and Moratelli (2011), observing the use of auto-guidance systems, obtained a cost of tractor-planter set of 76.43 US$ h^{-1} with a respective 75-25% cost distribution of the set and a field efficiency of 68%.

Cultivating and spraying have the source of their operation-costs extracted from FNP consultoria e comércio AGRAFNP (2012), which also provides the data for economic balance.

In harvesting operations, Salvi et al. (2010) proposed a method that first sets field efficiency (in his study of 65 %) and the number of harvesters necessary to conclude a certain project area, rounding up the non integer demand for machines in the site. The authors calculated costs per Mg of sugarcane harvested obtaining a cost of US$ 2.12, US$ 1.92 and US$ 1.70 Mg^{-1} for yields of 80, 90 and 100 Mg ha^{-1}, respectively.

The final economic and energy costs used herein for calculation of the manoeuvre cost balance are shown in Table 2.3.

Table 2.3 - Energy and economic costs for the operations

Operation	Energy input (MJ h^{-1})	Economic input [a] (US$ h^{-1})
Planting	1175.64	80.46 [b]
Cultivating	1103.10	36.53 [c]
Spraying	1118.58	38.86 [d]
Harvesting	3494.28	170.98 [e]

[a] operator hourly wage of US$ 2.55 added to each operation for a 8 hour daily shift labor (FNP CONSULTORIA E COMÉRCIO AGRAFNP, 2012).
[b] costs distributed in: 72.8% tractor (148.7 kW) and 24.13% sugarcane planter (BAIO e MORATELLI, 2011);
[c] 88.3 kW tractor with a two row triple operation implement: fertilizer distribution, subsoiling and cultivation (FNP CONSULTORIA E COMÉRCIO AGRAFNP, 2012);
[d] 18 m boom sprayer pulled by a 66.2 kW tractor (FNP CONSULTORIA E COMÉRCIO AGRAFNP, 2012);
[e] Salvi et al. (2010), considering a yield of 90 Mg ha^{-1} and a cost of harvest of 1.92 US$ Mg^{-1}.

2.2.3.5 The cost of a row-edge

The yearly cost of manoeuvring on a row-edge for an operation is herein designated as *CMRE* which is dependent neither on *WS* nor in the *ARL*, but on the time of manoeuvring, the time-cost of the operation, the frequency of operation currency along the plant life and the number of rows covered by the crop. Its calculation is given in Equation 2.17.

$$CMRE_{Oper} = TM_{Oper} \cdot \frac{TC_{Oper}}{3600} \cdot \frac{F}{NRC_{Oper}} \tag{2.17}$$

$$TCMRE = \sum_{Oper} \left(CMRE_{Oper} \right) \tag{2.18}$$

Where:

CRME is the cost of manoeuvring in a row-edge (MJ or US$);

Oper identifier of the field operation;

TC_{Oper} is the time cost of a manoeuvre (MJ h^{-1} or US$ h^{-1});

F is the yearly frequency of occurrence of the operation;

NRC_{Oper} number of rows covered by the operation;

TCMRE is the sum of manoeuvring operations costs in a row-edge (MJ or US$);

2.2.3.6 The manoeuvring cost per area

The manoeuvring cost per area is given by the number of manoeuvres in an area unit multiplied by the *TCMRE*. The area unit used herein is the hectare (ha).

The number of manoeuvres is obtained by dividing the area unit by an average of the area of one crop row. The calculation is pointed in Equation 2.19.

$$ICMA = \frac{10000}{ARL.Row\ width} \cdot TCMRE \tag{2.19}$$

Where:

ICMA is the input cost of manoeuvring per area (MJ ha^{-1} or US$ ha^{-1});

Despite *ARL* has a direct impact on the production cost, no studies exist pointing an average value in sugarcane fields, neither their quantitative impact in machine operations. Thus *ARL* is considered herein as a variable.

The width of the coverage of a machine will also impact directly in the spatial turning costs. Figure 2.7 illustrates the types of sugarcane harvester coverage capacity. In general, sugarcane is harvested one row at a time (as in "i"), but machine developments allowed harvesters to enlarge their width to harvest narrow twin-rows ("ii") and more recent works enlarged the width up to two sugarcane rows ("iii").

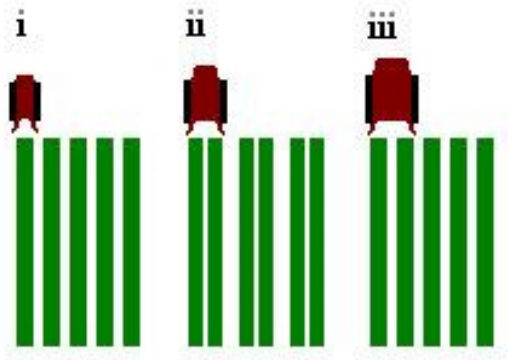

Figure 2.7 - Distinct width configuration available in sugarcane harvesters

2.2.3.7 The energy and economical balance

Both energy and financial liquid output of sugarcane can be calculated by the crop productivity. The energy balance is herein calculated after Macedo et al. (2008) which calculated the energy input and brute output of sugarcane to be of 233.8 MJ and 2185.2 MJ

respectively. The estimated yields along the harvest sequences, the financial input and output were extracted from FNP Consultoria e Comércio AGRAFNP (2012).

The financial balance fluctuates along the years because of the price paid for Mg of canes. The production costs are herein considered fixed for a five-year implantation set, but there are distinct costs for each harvest-year. Each sequential harvest from the same base-ratoon presents decreasing yields, until it reaches a critical economic point that requires it to be implanted again.

A total of five harvests from one implantation are common for the crop. The energy balance follows linearly while Table 2.4 displays the data used for the economic balance.

Table 2.4 - Economic balance of the sugarcane production

Harvest year	Yield (Mg ha^{-1})[a]	Cost (US$ ha^{-1})[a]	Profit (US$ ha^{-1})[a]
1	106	2822.27	832.64
2	84	2224.34	678.24
3	76	2333.67	273.57
4	66	2106.21	178.23
5	58	1952.84	35.75
Average	78	2287.87	399.68

[a] Yield, cost and profit extracted from FNP consultoria e comércio AGRAFNP (2012)

As the economic revenue may vary along the years because of factors like sugarcane price, yield or distinct case-sites of production costs, and because of the small fraction of economic revenue compared to the whole cost, unique costs (like manoeuvring) have significant influence in the final revenue. In order to study this influence, the net output shown in Table 4 be subject to increase profitability in the order of 50%, 75% and 100% within the scenario studies.

2.2.3.8 Impact of the manoeuvre within its row

Each crop-row is here considered to have a fixed *TCMRE* and a specific net output (energy or economic). By adding cost of manoeuvre per area (*ICMA*) to the final balance of sugarcane production, a net output is obtained free of manoeuvring costs. This value is adjusted to units of linear revenue of the crop row. Equation 2.20 shows the sugarcane balance to a row-meter.

$$EFB_{meter-row} = \frac{(EFB_{area} + ICMA) \cdot Row\ \ width}{10000} \tag{2.20}$$

Where:

$EFB_{meter-row}$ is the energy or financial balance per meter-row (MJ m^{-1} or US$ m^{-1});

EFB_{area} is the energy or financial balance per area (MJ ha^{-1} or US$ ha^{-1});

The ratio between *TCMRE* and $EFB_{row-meter}$ (Equation 2.21) is the length of a row necessary to pay for the manoeuvre. When a full row length is shorter than this, the respective row is considered unprofitable.

$$EMCRL = \frac{TCMRE}{EFB_{row-meter}} \tag{2.21}$$

Where:

EMCRL is the equivalent manoeuvre cost in row length (m);

2.2.4 Scenarios for calculating the impact of the manoeuvre-types

Planting and cultivating can be suitable options for replacing costly manoeuvres by U-turns (skipping rows) aiming to speed manoeuvring time and keeping reduced manoeuvring space. In this work scenarios were estimated and its values shown in Table 2.5 using the manoeuvring equations. A fixed number of 6*w* and 3*w* were used for skipping rows for the planting and cultivating operations respectively.

Table 2.5 - Turning types and their respective demands obtained for two operations

	Ω-turn		U-turn		T-turn	
	time (s)	space (m)	time (s)	space (m)	time (s)	space (m)
Planting [a]	46.8	22.1	25	10.9	80.5	10.9
Cultivating [b]	20.2	12.5	10.5	6.8	24.5	6.8

[a] Implement pulled by tractor's traction bar. Length of a manoeuvre calculated for planting with a *r* of 8 m; forward and rearward velocity of manoeuvring of 1.2 m s^{-1} and 0.6 m s^{-1}, DBA of 13cm and a total stopped time of 8 s

[b] Implement three point attached to the tractor. Length of a manoeuvre calculated for planting with a *r* of 4.5 m; forward and rearward velocity of manoeuvring of 1.5 m s^{-1} and 1 m s^{-1} respectively, DBA of 3 m and a total stopped time of 6 s.

Figure 2.8 illustrates how works the relation between manoeuvring space, time and cost of row-length for three manoeuvring types of a sugarcane carrier: Ω-turn, T-turn and P-turn. The sugarcane rows in green shift into grey after a transversal line. The length of the grey lines represent an equivalent time into row-length-cost for manoeuvres.

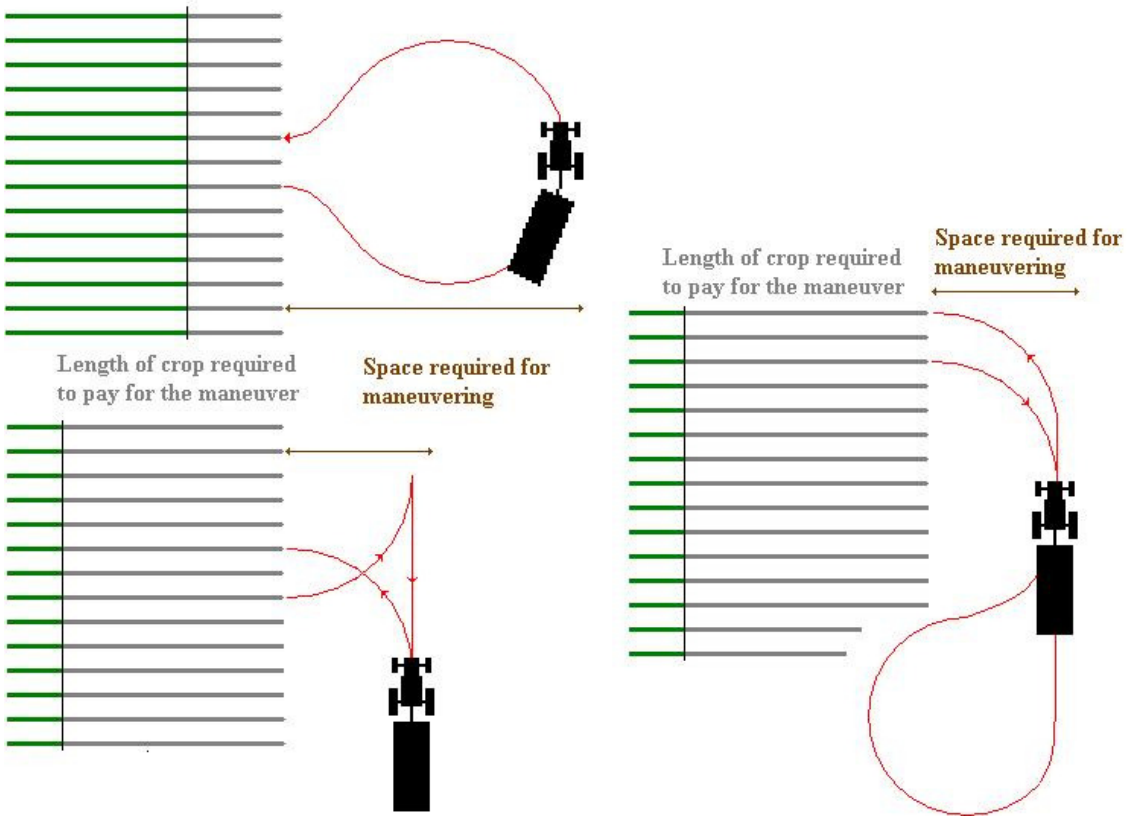

Figure 2.8 - Three distinct types of manoeuvres and their space and time equivalent costs

A study was carried estimating the impacts of these turns in the full cost of the manoeuvres (manoeuvre space + *EMCRL*) using the parameters presented in Table 2.6. The time and space parameters were obtained for: *w* of 1.5 m (working width); an implement width (for road turning) of 3 m; forward steering, rearward speed and forward straight distance of 1.5 m s^{-1}, 0.6 m s^{-1} and 2 m s^{-1} respectively; a general *D-MDS* arbitrarily set in 20 m.

Table 2.6 - Input data for comparison of three turning types and three carrier types to quantify cost of manoeuvring in row-length perspective

Carrier type	Turning radius (m)	Ω-turn		T-turn		P-Turn	
		Space (m)	Time (s)	Space (m)	Time (s)	Space (m)	Time (s)
Self-propelled carrier[a]	5	14.5	23.6	7.4	43.0	7.6	53.8
Single wagon[b]	7.5	21.3	35.8	10.3	57.1	10.9	71.4
Double wagon	10.8	23.6	48.1	na[c]	na[c]	15.2	89.0

[a] Distance between axles (DBA) of 5m
[b] Distance between axles (DBA) of 9m

[c] 'not applicable' - double wagon carrier unlikely uses reverse manoeuvring due to the difficulty to drive it rearwards

The variables to be simulated from the data in Table 2.6 were subject to comparison in the set of distinct economic revenue scenarios pointed earlier to observe its impact in the manoeuvring space cost. A model was built using the proposed equations in Microsoft Excel™ spreadsheet in order to answers the research questions posed.

2.3 Case studies, model sensitivity and discussion

2.3.1 Machine and field parameters influencing manoeuvres

The effects of two variables in the turning patterns were studied: turning radius (r) and angle of deviation from perpendicular border (θ). The width of the operation (w) was not studied, given the difficulty of significant enlargement of implement-width used in the sugarcane system.

In Figure 2.9, Ω-Turns are limited to be performed up to a 60 degrees of θ inclination, and above this another type of turn would follow ("Hook-turn" according to JIN;TANG, 2010). In practice, for sugarcane, P-turns would replace Ω-Turns under high θ inclination. A value of 10 degrees was assigned to θ for graphs 'b' and 'd'; and a r of 7 m was assigned for graphs 'a' and 'c'.

For T-turns, the DBA was set in 9m (trailed vehicle). The DBT for the U-turns is minimum distance of skipping rows considering r and w. The D-MDS was set in 20 m.

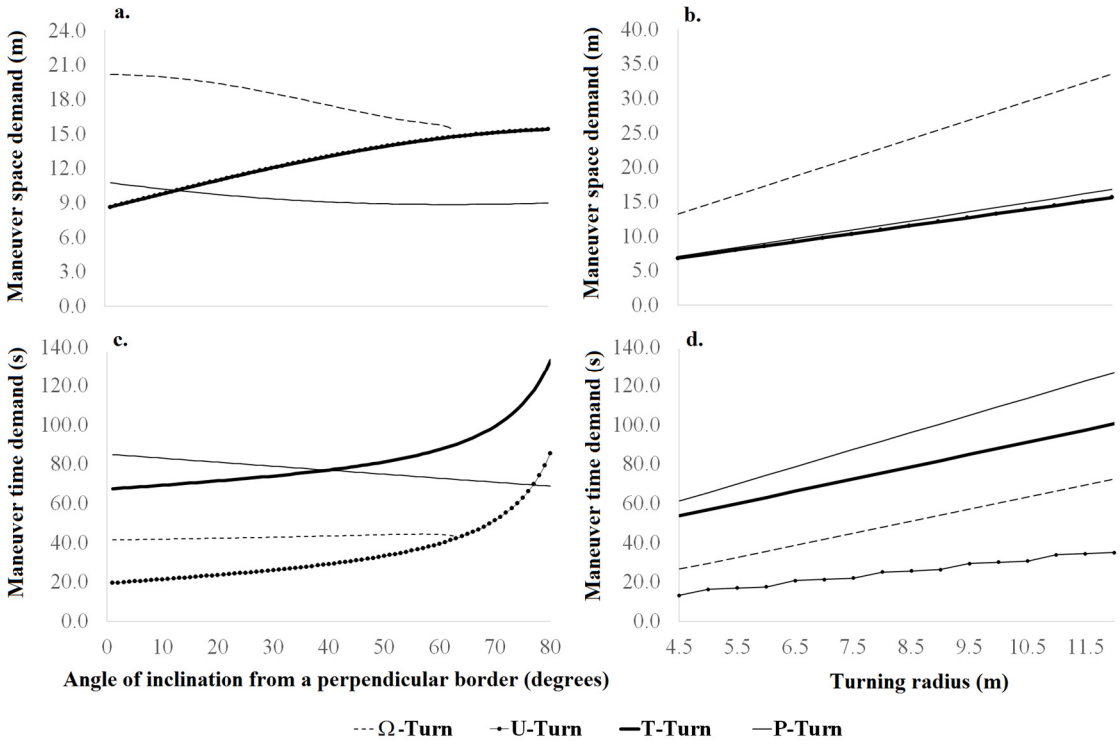

Figure 2.9 - Sensitivity analysis of the effects of the angle and turning radius in the manoeuvring length and space

The snake-shape in the graph for U-manoeuvres in Figure 2.9d is because of the effect of skipping rows, in which the increase in turning radius may lead to an immediate need to skip one more *w*.

The choice for P-turns for carrier-wagons can be understood regarding the low space demand for manoeuvre that it presents compared to the Ω-turn (for manoeuvres into adjacent rows). This additional space needed can be generically rounded and averaged to 9 m for along values of *r*.

The benefits of the use of U-turns decrease in steep θ values. This observation was also made for optimized choice of manoeuvres done by Spekken and DeBruin (2013), contrasting with the Ω-turns, where the space and time for manoeuvres decreases in steeper θ values.

Despite P-turns are the most common manoeuvring type for the harvesting operation (for the carrier-wagons), nonetheless they are the most time consuming. Even when the *MDS* is in its closest to the transport unit (*D-MDS* equal to 0), the manoeuvre time is still 69 s.

2.3.2 Time impact of manoeuvring

The sensitivity of the time impact of manoeuvres in sugarcane harvest was obtained simulating increasing ARL and TC. The operation speed was set on 1.575 m s^{-1} (SALVI et al., 2010). Results are shown in the graph of Figure 2.10.

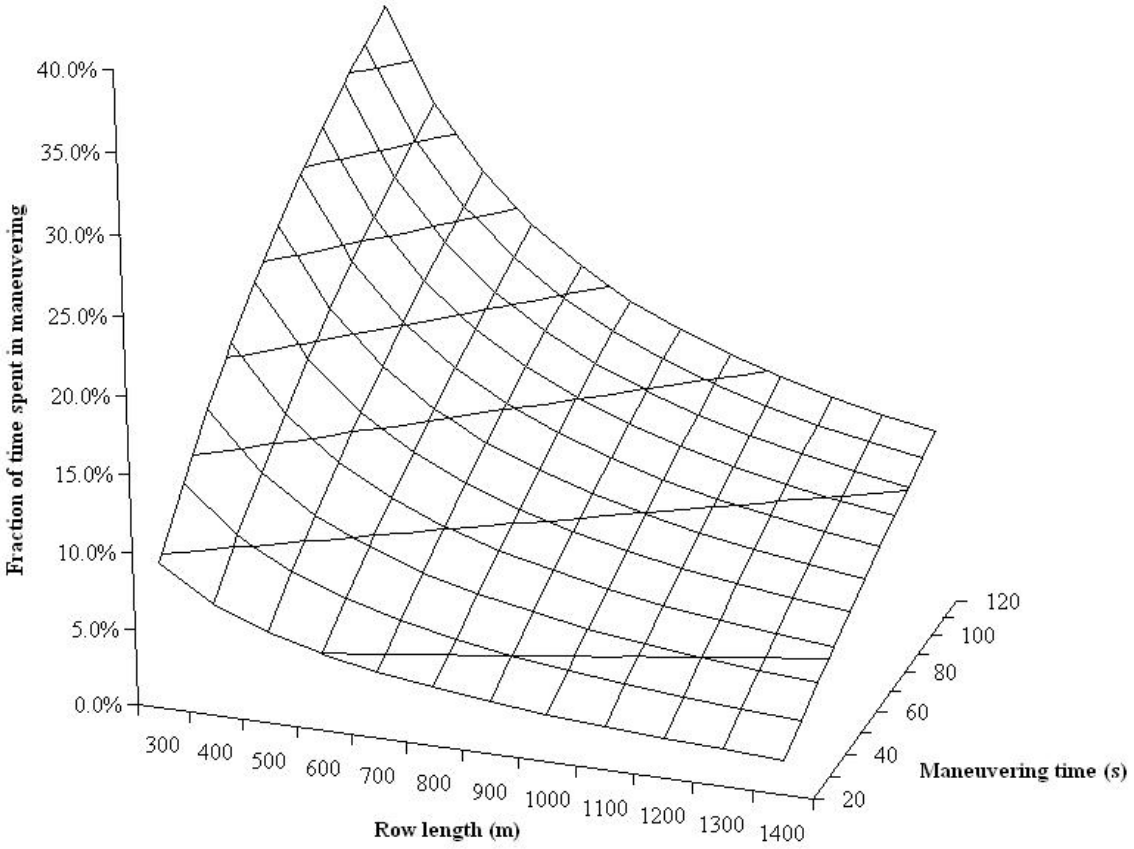

Figure 2.10 - Fraction of time spend in manoeuvring for a sugarcane harvester for its overall efficiency

A range between 2.2% to 38.7% of non-working time due to manoeuvres was found for harvesting. The analysis still doesn't consider that rows can be shorter than 300 m, mainly in corners of fields and obstacles. Regarding time spent, ranges up to 2 minutes (as 120 seconds in the graphs) were found in literature. As short rows are almost unavoidable in many fields, options for efficiency are limited to speed manoeuvring time or avoiding these regions.

A standard scenario was set for the model to calculate the *CMRE*. The variable settings can be seen in Table 2.7.

Table 2.7 - Standard setting parameters used for calculation of *CMRE* and its respective costs

NRC	*F*	Time energy cost (MJ s^{-1})	Time economic cost (US$ s^{-1})	Manoeuvre time (s)	*CMRE* (MJ)	*CMRE* (US$)

Planting	2	0.2	0.327	0.02	80.5	2.63	0.17
Cultivating	2	1	0.306	0.01	24.5	3.75	0.12
Spraying	12	1	0.311	0.01	20	0.52	0.02
Harvesting	1	1	0.971	0.05	89	86.4	4.14

The costs found for a single turning edge was of 93.29 MJ and US$ 4.45. The harvest operation comprises with the majority of the costs with 92.6 and 93.0 % of the respective energy and financial costs in the listed operations.

2.3.3 The manoeuvre cost per area

In the given CRME scenario, with a standard scenario of ARL and RW of 300 m and 1.5 m respectively, the obtained cost of manoeuvring per area was 2073 MJ ha^{-1} and US$ 98.9 ha^{-1}. A sensitivity analysis was applied into the model by varying a of row-length distance in a range between 50 to 1000 m, retrieving the respective turning costs.

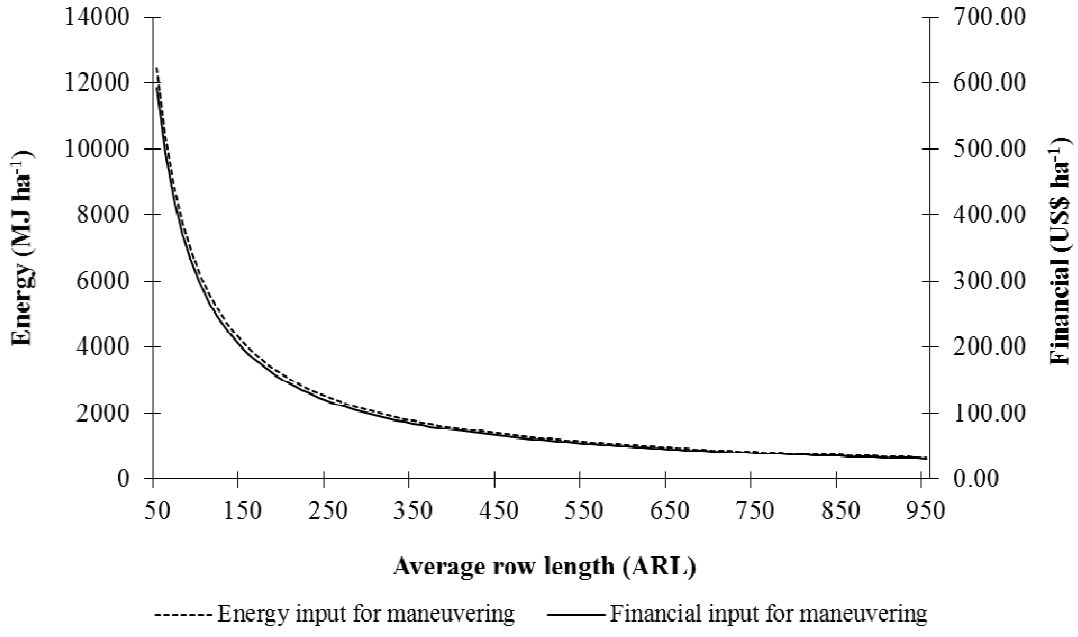

Figure 2.11 - Cost of manoeuvring per area with increasing row length

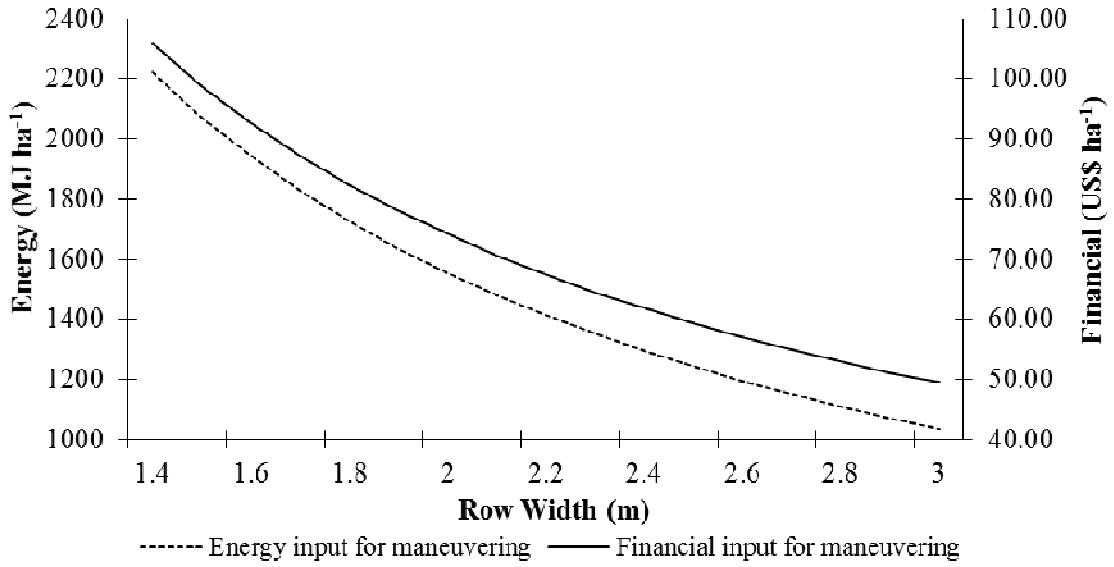

Figure 2.12 - Costs of manoeuvring per area with increasing coverage capacity of machines

Figure 2.11 points to the impact of manoeuvres in short rows, which may surpass the economic return (average of five years in Table 2.4) in rows shorter than 50 m. The same figure also shows that continuous efforts to lower manoeuvring costs by increasing the row length gives a decreasing benefit. This must be taken into account because longer rows can lead to problem of machine servicing, when these machines finish their product capacity (carrier baskets full or spraying and fertilizing tanks empty) far away from the roads where these can be unloaded/replenished, and the overall efficiency can be rather damaged than improved. Benedini and Conde (2008) suggest the length of the row to be within 500 m and 700 m, the benefit for extending the row from 700 m to 1000 m will yield a benefit of only 9.38 US$ ha^{-1} for manoeuvring. Considering that costs of servicing operations significantly surpass the non-servicing operations (like soil tillage every five years), studies towards the latter weren't carried.

For many sugarcane fields when roads are not limiting the length of row, but just cutting through it, no manoeuvre is needed and fully loaded transporting units can just steer to the roads. In such cases extending row length can continue yielding profits, if this is properly segmented by crossing roads.

Figure 2.12 quantifies the benefit in increasing coverage width of the sugarcane rows by decreasing the number of turns and the respective spatial turning costs. Above the width of 1.8 m the crop is herein considered to be implanted in twin-rows and the planting and cultivating

operations can no longer cover two rows (1.9 m width), slightly increasing the overall manoeuvring time.

The increasing width, despite its benefit in reducing manoeuvring costs, will also influence the servicing of machinery, mainly the sugarcane carriers, because it will fill the basket in a shorter harvested distance.

An optimization between crop yield, machine capacity, width of coverage and row length poses a topic for further study.

Considering the standard scenario of *ARL* and *CMRE*, increasing *ARL* in 150 m yields savings equivalent to reducing the manoeuvring times of planting and harvesting in 30 s.

2.3.4 The manoeuvring cost within sugarcane energy and economic balance

In a standard *TCMRE* scenario, the fraction of costs related for energy and economic perspectives are displayed in Table 2.8.

Table 2.8 - Fraction of manoeuvring in the total sugarcane input cost for the standard CMRE scenario

Annual harvest sequence from ratoon	Yield (Mg ha^{-1})	Fraction of the total input related to manoeuvres (%)	
		Energy	Economic
1	106	8.3%	3.6%
2	84	10.5%	4.5%
3	76	11.6%	4.3%
4	66	13.4%	4.8%
5	58	15.3%	5.2%
Average	78	11.8%	4.5%

The energy input represents 10.7 % of the brute output, contrasting with economic where the input represents 85.1 % of the brute output (average of 5 years). It strongly points that the full economic input is not so much related to financial costs of raw material (iron, rubber, fuel, etc) but rather to the cost of embedded technology (embodied knowledge cost). This suggests that the sustainability of sugarcane crop production is more fragile towards its economic balance than its energy balance.

In Table 2.8, the higher manoeuvring proportion of energy compared to economic in the total input shows the impact of embodied knowledge cost in the majority of other economic costs of sugarcane (administrative, land lease, technology patents, etc).

Despite the small fraction of manoeuvres in the economic total input, these can have a significant weight in the profit (which is less than 15% of the economic brute output). As an example, a cost of manoeuvring per area of 98.9 US$ ha^{-1} (found for a standard scenario) represents a fraction of 20% of the income (when considering the income Table 2.4 of net revenue, average of 5 years).

2.3.5 Cost impact of a manoeuvre translated in length of crop-row

The net output of the crop translated into length of crop-row can be seen in Table 2.9. A significant difference is found along the harvest sequences. While the net output of energy of fifth harvest represents 55.2% of the first, economically this value drops to 14.8%.

Table 2.9 - Energy and economic balance of a meter-row of sugarcane found

Harvest sequence	Yield (Mg ha^{-1})	Revenue per length of row	
		Energy (MJ m^{-1})	Economic (US$ m^{-1})
1	106	31.36	0.14
2	84	24.92	0.11
3	76	22.58	0.05
4	66	19.65	0.04
5	58	17.31	0.02
Average	78	23.16	0.07

Table 2.10 - Equivalent length of rows required to pay for the manoeuvre cost using different scenarios of economic net revenue

Harvest sequence	Energy	Economic scenarios of net output			
	Standard	Standard	+ 50%	+ 75%	+ 100%
	Equivalent row length to cover manoeuvre cost (m)				
1	2.21	32.6	21.7	18.6	16.3
2	2.78	39.0	26.0	22.3	19.5
3	3.06	81.7	54.5	46.7	40.8
4	3.52	110.0	73.3	62.8	55.0
5	4.00	228.0	152.0	130.3	114.0
Average	2.99	62.0	40.6	34.8	30.5

The data provided in Table 2.10 points to the length required for the crop to pay for its manoeuvring costs. The most optimistic scenarios of profitability still require 30.5 m of crop row.

Figure 2.13 shows a real spatial dataset of pre-planned sugarcane rows. This dataset represents a subset field located in the corner of a farm containing some obstacles. The rows in red are shorter than 50 m (threshold rounded from the results in Table 2.10, from the average length of tracks a profitable row need) which are located in edges of the fields and between obstacles, these represent 22.8% of the rows (and manoeuvres) in the dataset, but only 4.2% of the total area.

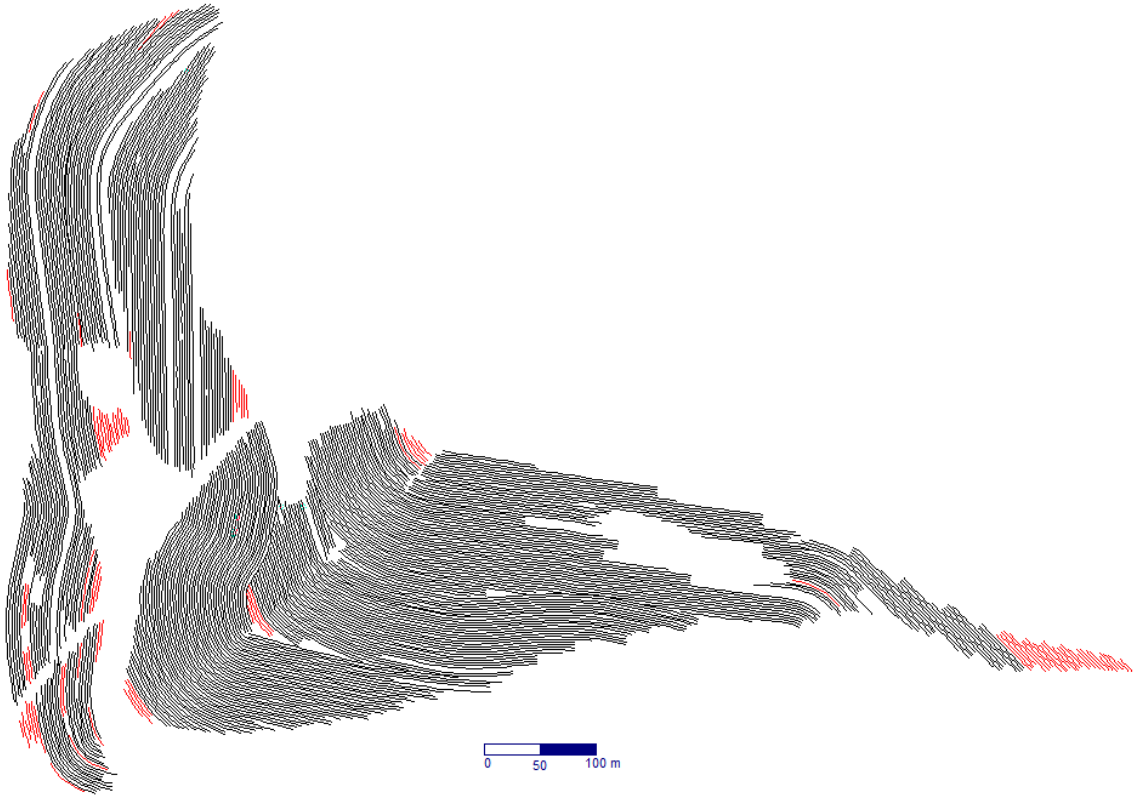

Figure 2.13 - Spatial pre-planned tracks for sugarcane rows. Rows in red are too short to pay for manoeuvre cost

2.3.6 Output for the scenarios proposed

Using the standard scenario of 300 m of average row length, an analysis was done comparing the costs of turning types feasible to be used in the planting and cultivating operations. The manoeuvring time costs were extracted from the parameters given in Table 2.5, with the frequency of 0.2 and 1 times per year for the planting and cultivating operations (Table 2.7). The space cost were obtained by an equivalent of spatial to row-length in the standard scenario (Table 2.9). The results are displayed in Table 2.11.

Table 2.11 - Cost impact obtained for the three manoeuvring types considering their space and time demanded for turning

	Cost for loss of cropped area		Cost of manoeuvring time		Total cost	
	Energy (MJ ha^{-1})	Economic (US$ ha^{-1})	Energy (MJ ha^{-1})	Economic (US$ ha^{-1})	Energy (MJ ha^{-1})	Economic (US$ ha^{-1})
Planting						
Ω-turn	511.8	3.18	33.9	2.20	545.7	5.38
U-turn	252.4	1.57	18.1	1.18	270.5	2.75
T-turn	252.4	1.57	58.4	3.78	310.8	5.35
Cultivating						
Ω-turn	289.5	1.80	68.8	2.23	358.3	4.03
U-turn	157.5	0.98	35.7	1.16	193.2	2.14
T-turn	157.5	0.98	83.41	2.71	240.91	3.69

In the three scenarios studied the economic costs, the T-turns almost reached the cost of the space demanding Ω-Turns. Also the savings in the use of U-turns, for large areas covered, may provide savings that allow the investment in guidance systems for skipping rows. The change of T-turns to skipping rows can amount a savings of 88 MJ ha^{-1} and 4.15 US$ ha^{-1} for both operations considered herein.

2.3.7 Impacts of enlarging manoeuvre space

The model result of the variables proposed in Table 2.6 for manoeuvring and carrier types is given in Table 2.12.

Table 2.12 - Four scenarios of summed time and space economic costs for three manoeuvring types and three sugarcane carrier machines

Carrier type	Summed space and time cost for manoeuvring (US$)		
	Ω-turn	T-turn	P-turn
Standard Scenario			
Self-propelled carrier	3.22	4.48	5.49
Tractor + single wagon	4.84	5.99	7.34
Tractor + double wagon	6.13	-	9.27
Net Output + 50%			
Self-propelled carrier	3.75	4.75	5.76
Tractor + single wagon	5.61	6.36	7.74
Tractor + double wagon	6.99	-	9.82
Net Output + 75%			
Self-propelled carrier	4.02	4.89	5.90
Tractor + single wagon	6.00	6.55	7.94
Tractor + double wagon	7.42	-	10.10
Net Output + 100%			
Self-propelled carrier	4.28	5.02	6.04
Tractor + single wagon	6.39	6.74	8.14
Tractor + double wagon	7.85	-	10.38

The loss of area for turning a machine in a space consuming manoeuvre (like the Ω-turn) is still more profitable because of its time savings benefit; and this was found for any of the scenarios tested. The current belief that narrow roads to reduce area loss leads to financial benefit is herein questioned. Also savings can be seen for using self-propelled and single-wagon carriers which can reduce considerably the necessity of too wide roads for turning.

If certain manoeuvres require wider roads by taking this space from productive areas, the time savings benefit can still excel the liquid outcome that a crop can produce.

In a standard scenario for an economic perspective, every second of harvest manoeuvring are the equivalent to 0.64 m of crop harvested in single row, 0.40 m of crop harvested in twin row and 0.32 m of crop harvested in double row harvester.

The methodology used here is applicable for other crop growing systems where it is expected high manoeuvring costs, but less likely to be found for wider machine coverage and lower biomass intake.

2.4 Conclusions

The cost of manoeuvring in sugarcane is herein calculated by a number of variables taking the machine hourly cost (energy and economic) into account. For the standard scenario energy and economic costs per manoeuvre were 93.3 MJ and US$ 4.45, respectively, for which harvesting comprises the majority of the costs, in agreement with other authors on the major impact of harvesting in the production of the crop.

The cost per area for manoeuvring is also dependent on width of coverage and length of rows. From a set of standard values for these, the cost of manoeuvring per area was obtained in 2073 MJ ha^{-1} and 98.9 US$ ha^{-1}. Efforts to keep increasing the length of the rows will give decreasing benefit in savings, suggesting the row length to be limited to 500 to 700 m regarding the logistic of transporting units. Increasing coverage width, which is usually limited by harvesting machines, showed potential to decrease the manoeuvring costs.

Manoeuvres comprise a small fraction in the final production costs, but higher impact in the final economic revenue. The high positive energy balance of the sugarcane crop points that the fragility of the production system is because of economic reasons.

The minimum length required to pay for a manoeuvre in a standard set scenario was of 62 m in average. More optimistic scenarios of economic revenue still demand more than 30 m of row length to start yielding economic revenue of it.

A real case-study site showed a number of pre-planned tracks that would be composed by 18.7 % of economic unprofitable tracks in a standard scenario.

The use of different turning patterns for planting and cultivating operations pointed to savings summing 88 MJ ha^{-1} and 4.15 US$ ha^{-1}. The cost implementing guidance systems in the machinery to orient the row skipping is not computed herein.

The scenarios of cane-carriers types, manoeuvre types and revenue obtained that the use of short width roads result in more cost than benefit. Optimized solutions were found with use of carriers with short turning radius and roads wide enough for Ω-turns.

References

BAIO, F.H.R. Evaluation of an auto-guidance system operating on a sugar cane harvester. **Precision Agriculture,** Dordrecht, v. 13, n. 1, p. 141-147, 2012.

BAIO, F.H.R.; MORATELLI, R.F. Avaliação da acurácia no direcionamento com piloto automático e contraste da capacidade de campo operacional no plantio mecanizado da cana-de-açúcar. **Engenharia Agrícola,** Jaboticabal, v. 31, n. 2, p. 367-375, 2011.

BENEDINI, M. S; CONDE, A. J. Sistematização da área para a colheita mecanizada de cana-de-açúcar. **Revista Coplana,** Jaboticabal, v. 25, nov. 2008. Disponível em: <http://www.coplana.com/gxpfiles/ws001/design/RevistaCoplana /2008/Novembro/pag23-24-25.pdf>. Acesso em: 20 maio 2015.

BOCHTIS, D.D.; VOUGIOUKAS, S.G. Minimising the non-working distance travelled by machines operating in a headland field pattern. **Biosystems Engineering,** London, v. 101, n. 1, p. 1-12, 2008.

BOWERS, W. Agricultural field equipment. **Energy in Farm Production,** Amsterdam, v. 10, p. 117-129, 1992.

CARIOU, C.; LENAIN, R.; THUILOT, B.; HUMBERT, T.; BERDUCAT, M. Manoeuvres automation for agricultural vehicle in headland. In: AgEng 2010, INTERNATIONAL CONFERENCE ON AGRICULTURAL ENGINEERING, 2010, Clermont-Ferrand. **Proceedings…** Clermont-Ferrand: CIGR, International Commission of Agricultural and Biosystems Engineering, 2010. p. 112-122.

COELHO, M.F. **Planejamento da qualidade no processo de colheita mecanizada da cana-de-açúcar.** 2009. 74 p. Tese (Mestrado em Máquinas Agrícolas) – Escola Superior de Agricultura "Luiz de Queiroz", Universidade de São Paulo, Piracicaba, 2009.

COMPANHIA NACIONAL DE ABASTECIMENTO. **Acompanhamento de safra brasileira:** cana-de-açúcar, segundo levantamento, agosto/2013. Brasília, 19p. 2013.

DE OLIVEIRA, M.E.D.; VAUGHAN, B.E.; RYKIEL, E.J. Ethanol as fuel: energy, carbon dioxide balances, and ecological footprint. **BioScience,** Cary, v. 55, n. 7, p. 593-602, 2005.

FNP CONSULTORIA E COMÉRCIO AGRAFNP. **AGRIANUAL 2012:** anuário da agricultura brasileira, São Paulo, 2012. 482 p.

GUIMARÃES, R.V. **Aplicação de geoprocessamento para aumento na eficiência do percurso em operações na cultura da cana-de-açúcar (*Saccahrum spp.*).** 2004. 82 p. Dissertação (Mestrado em Máquinas Agrícolas) - Escola Superior de Agricultura "Luiz de Queiroz", Universidade de São Paulo, Piracicaba, 2004.

JIN, J.; TANG, L. Optimal path planning for arable farming. In: ASABE ANNUAL INTERNATIONAL MEETING, 2006, Portland. **Proceedings…** St. Joseph: American Society of Agricultural Engineers, 2006. p. 304-312.

_____. Optimal coverage path planning for arable farming on 2D surfaces. **Transactions of the ASABE,** St. Joseph, v. 53, n. 1, p. 283, 2010.

MACEDO, I.C.; SEABRA, J.E.A.; SILVA, J.E.A.R. Greenhouse gases emissions in the production and use of ethanol from sugarcane in Brazil: the 2005/2006 averages and a prediction for 2020. **Biomass and Bioenergy,** Oxford, v. 32, n. 7, p. 582-595, 2008.

MANTOAM, E.J.; MILAN, M.; GIMENEZ, L.M.; ROMANELLI, T.L. Embodied energy of sugarcane harvesters. **Biosystems Engineering,** London, v. 118, p. 156-166, 2014.

MIKKOLA, H.J.; AHOKAS, J. Indirect energy input of agricultural machinery in bioenergy production. **Renewable Energy,** Oxford, v. 35, n. 1, p. 23-28, 2010.

MILAN, M. **Gestão sistêmica e planejamento de máquinas agrícolas.** 2004. 100 p. Tese (Livre-Docência em Mecânica e Máquinas Agrícolas) - Escola Superior de Agricultura "Luiz de Queiroz", Universidade de São Paulo, Piracicaba, 2004.

OKSANEN, T.; VISALA, A. Coverage path planning algorithms for agricultural field machines. **Journal of Field Robotics,** Hoboken, v. 26, n. 8, p. 651-668, 2009.

PAULA, V.D.; MOLIN, J.P. Assessing damage caused by accidental vehicle traffic on sugarcane ration. **Applied Engineering in Agriculture,** St Joseph, v. 29, n. 2, p. 161-169, 2013.

ROMANELLI, T.L.; MILAN, M. Material flow determination through agricultural machinery management. **Scientia Agricola,** Piracicaba, v. 67, n. 4, p. 375-383, 2010.

SALVI, J.V.; OLIVEIRA, M.P.; FIORAVENTE FILHO, S.R.; SANTOS, J.A. Análise do desempenho operacional e econômico da colheita mecanizada em um sistema de produção de cana-de-açúcar. **Anais do congresso da sociedade brasileira de economia, administração e sociologia rural**, 48., 2010, Campo Grande. Disponível em: <http://www.sober.org.br/palestra/15/157.pdf>. Acesso em: 28 maio 2015.

SPEKKEN, M.; DE BRUIN, S. Optimized routing on agricultural fields by minimizing manoeuvring and servicing time. **Precision Agriculture,** Dordrecht, v. 14, n. 2, p. 224-244, 2013.

SPEKKEN, M.; MOLIN J.P. Optimizing path planning by avoiding short corner tracks. In: INTERNATIONAL CONFERENCE ON PRECISION AGRICULTURE, 11., 2012, Monticello. **Proceedings…** Monticello: International Society in Precision Agriculture, 2012. p. 314-328.

TAÏX, M.; SOUÈRES, P.; FRAYSSINET, H.; CORDESSES. Path planning for complete coverage with agricultural machines. In: ZELINSKY A. **Field and service robotics.** Berlin; Heidelberg: Springer, 2006. p. 549-558.

WITNEY, B. **Choosing and using farm machines.** Edinburgh: Land Technology, 1996. 412 p.

ZACHARIAS, R.; SANTOS, F.L.; DE JESUS, V.A.M. Custos operacionais do plantio mecanizado e semi mecanizado de cana-de-açúcar. **Revista Engenharia na Agricultura,** Vicosa, v. 19, n. 2, p. 118-124, 2011.

3 PLANNING MACHINE PATHS AND ROW CROP PATTERNS ON STEEP SURFACES TO MINIMIZE SOIL EROSION

Abstract

In arable fields, irregular steep surfaces present a problem for operating machinery and establishment of row crops. Contouring (i.e., performing field operations perpendicular to slope direction) is a common practice to reduce runoff and increase water infiltration. Unfortunately, elevation contours are never perfectly parallel, while this would be required for optimal machine operation. In this work, a method is presented to assess spatial patterns of machine paths and row crops on irregularly sloping land in terms of susceptibility to water erosion. The approach comprises three main process-steps: (1) assembling a comprehensive set of reference tracks and introducing hybrid contour lines; (2) adjust these curved tracks into steerable parallel tracks for agricultural machines; and (3) assess water flow accumulation and susceptibility to soil loss of the corresponding pattern. The methods were implemented in open source software and applied on three case studies concerning sugarcane production in the São Paulo region in Brazil. The results suggest that soil loss could be reduced over 50% by inserting one single change in the cropping pattern while reductions up to 75% could be obtained by the model when compared to a human-suggested coverage pattern.

Keywords: Path planning; Soil loss; Runoff; Controlled traffic farming; Machine efficiency; GIS

3.1 Introduction

3.1.1 Overview of machine path and crop row establishment on steep surfaces

Soil conservation often antagonizes with traffic of machinery on fields because of the increase in soil density created by the latter. In order to reduce the area subject to compaction, the practice to confine the work of a machine to predetermined paths, known as Controlled Traffic Farming (CTF), is becoming an increasing trend in agricultural fields. This is being enabled by the availability of guidance systems, which are capable of steering a machine along predefined tracks with high accuracy and without human intervention. State of the art technology allows pre-planned paths to be inserted in the machine's guidance system prior to performing field operations.

CTF has its benefits already studied in reduction of compacted area and yield increase (HAMZA; ANDERSON, 2005; TULLBERG et al., 2007). However, intense repeated traffic on the same tracks reduces water infiltration and leads to the formation of depressions along these (LI et al., 2007). This promotes runoff and accumulation of water in certain spots, which are potentially dangerous in steep terrains. Liu et al. (2013) studied directional effects of ridging

and furrows and specifically assessed ridges being damaged by accumulated water on steep slopes. The authors pointed to the necessity of accurate contouring or increased ridge height.

The practice of contouring, i.e., performing field operations perpendicular to slope direction, significantly reduces water runoff. Carvalho et al. (2008) found that contouring reduced soil loss owing to water erosion by 68.7 % compared to crop rows established in the direction of slope. It was also found that the pattern of crop establishment had a higher conservation effect than the type of coverage. Contour lines on steep terrains are rarely parallel. Figure 3.1 shows an image of a terrain crossed by a number of dirt ridges along contours (terraces for water infiltration) to hold water flow. The non-parallel shapes of sub-fields between the ridges, aggravated by the fact that these are typically not crossed by most machines undermines the efficiency of mechanized operations.

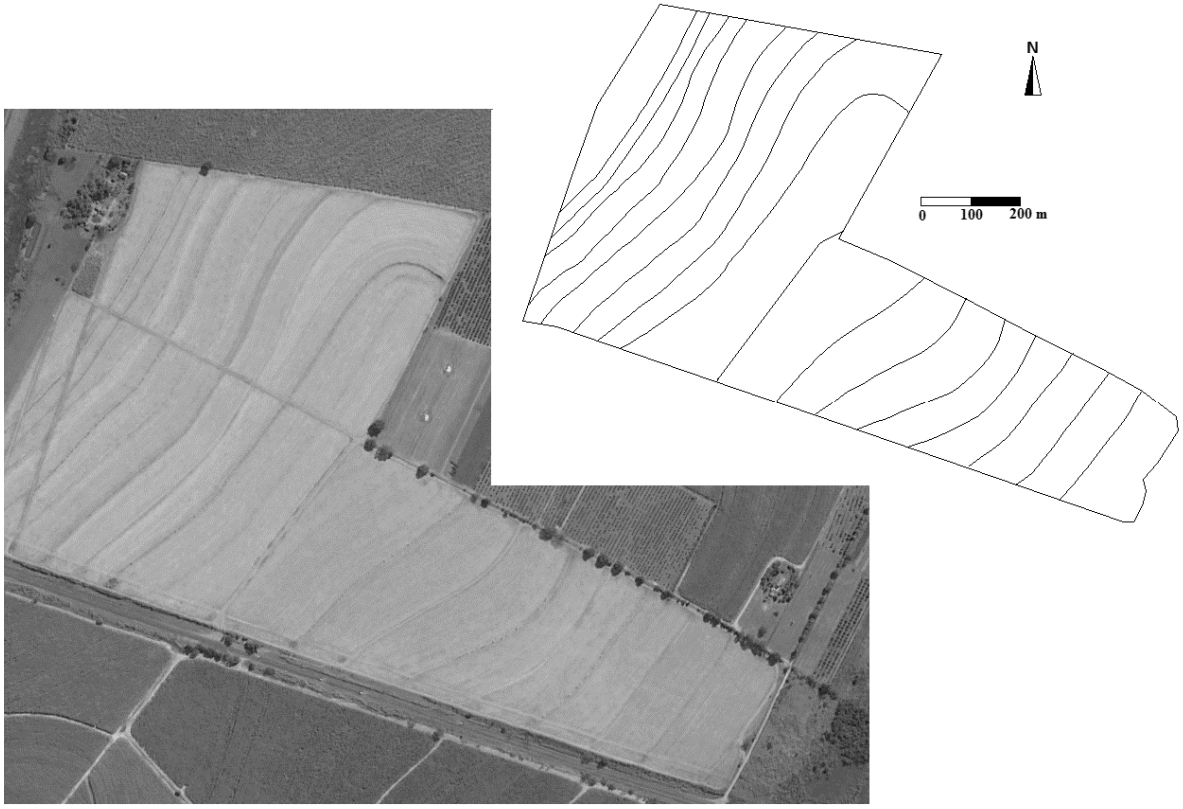

Figure 3.1 - Field with terraces at elevation contours (see inset)

Rolling arable areas in tropical countries show an intense susceptibility to erosion, owing to frequent occurrence of intense precipitation events and widely spread weathered soils. In Brazil, it is estimated that 600 million Mg of soil are lost by water erosion every year (GRIEBELLER et al., 2000). Therefore, a common procedure followed by land owners was to establish systematic sequences of terraces on terrain contours (like in Figure 3.1). This practice became, for some decades, a traditional guide for soil conservation towards water erosion.

However, in the past two decades, this rule has been defied by two trends: (1) adoption of conservation agriculture by eliminating scorching and tillage, which became a replacement technique for soil conservation (SOUZA et al., 2005); and (2) an increase of mechanized operations (particularly in sugarcane) for which more regular field shapes are required to increase machine efficiency (BENEDINI; CONDE, 2008).

Machine patterns considered in this work are parallel, which leads to a perfect coverage in rectangular fields of proper dimensions. However, in fields with irregular boundaries, short rows will be inserted along edges. The consequence of such practice is an increased number of manoeuvres and higher complexity of these. Spekken et al. (2015) showed that attempting to achieve full machine coverage by inserting short rows in a sugarcane crop can compromise its revenue.

Farmers prefer a single set of parallel machine tracks covering a surface because changing the direction of coverage patterns requires lanes between sub-fields to allow turning of machines (Figure 3.2). These lanes must have enough width for manoeuvring and occupy an area that could otherwise be used for crop production. The absence of such lanes would lead to unavoidable overrunning of standing crops.

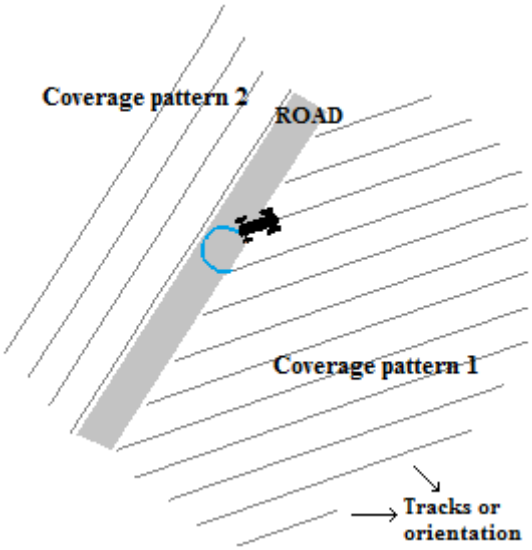

Figure 3.2 - Road/space required for machine manoeuvres between two working patterns

Recently, terraces have been partly (at times completely) abolished in many growing areas, with re-orientation of row-crop patterns (GUIMARÃES, 2004). In the process of such work, decision makers choose either a conservative approach, by still keeping potential unnecessary terraces dividing their fields; or a risky approach which eliminates most (or all)

terraces and relying on the fact that the newly intuitively drawn patterns will suffice to prevent substantial soil losses.

3.1.2 Computer path planning and soil erosion

The increased availability of guidance systems pushed the development of path planning. Path planning attempts to optimize tracks in fields in terms of avoiding overlap of machine coverage (PALMER et al., 2003; DE BRUIN et al. 2009); reducing manoeuvring time (JIN; TANG, 2010; SPEKKEN; DE BRUIN, 2013); minimizing soil compaction (BOCHTIS et al., 2012); and combined cost aspects (BOCHTIS et al., 2010). Few studies have assessed the impact of machine and row patterns in rolling landscapes on soil erosion.

Calculation procedures have been developed to obtain the dimension of terraces and spacing between them by accounting for soil and surface parameters (LOMBARDI-NETO et al., 1994). The calculations have been embodied in software for geo-spatial allocation of terraces (DA CUNHA et al., 2011); however, such tools are strictly dedicated to soil conservation practices while they disregard consequences for the efficiency of machines.

Recent developments on spatial tools embodying machine efficiency with soil conservation were done by Jin and Tang (2011), who proposed a method for optimizing machine paths on irregular surfaces. Despite its advances in computing the practices of contouring, the study lacks a method that considers water flow along its preferred way: along the track; the method creates steerable machine paths along curves, however it does so under the cost of leaving uncropped areas when narrow turns compromise the steering; suggested scenarios from the model demand many change in machine patterns, which is an user undesirable option. Finally, the model is incapable of detecting spatial variability in soil loss, water flow and water accumulation.

Perfect contouring is incompatible with full parallel coverage of fields. Nonetheless there exists a reference curve in a field that minimizes soil erosion. This work proposes a new approach for path planning that aims to reduce soil loss by assessing and visualizing cumulative water flow along tracks, which is dependent on geographical data of the field’s boundary and surface altimetry.

3.2 Methods

Crop rows are always established in line with the driving direction of planting machines, in row crops, planting patterns are important for erosion control (CARVALHO et al., 2008).

A sequence of steps is proposed to find an optimized track reference to be used as pattern in a (sub-) field. These are shown in the flowchart of Figure 3.3, which represents the conceptual model for path optimization on rolling land.

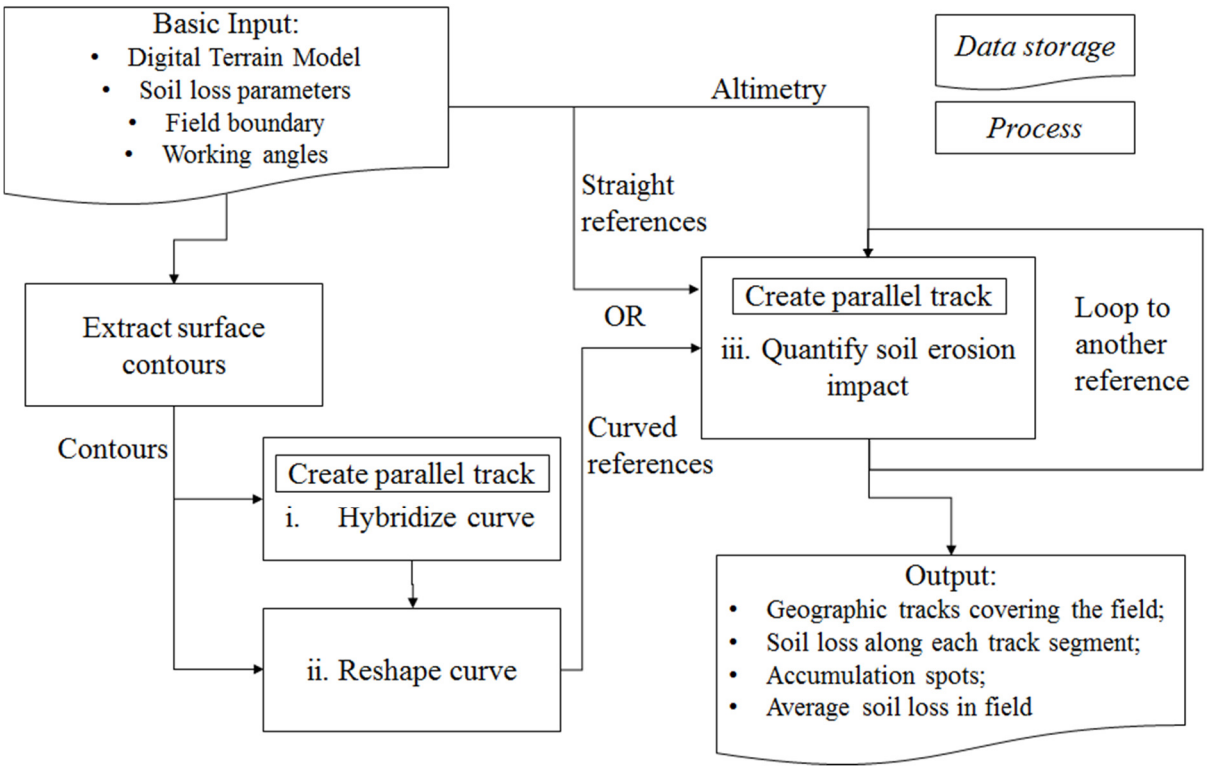

Figure 3.3 - Conceptual model of the planning procedure: data flow and processes

Given their multiple options of changes in direction, curved patterns have an infinite number of spatial configurations to be explored. To narrow down the options, contour lines are the most suitable geographical resource to find a minimized soil loss pattern. The process to extract surface contours is a known procedure within geo-information tools and carried to extract a basic inputs for curved references.

A generic process-tool identified in the diagram as “Create parallel track” is used within two of the main processes of the algorithm. Three of the processes in the conceptual model propose new or modified methods for path planning in irregular terrains (identified by numbering):

i. Hybridize curved lines, is an interactive step method creating a line in the exact middle of two existing contours. This is an optional step of the method.

ii. Reshape curve to create a suitable reference to be replicated in a set of steerable machine tracks.
iii. Quantify soil erosion using the Revised Universal Soil Loss Equation (RUSLE; RENARD, 1997).

Detailed descriptions of the methods are provided in the following sections.

3.2.1 Input data

3.2.1.1 Basic input

The Digital Terrain Model (DTM) is a grid of uniform cells each containing a value of elevation within the geographical limits of the field being studied. The DTM is used for retrieving contour lines and slope.

The field boundary is given by a 2D vector-polygon while, crop rows, machine paths, terraces are 2D vector polylines. All data are provided to the model in metric coordinates.

Polylines are vertices connected by segments, the term “track” is understood by the model as a polyline.

3.2.1.2 Digital terrain model and erosion parameters

Similar to Jin and Tang (2011) this work employs the RUSLE for assessing soil loss by water erosion (Equation 3.1):

$$A = R * K * LS * C * P \tag{3.1}$$

Where:

A is the estimated average soil loss (Mg ha^{-1} $year^{-1}$);

R is the rainfall-runoff erosivity factor;

K is the soil erodibility factor;

LS is the combination of the slope length and steepness factor;

C is the cover-management factor;

P is the support practice factor.

The factors R, K and C were considered constant representing an agricultural field with a uniform soil and rainfall regime that is covered by a single crop. The calculation of soil loss

from a certain track pattern is influenced by orientation with respect to the slope direction and is expressed in two RUSLE factors: the support practice factor (*P*) and the slope length (*LS*).

The support practice factor is based on the establishment of barriers in contours towards slope holding the water flow. It is dependent on the size of the barrier, which is considered fixed for a soil disturbance operation, and the deviation it has from a perfect contour (off-grade contouring). The latter effect is calculated as in Equation 3.2.

$$P_g = P_o + (1 - P_o)\sqrt{Sf/_{Sl}} \tag{3.2}$$

Where:
Pg is the *P* factor of off-grade contouring;
Po is the *P* factor for on-grade contouring;
Sf is the grade along the furrow (path) direction;
Sl is the local steepness of the land.

Erosion along furrows (tillage furrows or strip tilled rows) can be retrieved by calculating the factor *LS* parallel to the track orientation instead of the slope. For such, the *P* factor will be considered fixed (which for an open plough ditch would equal to an open bare furrow) equal to 1.

The Rainfall factor (*R*) was calculated by the method proposed by Lombardi-Neto and Moldenhauer (1992):

$$R = 68{,}73 * (p^2 / P)^{0{,}841} \tag{3.3}$$

Where:
p is the average monthly precipitation (mm);
P is the average annual precipitation (mm).

The soil factor (*K*) was calculated after Lombardi-Neto & Bertoni (1975). The authors base the erodibility on the soil particle fractions in the Horizon A of the soil (0.3m of depth):

$$K = \frac{\%\ Sand + \%\ Silt}{\%\ Clay * 100} \tag{3.4}$$

3.2.2 Processing steps

3.2.2.1 Creating parallel tracks

A straight track was defined as a working angle (direction) resulting in a straight line limited by the field boundary; its erosion impact calculated without prior modification in its shape (as shown in the flowchart in Figure 3.3). As an arbitrary rule, the model creates the first base straight track from the first vertex composing the polygon boundary of the field, it is considered that shifting it in small distances sideways will have no significant influence in the soil loss by water in the final track coverage.

Obtaining parallel tracks by offsetting a reference is more complex for curved references than for straight lines, because curves change shape when parallel offsets are created (see Figure 3.4a). In applied path planning, Oksanen and Visala (2009) made use of the angular bisector method (AICHHOLZER et al., 1996) to offset curved paths, yet still keeping the sharp edges along the tracks (Figure 3.4a). A modified approach is here used employing bisectors between angles in concave vertices while creating a composite of equidistant points in form of arcs around convex vertices (Figure 3.4b). This results in a curved track with a higher degree of smoothness along vertices (Figure 3.4c).

Figure 3.4 - Offsetting issues of the original angular bisector method (in 'a'); implementation of the modified approach (in 'b'); and the result of replicated tracks derived from the approach used (in 'c'). The blue ellipse and arrow show limitations of the offsetting procedures for the steerability of machines

In polygon offsetting, when tracks converge towards each other in concave corners (like indicated by the arrow in Figure 3.4c), a sharp turning angle results. This angle is not steerable by a machine, requiring changes in the original reference. This issue is elaborated and solved further in this manuscript.

3.2.2.2 Hybridize curved lines

In order to find track patterns that are capable to keep themselves in closer surface grade for the full area, a method is here proposed to merge shape properties of different curves in a hybrid curve.

Figure 3.5a shows a hybrid line (in red) crossing in the middle of two contours (in green). This created curve, for which the shape may not follow any contour, is capable be replicated on the field following its grade better than its seed contours (Figure 3.5b).

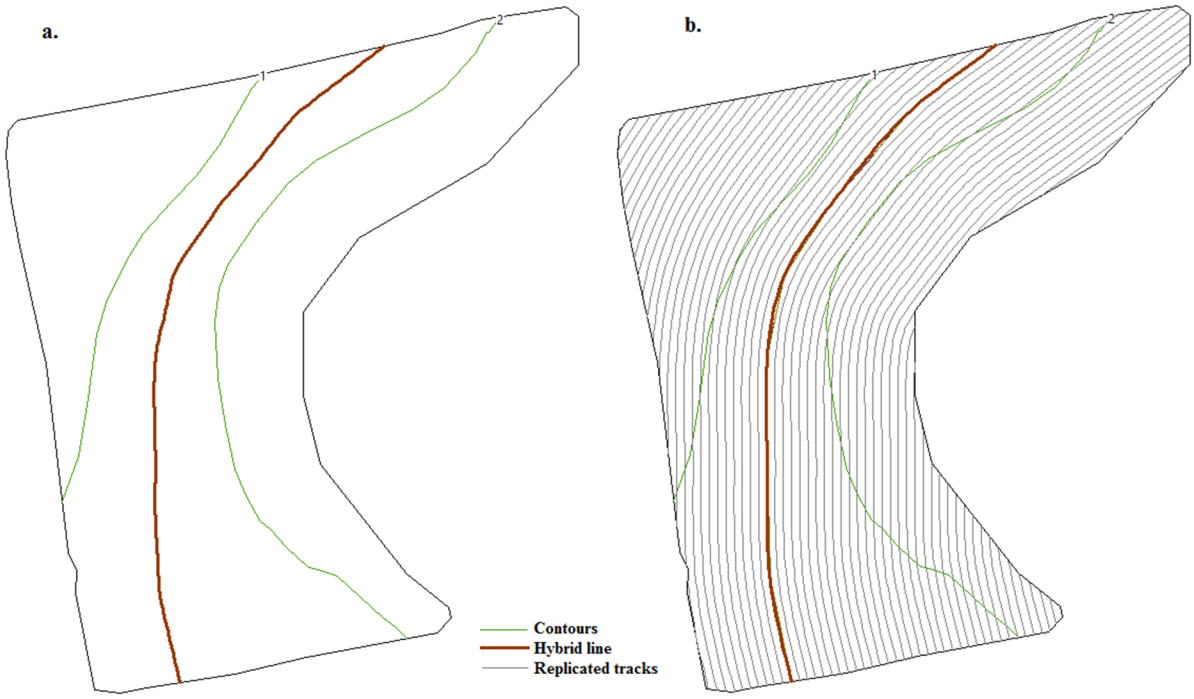

Figure 3.5 - Hybrid line obtained from two surface contours (in ‘a’) and replicated in parallel passes over the field (in ‘b’)

The embodied shapes of both origin contours in the hybrid curve suggests it to be an option for irregular surfaces, yet this is not a proven fact of its superiority. Hybrid lines are considered, in this work, an additional option for field coverage along with the contours.

Hybrid curves are constructed from the intersection points between tracks created in parallel to its references (Figure 3.6).

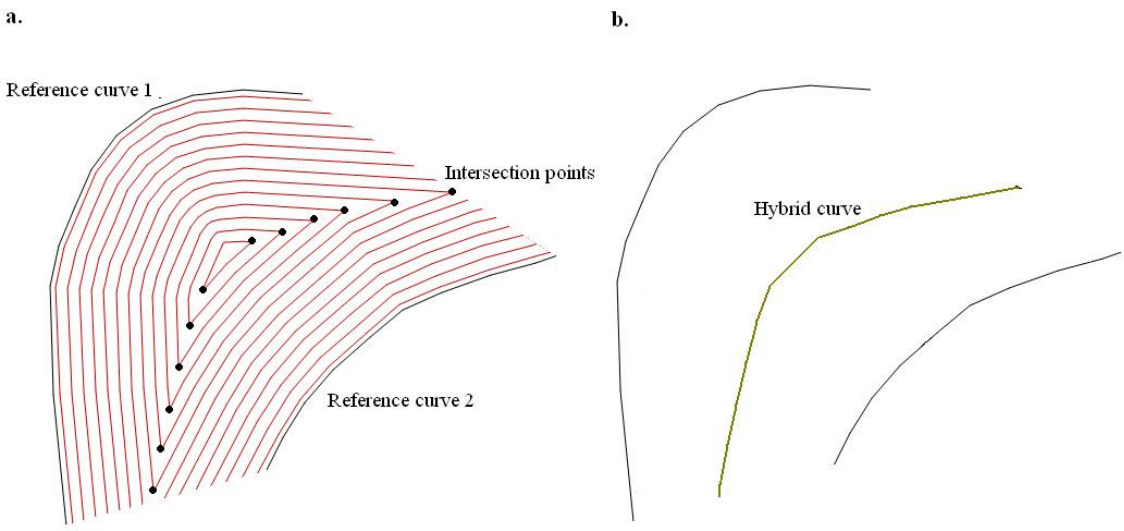

Figure 3.6 - In ‘a’, sequences of parallel tracks offset towards each other from the two original references, and intersection obtained from the encounter of these. In ‘b’ the resulted hybrid curve derived from linking the intersections found

A sequential hybridization for a larger group of reference lines allows an improved reference curve to be found for a whole field. This process is shown in Figure 3.7a where four contour lines (in green) are double hybridized into new curves indicated by the arrows, emerging in two new curves (in dark yellow) that are again hybridized into a final curve (in black). The coverage obtained by the final curve is shown in Figure 3.7b.

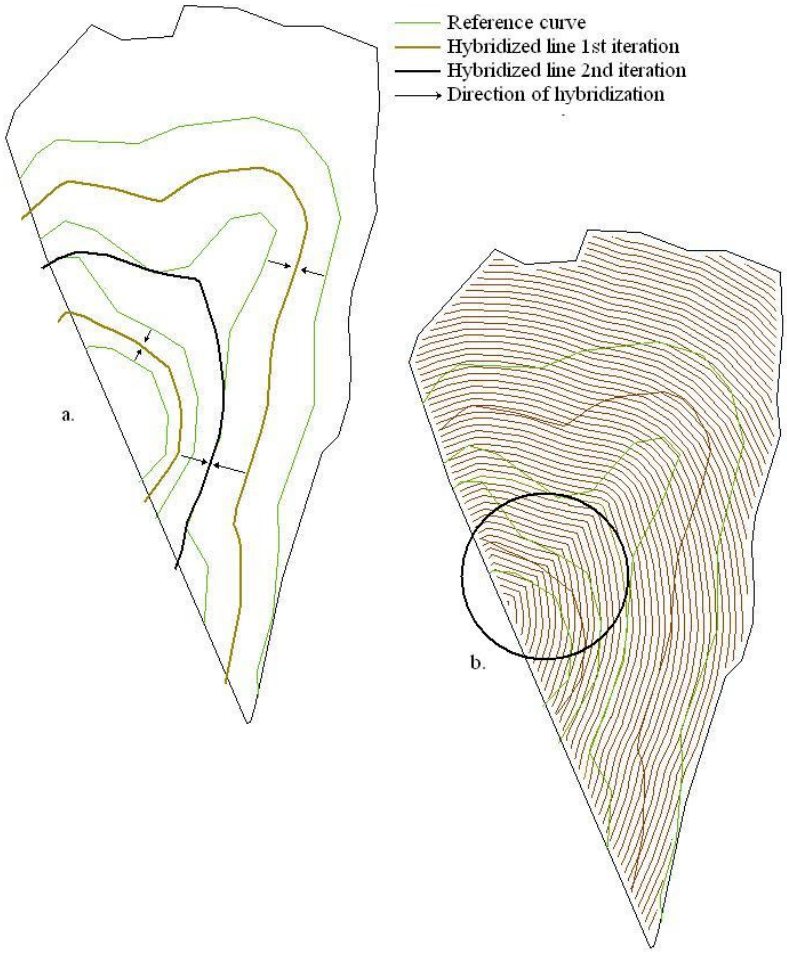

Figure 3.7 - Double hybridization of existing contour lines on a field into a single pattern for field coverage. In ‘a’ reference curves (green) are first hybridized following the arrows into dark yellow curves, which are again hybridized into a final curve (in thick black). In ‘b’ the latter curve is replicated in parallel passes over the field and the ellipse points a regions where steerability along tracks is still be compromised by rough turns

The hybridization process tends to smooth irregular curved shapes, although it does not guarantee to produce a steerable track. In Figure 3.7b, the ellipse indicates sharp turns that compromise steerability by machines.

3.2.2.3 Reshaping contour line in a steerable reference

Three issues are considered when using a certain line as a template for machine tracks: undulation, shape concavity and smoothness. Figure 3.8a shows an agricultural field with its contour lines where these issues are overcome in a sequence of steps where each.

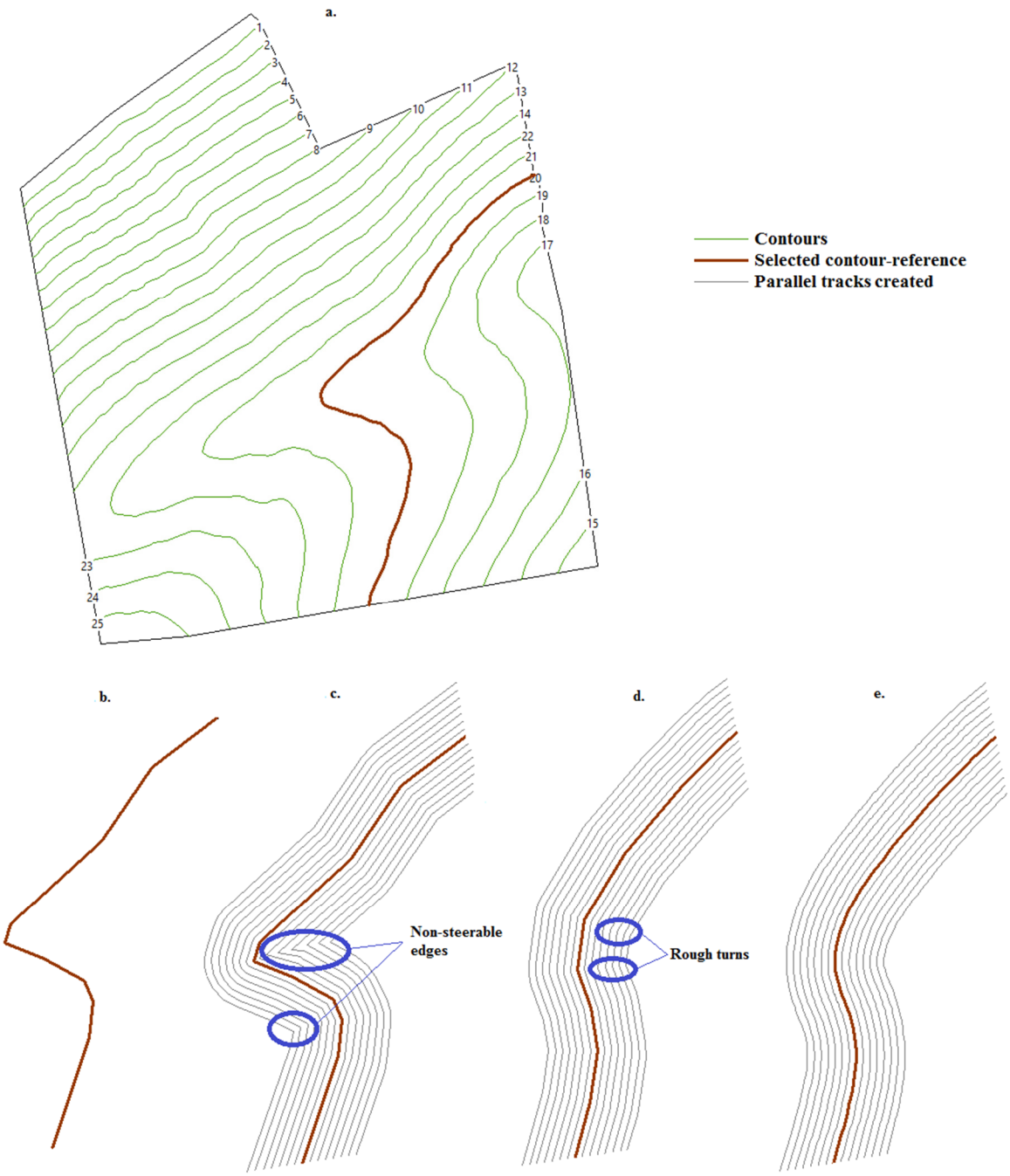

Figure 3.8 - Steps for achieving steerability applied to a contour line as extracted from the DTM (in 'a'). In 'b', 'c', 'd' and 'e' it is shown sequentially the steps applied for transforming the respective contour into a steerable machine path. For each step followed, it is pointed the remaining issue to be solved

Undulation: Digital Terrain Models, usually derived from interpolation of elevation points, may contain a small degree of variation. Contours extracted from such data display some tremor in their shape, making them unsuitable references for machine paths. Figure 3.8a shows a field from which contour lines (in green) were derived from the Data Terrain Model enhancing one specific line (in red). It is possible to observe the tremor in the line which undergoes a process of vertices simplification using Ramer-Douglas-Peucker algorithm (DOUGLAS; PEUCKER, 1973), resulting in the simplified line seen in Figure 3.8b.

Shape concavity: In Figure 3.8c, continuous parallel passes on a concave face of a track converge into each other narrowing the angle in between them (indicated by the ellipses). This issue, also indicated previously (Figure 3.4c), is solved by averaging the coordinates of the segments composing a reference track. This process is repeated until the steerable angle between all segments is lower than a threshold (like used by OKSANEN; VISALA, 2009). In Figure 3.8d, this process removed narrow edges, yet still leaving some rough turns (blue ellipses) because of the limited number of edges to compose a curved shape.

Smoothness: Most agricultural machines steers into a desired direction following an arc shape. This makes most agricultural machines incapable of immediate turns on vertices (shown in Figure 3.8d), requiring a gradual steering along curves. To overcome this, new vertices are created by parametric cubic spline interpolation across the existing ones resulting in a final steerable track (Figure 3.8e). This approach was used by Spekken & DeBruin (2010) who employed cubic splines to reduce roughness of machine paths while evaluating the coverage accuracy of the machine.

In the approach of Jin and Tang (2011), B-splines were used for interpolation of a whole new line in between (and not across) the existing edges, simultaneously solving the issues of vibration and smoothness. However, the authors did not reshape the curve to reduce the concavity, proposing to skip narrow corner edges (not possible to be steered by the machine) and adding the loss of uncovered area to the final path costs.

Depending on the source data, contours may not need reshaping. In traditional procedures, when terraces are established in fields by topographic equipment, the curves are already adjusted to fit into machine and operation constraints. The use of the terrace data as a reference may not require any reshaping procedure.

3.2.2.4 Soil erosion impact

Soil Loss from Track Pattern Coverage

In our approach, sequences of segments with the same direction of water flow are extracted. For each sequence a cumulative soil loss is calculated using the methods proposed by Foster and Wischmeier (1974) and Wischmeier and Smith (1978). To account for sequences of segments (identified by in following equations by "i') with different lengths and slope steepness, the approach of Renard et al. (1997) is followed.

First, the slope length factor (L) is calculated for each segment *i* of a sequence composed by *n* segments (L_i, $i \leq n$):

$$L_i = \left(\frac{i}{22.13} \right)^m \tag{3.5}$$

Where the variable *m* is determined by an evaluation of the steepness of the slope (*StSl,* mm^{-1}) for the segment length, given by: $m = 10*StSl$, with *m* value adjusted within lower and upper limits to 0.3 a 0.5.

The slope steepness factor (S_i) is calculated by:

$$S_i = 65.41 \frac{StSl_i^{\,2}}{1 + StSl_i^{\,2}} + 4.56 \frac{StSl_i}{\sqrt{1 + StSl_i^{\,2}}} + 0.065 \tag{3.6}$$

The *LS* factor at the end of the segment is calculated by:

$$LS_i = L_i S_i P_i \tag{3.7}$$

Where *Pi* is a weighting factor calculated by:

$$P_i = \frac{i^{m+1} - (i-1)^{m+1}}{i^{m+1}} \tag{3.8}$$

Finally, each segment that composes the track has its own *LS* factor calculated and multiplied by the other RUSLE factors Eq. (3.1) obtaining A_i (Mg ha^{-1} $year^{-1}$).

The final estimate of average soil loss over all the tracks on the field is calculated by the weighted average of all *Ai* values by their length (L_i):

$$ASSL = \frac{\sum_{j=1}^{nft} \sum_{i=1}^{nts} A_i * L_i}{\sum_{j=1}^{nft} \sum_{i=1}^{nts} L_i} \quad (3.9)$$

Where *ASSL* is the average surface soil loss along tracks for a field; *nft* is the number of tracks covering the field; *j* is the index of a track; *nts* is the number of segments that compose a track; and *i* is index of a segment.

Identifying Critical Spots of Flow Accumulation within a Track

Under certain rainfall events, the water will accumulate in some regions, with potential risk for overflow and water running downhill across tracks. This process characterizes the formation of a gully.

Such accumulation of water occurs when: water flows along a track converging towards a single location (as in Figure 3.9a); or water flows on the same direction along a track but a significant difference in steepness along it makes one location to receive more water than it can carry on (as in Figure 3.9b).

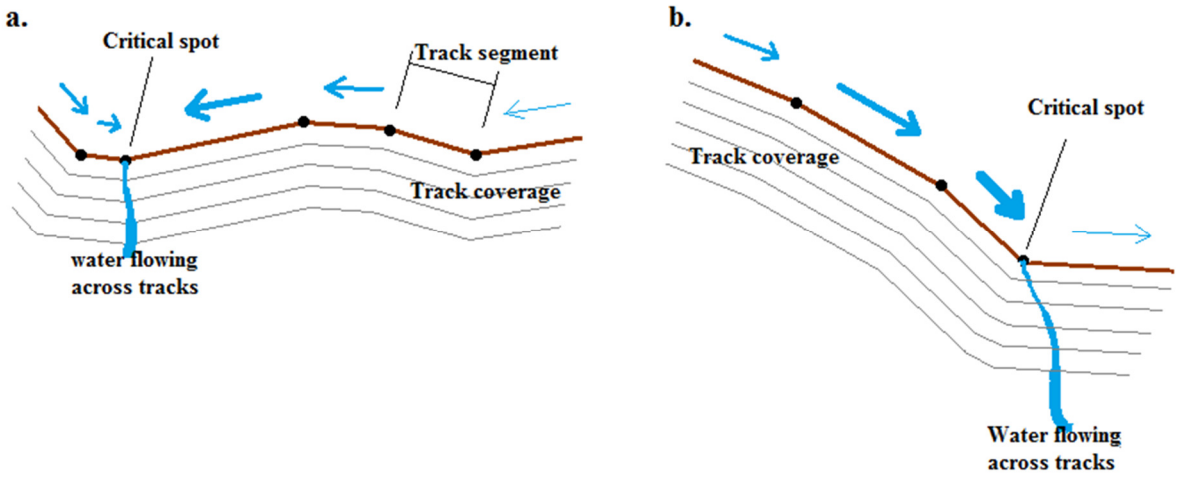

Figure 3.9 - Two sets of tracks (in grey) parallel to their references (in brown). Intensity of water runoff along the references is proportional to the size of the blue arrows. Critical spots are identified when water accumulates and overflows across tracks

While the altimetry data can identify the water flow and the basal position along the tracks, the intensity of water runoff is here considered to be proportional to the calculated soil loss at the edge of the segment (A_i). Thus, an accumulation parameter is found accounting *Ai* and the facet condition of neighbouring segments as shown Figure 3.9, where: in "a" the accumulation in the critical spot is proportional to the sum of the soil losses of the neighbouring

segments; and in “b” the accumulation in the critical spot is proportional to the difference between the soil loss of the neighbouring segments.

When the sum or difference of A_i with A_{i+1} is higher than a defined threshold, the vertex in between the segments is defined as a critical flow accumulation spot (*CFAS*). The identification of these spots offers no quantitative basis, however, identifying them spatially provides a guide of the potential risk spots for the decision makers.

3.2.3 Finding an optimized track reference

We now turn to the problem of finding an optimized pattern on sloping land.

Simulation of Patterns

Searching for the least erosive coverage pattern over an irregular surface is here done by simulating track options (working directions and/or curves). A simulation consists of replicating a reference in parallel tracks until full coverage of a field (or sub-field) and computing: (1) average Surface Soil Loss (*ASSL*); (2) number of critical flow accumulation spots (*CFAS*) and (3) the number of tracks required for field coverage (as a raw machine manoeuvring parameter).

The model loops this procedure for either:

1. Straight tracks, testing 180 angles spaced by 1 degree angle; or
2. Curved lines, which are contour lines or hybrid lines loaded along with the input data. The procedure is applied to all existing curved options.

Each loop adds the calculated impacts to a list from which the least erosive reference can be identified.

The possibilities for coverage of field is not only limited to a number of working directions and/or a set of curved lines. If a divisor is inserted in the field (usually upon a contour), to change track orientation to increase their on-grade pattern, it results in two sub-fields capable to be covered by a number of contour lines within them. For a field crossed by n contour lines ($n > 1$), in which each of these is a possible field divisor, the number of options is a permutation of n.

For the hybridization options and insertion of divisor, no solution was implemented to exhaustively try all the possibilities or heuristically solve the full array of combinations in this study.

3.2.4 Model implementation

The methods here proposed were implemented using the object-oriented programming platform Lazarus 1.2© (1993-2013 Lazarus and Free Pascal).

Vector data like fields and curved lines (contour lines, terraces, or even free-hand drawn lines) are loaded as text files containing the metric coordinates in the form of 2D maps and stored in the form of an array. Raster data are loaded as an accompanying file in an ASCII form also in metric coordinates and stored in a double-numeric-type matrix.

The methodology proposed was implemented in two separate applications. The first elaborates reference curves into steerable machine paths, creates hybrid lines and determines field divisors. The output of this first algorithm is fed into the second where the DTM is loaded and soil erosion impacts are calculated and spatialized. The first algorithm is unnecessary when only straight references apply.

3.3 Case studies and results

The application developed to evaluate the soil loss impact of created references is shown in Figure 3.10. The ellipses point to the graphic outputs that orient the decision making process for minimizing the soil loss.

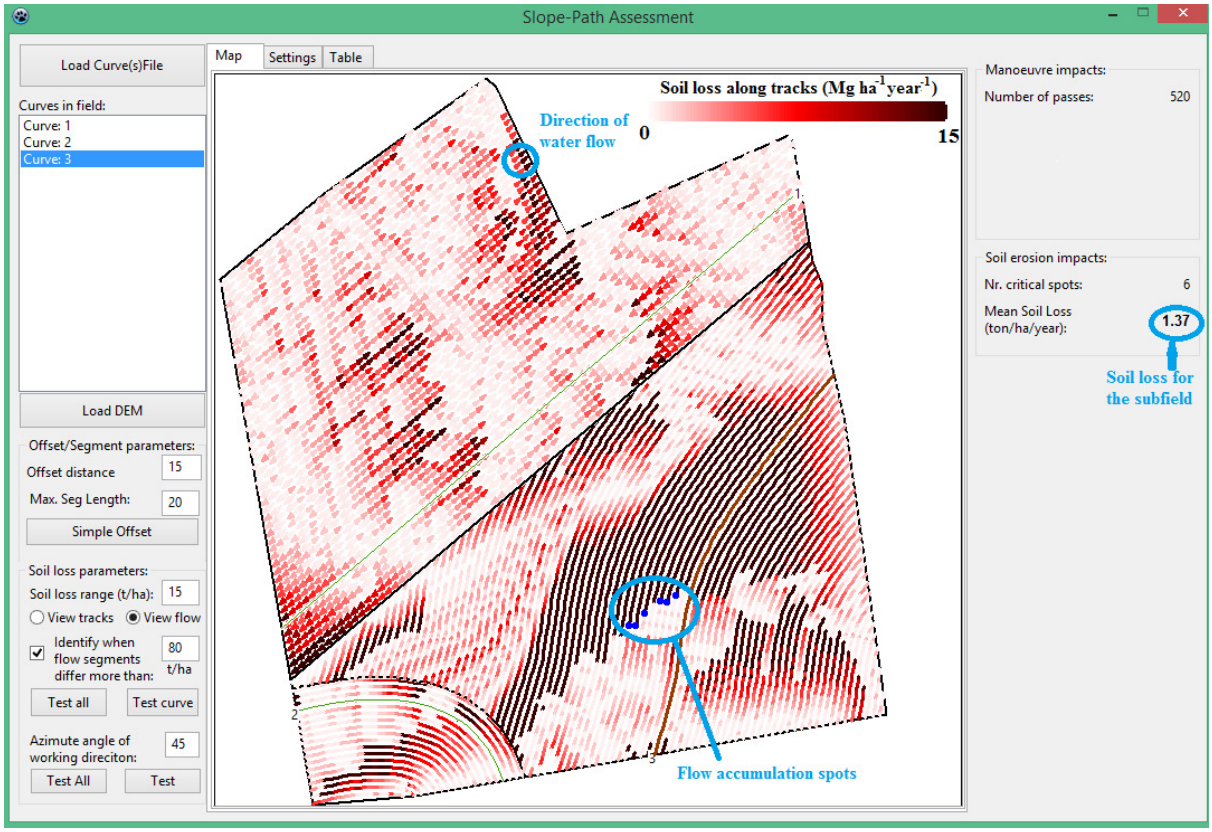

Figure 3.10 - View of the application-algorithm developed for assessment of soil erosion from tracks

In Figure 3.10, tracks cover the field in a specific offset distance with its soil loss identified by red intensity (darker red meaning more soil loss), along with a mean retrieved for a corresponding sub-field. Blue dots identify the flow accumulation spots, which are usually located in a row-track with a cumulative sequence of soil loss. The tracks can be visualized as a line or as a sequence of arrows pointing to the estimated flow of water along the track.

3.3.1 Path-planning in sugarcane

The methods presented here are applicable to row crops in general. However, the case studies concern sugarcane (*Saccharum spp.*). Belardo et al. (2015) compiles information in the subject for the scope of mechanization and path planning in the crop. Sugarcane is widely grown in tropical and subtropical regions of Brazil over rolling landscapes. The crop covers 9 million hectares in the country (CONAB, 2014) and its production system has some specific soil, machine and operation properties:

- Intense mobilization of soil along the rows when the crop is being planted, leaving an open bare furrow (Figure 3.11);

- High demand for driving accuracy in between the rows because driving errors lead to damages on the plant's ratoon which has to re-grow and be harvested up to 5 times until the crop is uprooted and replanted (NORRIS et al., 2000; DE PAULA; MOLIN, 2013);
- Huge biomass being harvested row-by-row (in a common width of 1.5 m) leading to an intense and costly mechanization and logistic system, as well as a large fraction of the area under machine traffic;
- Small coverage capacity of machines demanding a large window of continuous harvesting of 24 hours per day and 9 months per year.

The need for steering accuracy and night-working shifts made the crop a leader in the adoption of CTF and automatic pilot systems in Brazil (39% of harvesters, according to SILVA et al., 2011).

The availability of guidance systems and need for increasing the machine efficiency created a trend within the production system, in which large-scale predefined machine tracks are inserted in the navigation systems for the crop implantation and harvest. The elaboration of the track patterns, done in computer aided design (CAD) programs, became a practice which is colloquially known as "sistematização" (systematizing). This demand for pre-planned tracks resulted in dedicated software tools developed in CAD concept, which speeds the computer replication of machine tracks on fields.

Despite the fact that such tools were effective in achieving higher machine efficiency, they are still based on human intuition neither capable to combine aspects of intense simulation of machine tracks (like in path planning) nor measuring the water erosion impact for different scenarios.

The sugarcane planting phase is the most critical moment of soil loss because of the high susceptibility of water flow along the rows (Figure 3.11). This is aggravated by the fact that most of the Brazilian sugarcane production is located on steep areas with occurrence of intense tropical rain events.

Figure 3.11 - Recently emerged sugarcane on steep slope, within furrows created by the planting operation

The municipality of Pradópolis in São Paulo state (Latitude 21º 21'and Longitude 48º 04') has the majority of its land dedicated to sugarcane production. In this region, three representative case studies (Figure 3.12) were selected demonstrate the method.

The average annual rainfall is 1300 mm. The month with the highest rainfall (January, 250 mm of precipitation) was selected as a reference for soil loss estimation. The calculated RUSLE *R* factor is 1785. The soil of the region can be classified as Ferrasol (INTERNATIONAL SOIL REFERENCE AND INFORMATION CENTRE, 1998), with a soil particle classification as sandy-clay with composition in the A horizon of 45-10-45 (clay-silt-sand). The RUSLE *K* factor was estimated as 0.012. Based on Machado et al. (1982) a coverage factor C of 0.307 was used. A standard value for the conservation practice *P* is 1 (bare furrow along recently planted rows).

Figure 3.12 - Spatial identification and surface arrangement of the three case study fields

Altimetry data was available from logged RTK (Real Time Kinematic) measurements, retrieved from the auto-guidance system during the planting operation. These data were interpolated to a 5 m regular-grid by ordinary kriging using VESPER 1.6 (MINASNY et al., 2006). A global generalized cauchy variogram presented the best model fit with a maximum root mean square error of 0.01361 for all three cases. The obtained DTM was loaded in the software Quantum GIS 2.4.0 Chugiak (QUANTUM GIS DEVELOPMENT TEAM, 2014) for extraction of the surface contours every 2 m of elevation apart. These are shown in Figure 3.12 (elevation of the field directly proportional to brightness) along with their respective contour lines.

The area and the slope were retrieved and are shown in Table 3.1. Over 60% of the surface in all case studies present slope higher than 0.04 m m^{-1}.

Table 3.1 - Area and average surface properties of the case study fields

	Cartographic area (ha)	Average surface slope (m m^{-1})
Field 1	82.99	0.0436
Field 2	142.73	0.0512
Field 3	143.27	0.0452

The field coverage simulations done for all the case studies create parallel tracks in offsets of 9 m (equivalent to 6 sugarcane rows of 1.5 m). The threshold value used for identifying the critical flow accumulation spots (*CFAS*) was set in 80 Mg ha^{-1} $year^{-1}$.

3.3.2 Optimal coverage in a single pattern

In the first case study, simulations were carried by the algorithm to find the minimum soil loss by water for one single pattern of coverage for the whole field. Figure 3.13a displays the field and its respective contour lines; for which three methods were compared: 1) finding the least erosive among the existing contour line options (Figure 3.13b); 2) hybridizing contour lines (Figure 3.13c); and 3) selecting the optimal out of all straight patterns possible (Figure 3.13d). Quantitative outputs are presented in Table 3.2.

From all contour lines existing in the field, only those whose length cross the main field were selected as coverage options (twelve selected contour lines identified numerically in Figure 3.13a). These were reshaped using: vertices simplification for 5 m of deviation tolerance; reduction of concavity by averaging the vertices coordinates until a maximum steering angle of 5 degrees was obtained between them; and spline interpolation of 20 m between new vertices.

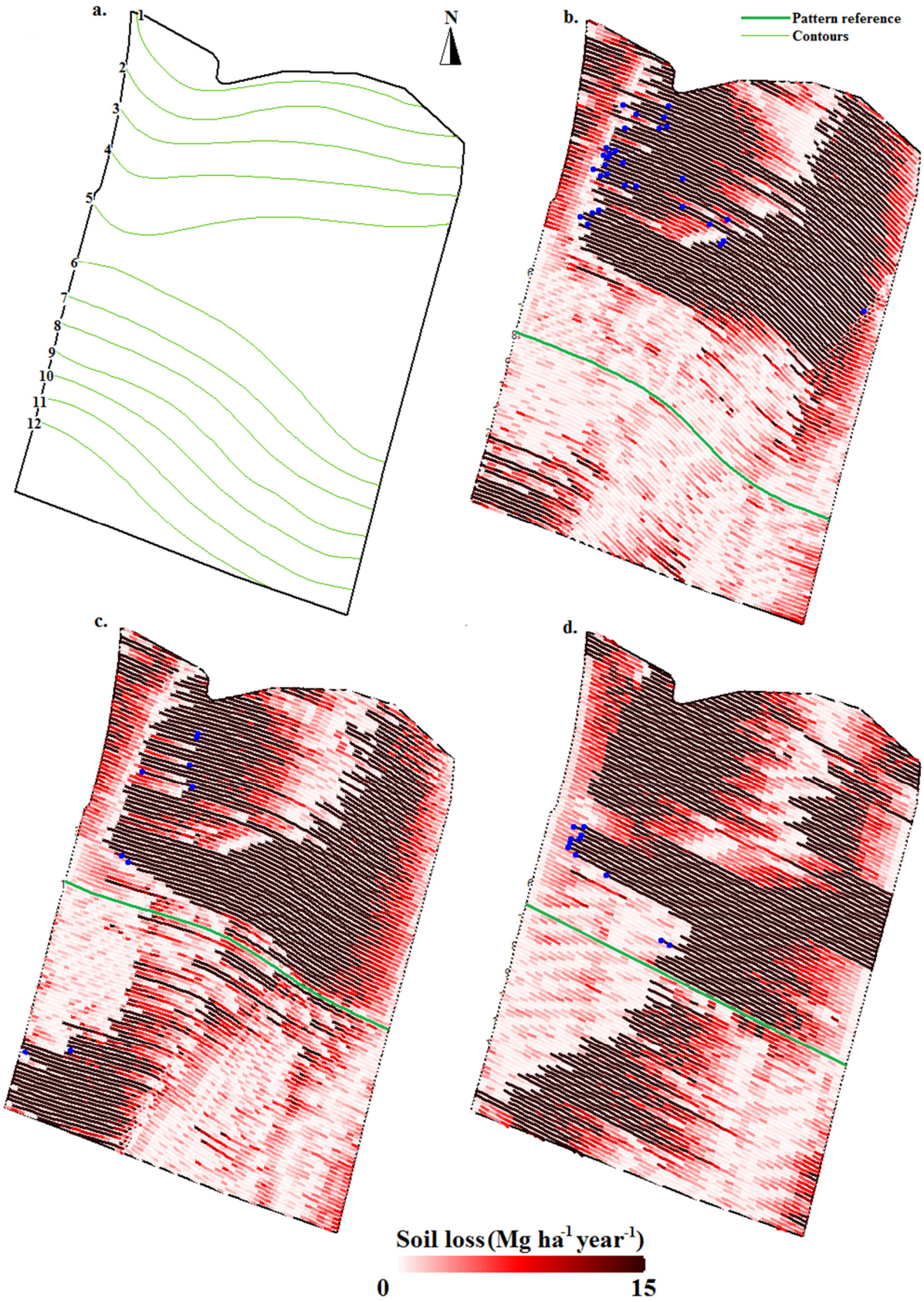

Figure 3.13 - Selected and reshaped contour lines for track reference (“a”) and the coverage results of three coverage patterns: “b” as the optimal contour line; “c” as the generated hybrid line; and “d” as the least erosive straight direction

Table 3.2 - Outputs of least erosive track pattern among simulations within the three methods of field coverage

	Average surface soil loss (Mg ha^{-1} $year^{-1}$)	Number of tracks for full field coverage
Contour line	18.28	138
Hybrid line	15.26	136
Straight pattern	15.9	136

3.3.2.1 Optimal contour line coverage

Simulations were carried out for each of the selected contour lines. The graph in Figure 3.14 shows quantitative differences found for surface soil loss between the contour line options, pointing contour line 8 as the least erosive option. Figure 3.13b shows the field coverage from this reference line (in green).

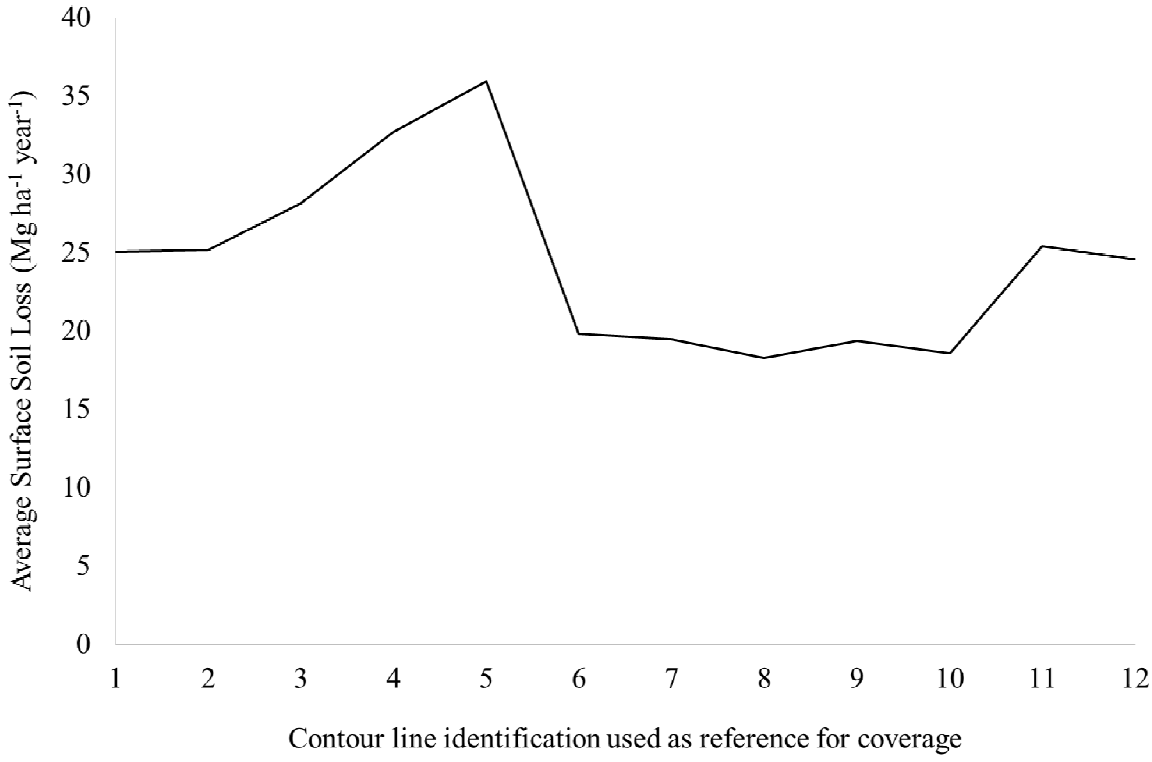

Figure 3.14 - Average surface soil loss for the existing contour line options of the case study

Regarding manoeuvring efficiency, a range of 135 to 143 of tracks were found among the options, counting 138 tracks for the excelling option. In case of the demand for a more

efficient path, contour line 9 presented the lowest track count (135) with relative low increase in erosive impact.

3.3.2.2 Hybrid contour lines

Some hand-picked contours were used for creating hybrid lines. Selection was done by first grouping similar line-shapes and selecting one of the references for hybridization from each group. Two groups were defined: i) lines from 1 to 5; and ii) lines from 6 to 12.

Hybrid combinations were tried, from which the best results were found from first combining any line from group “i” with any other line of group “ii” and the obtained line re-combined with the same line of group “ii”. Any outcomes of this procedure resulted in a less erosive reference than line 1 (shown in case study Figure 3.12b). Recursively hybridizing all the available lines led to an almost straight line with no better results than following the best contour or the best straight line.

Figure 3.13c shows a double hybrid line (in green) found by first crossing contour lines 4 and 8, and the resulting hybrid crossed again with line 8. The final solution found was less erosive than any of the contour lines or straight angles simulated. Regarding machine efficiency, this option had a track count of 136, which is also lower than that of the optimal contour line.

3.3.2.3 Optimal straight coverage pattern

A total of 180 straight pattern directions were tried, the least erosive option (117 degrees from the azimuth) is displayed on Figure 3.13d. Remarkably, this option is more suitable than any of the surface contour options tested, and reaches closer soil loss to the optimal hybrid option found.

Figure 3.15 - Surface soil loss and critical flow points for all straight directions of coverage pattern

The straight option found also presented a low track count of 136 similar to the least erosive solution. Further work can be carried to filter out some obvious unsuitable patterns (like track directions going downhill) in the processing of the model. Nevertheless, the compiled algorithm took less than 3 seconds to retrieve the list of impacts for all directions tried in this case study, thus time is not presenting to be an issue in this work.

The east-west orientation of the contours, showing some degree of parallelism, makes a hand-drawn design to keep tracks in grade not so challenging. Nevertheless, a CAD path designer suggested a contour line in the middle of the field as reference, deviating from the best contour line (as found by the model). Determining intuitively a straight pattern by drawing a straight line in the centre of lines 5 and 6 (108 degrees) would increase average yearly soil loss in 4 Mg ha^{-1} in comparison to the optimal direction (117 degrees), also doubling the number of critical flow accumulation spots.

3.3.3 Varying track orientations within a field

In some irregular terrains, forcing a single machine coverage pattern (curved or straight) on steep surface will likely lead to many tracks not being perpendicular to the slope, and

consequently to water erosion. In these cases, it might be suggestive to work the field in more than one arrangement (pattern divisors).

In Figure 3.16, case study 2 shows in “a” the contour lines, from which two lines were selected as options for field divisor (in blue). The criteria for the selection was: a line that represents a shape-change in the sequence of lines (line 12) and another that creates a regular field with the south border of the field (line 29). The field coverage by tracks with its potential soil loss intensity is given for: no field divisors, with one divisor (divisor 12) and two divisors (divisors 12 and 29) respectively by “b”, “c” and “d”. Within these, the reference contour line or straight pattern with lowest calculated soil loss is shown in a green line for each field.

Quantitative soil loss parameters are shown in Table 3.3 for the simulation of all existing contour lines and straight directions for the whole field. Except for straight patterns and some contour references, no critical flow accumulation spots were identified in this case study.

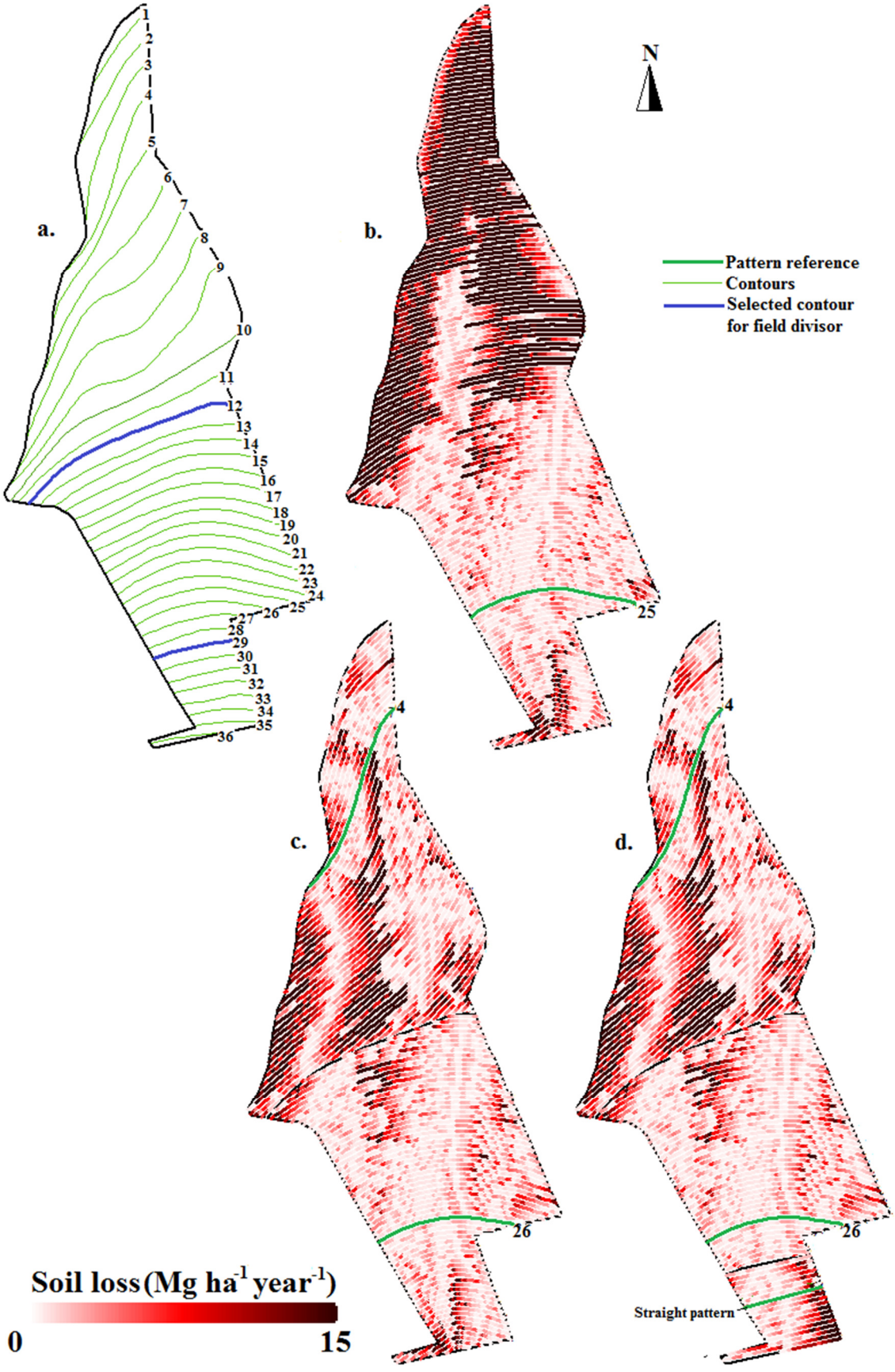

Figure 3.16 - Distribution of contour lines (in “a”) and selection of these as field divisors and least soil loss option (in “b”, “c” and “d”)

Table 3.3 - Soil loss and track count for the increased number of divisors for the case study

	Coverage pattern following contours				Straight Coverage Pattern	
	Average Soil Loss (Mg ha^{-1} year^{-1})			Track count (best contour)	Min. Average Soil Loss (Mg ha^{-1} year^{-1})	Track count
	Best contour(s)	Worse contour(s)	Average of contours			
No divisors	11.24	259.56	43.04	311	16.85	305
1 Divisor	4.45	28.27	9.57	265	11.06	293
2 Divisors	4.36	26.25	8.56	259	10.8	295

As expected, insertion of divisors reduced soil loss; the most significant decrease in soil loss occurred on the insertion of the first divisor while with the second, some minor additional benefit was obtained in soil conservation and efficiency (regarding track-count and more straight tracks in the sub-field).

The southern part of the field presents a boundary complexity (narrow corner), and the decrease in track-count occurred because such regions are more efficiently worked when different working patterns are used. Previous studies achieved higher efficiency by splitting fields in units to be worked in distinct patterns (JIN; TANG, 2006; OKSANEN; VISALA, 2009). Though in general, continuous addition of divisors based on contour lines tends to decrease field efficiency (as pointed previously in the introduction).

3.3.4 Intuitive vs. calculated path planning

A comparison was done between a human-drawn track design and the model optimized solution. This intuitive design was retrieved for case study three (from our data provider) and submitted to the model for its evaluation. Likewise, the model submitted the case study to a full search among all of its contours retrieving the best option. The intuitive-based and algorithm-based results are displayed in Figure 3.17.

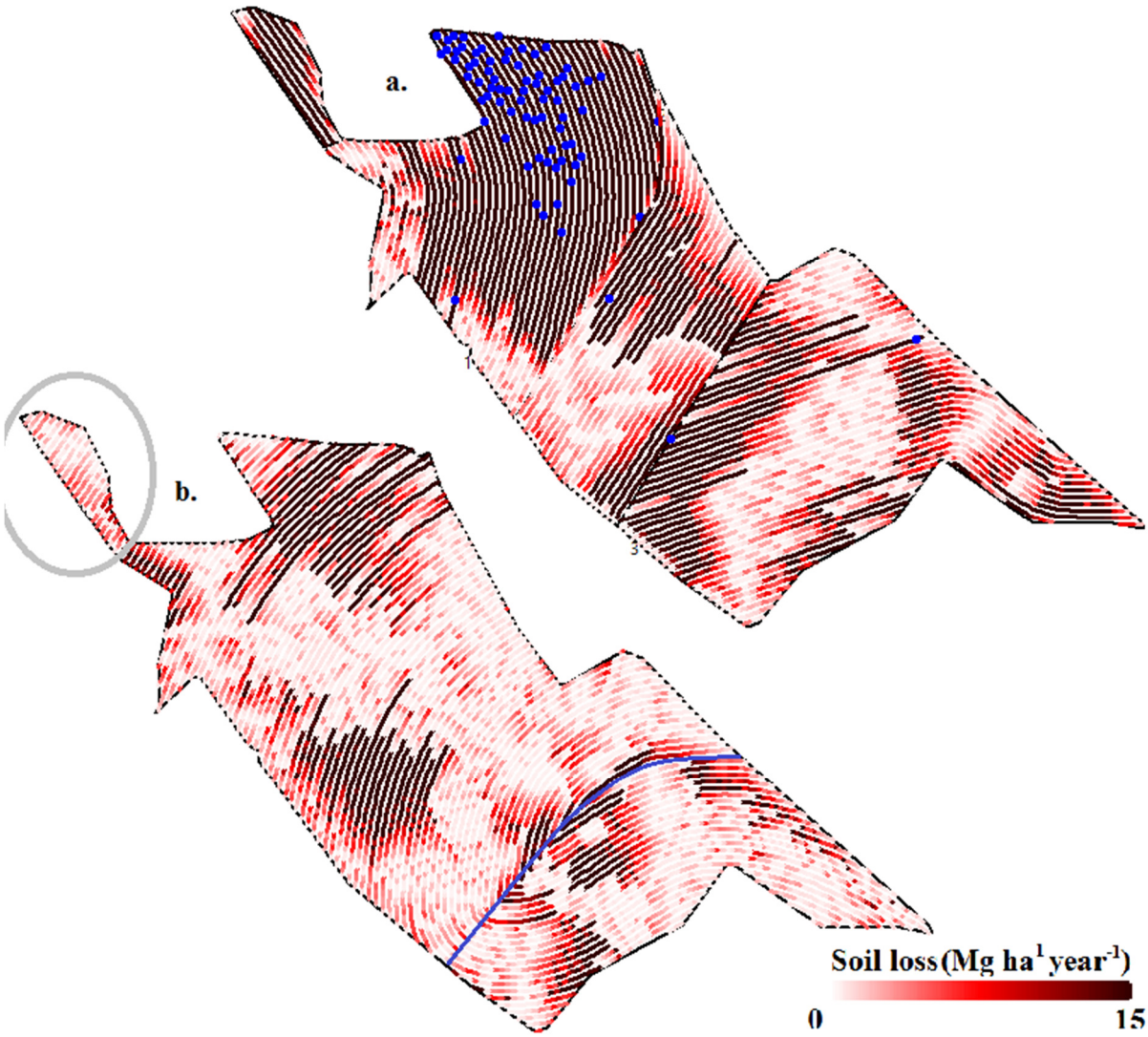

Figure 3.17 - Case study three in intuitive-base and algorithm-based coverage patterns given respectively by “a” and “b”

In Figure 3.17, in between the pattern changes in “a” three roads will be necessary. In “b” one road was hand-drawn (line in blue) along a sequence where the shape of tracks fold into themselves in a narrow angle which is impossible to be steered by a machine, demanding a road space for such.

A dense net of roads is necessary in sugarcane production given its intense logistics (crop harvests up to 100 Mg ha^{-1} of biomass); fields are thus subdivided in logistic units and for fire spreading prevention. Therefore, in the simulation of Figure 3.17b, additional roads will be necessary, yet if these are kept parallel to the tracks, it would result in long and reduced number of tracks (and manoeuvres). Besides, no manoeuvres are needed in roads parallel to the

tracks, allowing their width to be limited by the machine's width and not by their wide turning radius (like the example shown previously in Figure 3.2).

Regarding the soil erosion impacts, majority of the soil flow accumulation spots obtained for the intuitive based design (Figure 3.17a) are concentrated in a specific region of the field where tracks are more parallel to slope presenting a high potential for soil loss and formation of gullies. Table 3.4 shows a significant decrease in soil erosion by water in the option found by the algorithm-based search, pointing to dangers of intuitive based approaches which, in fact, did not result in reduction in tracks.

Table 3.4 - Estimated soil erosion and efficiency impacts of field coverage between the two designs

	Average Soil loss ($Mg\ ha^{-1}\ year^{-1}$)	Track count
Intuitive based	30.09	264
Algorithm based	6.99	258

One subset of the field is identified by an ellipse in Figure 3.17b, regarding a region of the field in which a clear contrast exists for track patterns aiming at machine efficiency or low soil loss. The average surface soil loss in the subset was of 4.27 and 33.7 $Mg\ ha^{-1}\ year^{-1}$ and track counts (for a 3 m width between tracks) of 145 and 43 for calculated and intuitive methods respectively.

3.4 Limitations and advances of the model

One subset of the field is identified by an ellipse in Figure 3.17b, regarding a region of the field in which a clear contrast exists for track patterns aiming at machine efficiency or low soil loss. The average surface soil loss in the subset was of 4.27 and 33.7 $Mg\ ha^{-1}\ year^{-1}$ and track counts (for a 3 m width between tracks) of 145 and 43 for calculated and intuitive methods respectively.

Many aspects of the model are still intuitive: reshaping contour lines into track-references still require user-given parameters to simplify and straighten these into steerable tracks; the location and number of field divisors is still an unsolved permutation with eye picking solutions; the selection of references for hybridization and their proper sequence is not yet automatic; identifying potential consequences by the spatial concentration and pattern of the flow accumulation spots in the output of the model is still done by human observation.

Hybridization of lines is still a method to be tested and adapted, yet is has shown promising results regarding establishment of a unique pattern for coverage on surfaces.

The locations of the critical flow accumulation spots are also important for decision making. Spatial concentration of such spots (like in Figure 3.13d) makes the measures for soil conservation confined to one region (like terraces or grassways), while dispersed spots would make interventions more costly. Such a study can be visually done by the user, though no automated method was herein implemented addressing this issue.

Small changes in track direction have low influence in soil loss (Figure 3.15). This suggests that a heuristic method for finding an optimized straight direction (as in OKSANEN; VISALA, 2009) could be applied to reduce processing, if this shows necessary.

The automatic procedures for simulating all contour-references within a field (or sub-fields if divisors exist) and the automatic exhaustive search for a straight pattern makes more accurate the decision of field coverage pattern. A list is generated for each simulated option with the quantitative values for average surface soil loss, number of flow accumulation spots and number of tracks. The latter still requires to be replaced by the requirements of time and space for manoeuvring, which is dependent on some parameters derived from the model (like angle between track and boundary) and user parameters (like turning radius, width and machine speed).

The model does not account for across-track water runoff, making the soil loss estimates equal to zero when a track is following perfect contour even when a steep slope is perpendicular to it. Despite the fact that such limitation compromises the real soil loss estimates for some crops, it still finds, qualitatively, more on-grade patterns.

Soil loss estimation made from RUSLE equation does not account for soil displacement, which would likely affect the soil loss estimates. Ranieri et al. (2002), implementing a similar water cumulative approach, found that soil loss calculated by WEPP and RUSLE obtained more than the double of the estimations for the latter. Nevertheless, the use of the method of Foster and Wischmeyer (1974) for flow accumulation makes a more realistic identification of the critical spots, where the soil re-sedimentation to it makes the start of a gully more likely.

For the increase of accuracy of the model, adding a grid erosion susceptibility based on the soil attributes could retrieve more appropriate values (if a significant degree of contrast is found spatially).

Another aspect that has to be accounted for is that track-count (which equals to number of manoeuvres) does not fully relate to the time required for manoeuvring with a machine into the field. Machine and operation properties like turning radius, width and angle of machine

towards road/boundary influence the choice of a suitable type of manoeuvre and also its required time. Jin and Tang (2010), using kinematic equations to model machine turns, found that some coverage patterns with minimized number of tracks can actually increase the manoeuvring time when these properties are considered. Spekken et al. (2015) also proposed a number of model-equations to calculate time and space necessary for machine manoeuvres, applying it in sugarcane operations. These have to be integrated inside the algorithm in order to provide a consistent parameter of machine productivity and cost of areas taken as road-space for manoeuvres.

A common denominator still has to be found for the contrasting issues of best on-grade tracks towards most machine efficient track. Spekken et al. (2015) proposed methods to calculate a unique cost for manoeuvres in each sugarcane row, achieving values of US$ 4.45 for a standard scenario. The authors also calculated that sugarcane rows shorter than 50 m may have its revenue compromised, which happens in 29% of the rows in “a”. De Andrade et al. (2011) proposed a method to translate soil loss into economical values by loss of nutrients; Jin and Tang (2011) used soil loss cost by the RUSLE *P* factor for its off-grade intensity and normalizing this within a weight scale, adding costs of manoeuvring time and loss of area in sharp steering points along the track. This issue is addressed to future works.

Crop, weather, soil and machine aspects must be taken into account for the decision of the optimal path planning. Under its limitations, the proposed model allows to quantify erosion impacts with their spatial distribution on field, which is an advance on previous models.

3.5 Summary and Conclusion

An algorithm is presented to find a suitable pattern for establishment of crops on rolling terrains. The model proposes: 1) shaping elevation contours in steerable machine paths; 2) replicating a reference in tracks covering the field; 3) retrieving two erosive aspects of the tracks while they are being created; 4) automatically repeating procedures 2 and 3 for listing the erosion impacts of each reference. An additional method is proposed to obtain a more satisfying reference on the field by merging of two contour shapes into a single reference (hybridization).

The model was applied to three case studies working a number of aspects related to the design of a coverage pattern, considering its performance, sensitivity and limitations. The proposed method of hybridizing curves resulted in a better reference for coverage than the use of contour lines, though procedures have to be improved for its applicability. Using a straight

options of coverage pattern achieved improved results that are not intuitively obvious, even for a simple case.

Quantitative outputs of the model give a more robust guidance for decision-making of field operations on steep surfaces. Comparative scenario studies showed a decrease of soil loss by more than half by one single change in pattern within a field, and by four times towards a human designed pattern.

References

AICHHOLZER, O.; AURENHAMMER, F.; ALBERTS, D.; GAERTNER, B. **A novel type of skeleton for polygons.** Berlin; Heidelberg: Springer, 1996.

BENEDINI, M.S; CONDE, A.J. Sistematização da área para a colheita mecanizada de cana-de-açúcar. **Revista Coplana,** Jaboticabal, v. 25, nov. 2008. Disponível em: <http://www.coplana.com/gxpfiles/ws001/design/RevistaCoplana /2008/Novembro/pag23-24-25.pdf>. Acesso em: 03 mar. 2015.

BOCHTIS, D.D.; SØRENSEN, C.G.; GREEN, O. A DSS for planning of soil-sensitive field operations. **Decision Support Systems,** Amsterdam, v. 53, n. 1, p. 66-75, 2012.

BOCHTIS, D.D.; SØRENSEN, C.G.; BUSATO, P.; HAMEED, I.A.; RODIAS, E.; GREEN, O.; PAPADAKIS, G. Tramline establishment in controlled traffic farming based on operational machinery cost. **Biosystems Engineering,** London, v. 107, n. 3, p. 221-231, 2010.

COMPANHIA NACIONAL DE ABASTECIMENTO. **Acompanhamento de safra brasileira:** cana-de-açúcar, segundo levantamento, agosto/2013. Brasília, 2013. 19 p.

DA CUNHA, F.F.; FREITAS, A.J.F.L.J.; LEAL, L.; ROQUE, C.G.R.G.R. Planejamento de sistemas de terraceamento utilizando o software Terraço 3.0. **Brazilian Geographical Journal: Geosciences and Humanities research medium**, Uberlandia, v. 2, n. 1, p. 182-196, 2011.

DE ANDRADE, N.S.; MARTINS FILHO, M.V.; TORRES, J.L.; PEREIRA, G.T.; MARQUES JÚNIOR, J. Impacto técnico e econômico das perdas de solo e nutrientes por erosão no cultivo da cana-de-açúcar. **Engenharia Agrícola,** Jaboticabal, v. 31, n. 3,p. 539-550, 2011.

DE BRUIN, S.; LERINK, P.; KLOMPE, A.; van der WAL, T.; HEIJTING, S. Spatial optimization of cropped swaths and field margins using GIS. **Computers and Electronics in Agriculture,** Amsterdam, v. 68, n. 2, p. 185-190, 2009.

DE CARVALHO, D.F.; DA CRUZ, E.S.; PINTO, M.F.; SILVA, L.D.B.; GUERRA, J.G.M. Características da chuva e perdas por erosão sob diferentes práticas de manejo do solo. **Revista Brasileira de Engenharia Agrícola e Ambiental**, Campina Grade-PB, v 13, n 1, p. 3-9, 2009.

DE PAULA, V.R.; MOLIN, J.P. Assessing damage caused by accidental vehicle traffic on sugarcane ration. **Applied Engineering in Agriculture,** St Joseph, v. 29, n. 2, p. 161-169, 2013.

DOUGLAS, D.H.; PEUCKER, T.K. Algorithms for the reduction of the number of points required to represent a digitized line or its caricature. **Cartographica: The International Journal for Geographic Information and Geovisualization,** Toronto, v. 10, n. 2, p. 112-122, 1973.

FOSTER, G.R.; WISCHMEIER, W.H. Evaluating irregular slopes for soil loss prediction. **Transactions of the ASAE,** St Joseph, v. 17, n. 1, p. 305–309, 1974.

GRIEBELER, N.P.; DE CARVALHO, D.F.; DE MATOS, A.T. Estimativa do custo de implantação de sistema de terraceamento, utilizando-se o sistema de informações geográficas. estudo de caso: bacia do rio caxangá, PR. **Revista Brasileira de Engenharia Agrícola e Ambiental,** Campina Grande, v. 4, n. 2, p. 299-303, 2000.

GUIMARÃES, R.V. **Aplicação de geoprocessamento para aumento na eficiência do percurso em operações na cultura da cana-de-açúcar (*Saccahrum spp*.).** 2004. 82 p. Tese (Mestrado em Máquinas Agrícolas) - Escola Superior de Agricultura "Luiz de Queiroz", Universidade de São Paulo, Piracicaba, 2004.

JIN, J.; TANG, L. Optimal path planning for arable farming. In: ASABE ANNUAL INTERNATIONAL MEETING, 2006, Portland. **Proceedings…** St. Joseph: American Society of Agricultural Engineers, 2006. p. 304-312.

_____. Optimal coverage path planning for arable farming on 2D surfaces. **Transactions of the ASABE,** St. Joseph, v. 53, n. 1, p. 283, 2010.

_____. Coverage path planning on three-dimensional terrain for arable farming. **Journal of Field Robotics,** Hoboken, v. 28, n. 3, p. 424-440, 2011.

LI, Y.X.; TULLBERG, J.N.; FREEBAIRN, D.M. Wheel traffic and tillage effects on runoff and crop yield. **Soil and Tillage Research,** Amsterdam, v. 97, n. 2, p. 282-292, 2007.

LIU, Q.J.; ZHANG, H.Y.; AN, J.; WU, Y Z. Soil erosion processes on row sideslopes within contour ridging systems. **Catena,** Amsterdam, v. 115, p. 11-18, 2014.

LOMBARDI-NETO, F.; BERTONI, J. **Tolerância de perdas de terra para solos do Estado de São Paulo.** Capinas: Instituto Agronômico de Campinas, 1975. 12 p. (Boletim Técnico, 28).

LOMBARDI-NETO, F.; MOLDENHAUER, W.C. Erosividade da chuva: sua distribuição e relação com perdas de solo em Campinas, SP. **Bragantia,** Campinas, v. 51, n. 2, p. 189-196, 1992.

LOMBARDI-NETO, F. JUNIOR, R.B.; LEPSH, I.G.; OLIVEIRA, J.D.; BERTOLINI, D.; GALETI, P.A.; DRUGOWICH, M.I. **Terraceamento agrícola.** Campinas: CATI, 1994. 39 p.

MACHADO, E.C.; PEREIRA, A.R.; FAHL, J.I.; ARRUDA, H.V.; CIONE, J. Índices biométricos de duas variedades de cana-de-açúcar. **Pesquisa Agropecuária Brasileira,** Brasília, v. 17, n. 9, p. 1323-1329, 1982.

MANNIGEL, A.R.; DE PASSOS, M.; MORETI, D.; DA ROSA MEDEIROS, L. Fator erodibilidade e tolerância de perda dos solos do Estado de São Paulo. **Acta Scientiarum. Agronomy,** Maringa, v. 24, p. 1335-1340, 2008.

MINASNY, B.; MCBRATNEY, A.B.; WHELAN, B.M. **Vesper:** version 1.6. Sidney: The University of Sidney; Australian Centre for Precision Agriculture, 2002. Disponível em: <http://sydney.edu.au/agriculture/pal/software/download_vesper.shtml>. Acesso em: 03 jun. 2015.

NORRIS, C.P.B.G.; ROBOTHAM, T.A. BULL. High density planting as an economic production strategy: (c) a farming system and equipment requirements. In: CONFERENCE OF THE AUSTRALIAN SOCIETY OF SUGAR CANE TECHNOLOGISTS, 2000, Bundaberg. **Proceedings…** Bundaberg: PK Editorial Services, 2000. p. 113-118.

OKSANEN, T.; VISALA, A. Coverage path planning algorithms for agricultural field machines. **Journal of Field Robotics,** Hoboken, v. 26, n. 8, p. 651-668, 2009.

PALMER, R. J.; WILD, D.; RUNTZ, K. Improving the efficiency of field operations. **Biosystems Engineering,** London, v. 84, n. 3, p. 283-288, 2003.

QUANTUM GIS DEVELOPMENT TEAM. **Quantum GIS geographic information system:** open source geospatial foundation project. 2014. Disponível em: <http://qgis.osgeo.org>. Acesso em: 03 jun. 2015.

RANIERI, S.B.L.; VAN LIER, Q.D.J.; SPAROVEK, G.; FLANAGAN, D.C. Erosion database interface (EDI): a computer program for georeferenced application of erosion prediction models. **Computers & Geosciences,** Amsterdam, v. 28, n. 5, p. 661-668, 2002.

RENARD, K.G.; FOSTER, G.R.; WEESIES, D.K.; TODER, D.C. (Coord.). **Predicting soil erosion by water**: a guide to conservation planning with the revised universal soil loss equation (RUSLE). Washington: USDA, 1997. 407 p. (Agriculture Handbook, 703).

SILVA, C.B.; DE MORAES, M.A.F.D.; MOLIN, J.P. Adoption and use of precision agriculture technologies in the sugarcane industry of São Paulo state, Brazil. **Precision Agriculture,** Dordrecht, v. 12, n. 1, p. 67-81, 2011.

SOUZA, Z.M.; DE MELLO PRADO, R.; PAIXÃO, A.C.S.; CESARIN, L.G. Sistemas de colheita e manejo da palhada de cana-de-açúcar. **Pesquisa Agropecuária Brasileira,** Brasília, v. 40, n. 3, p. 271-278, 2005.

SPEKKEN, M.; DE BRUIN, S. **Coverage accuracy using curved swaths within agricultural fields.** 2010. Thesis (PhD) - Wageningen University, Wageningen, 2010.

SPEKKEN, M.; DE BRUIN, S. Optimized routing on agricultural fields by minimizing manoeuvring and servicing time. **Precision Agriculture,** Dordrecht, v. 14, n. 2, p. 224-244, 2013.

SPEKKEN, M.; MOLIN, J.P.; ROMANELLI, T.L. Cost of boundary manoeuvres in sugarcane production. **Biosystems Engineering,** London, v. 129, p. 112-126, 2015.

TULLBERG, J.N.; YULE, D.F.; MCGARRY, D. Controlled traffic farming: from research to adoption in Australia. **Soil and Tillage Research,** Amsterdam, v. 97, n. 2, p. 272-281, 2007.

WISCHMEIER, W.H.; SMITH, D.D. **Predicting rainfall erosion losses:** a guide to conservation planning. Washington: USDA, 1978. 58 p. (Agricultural Handbook, 537).

4 SITE-SPECIFIC COSTS OF MACHINE PATH ESTABLISHMENT IN AGRICULTURAL FIELDS

Abstract

In the current agricultural context, machine unproductivity on fields and their impacts on soil along pathways are unavoidable. This work was carried out seeking to gather different impacts calculated in computational path planning and distribute them spatially to their respective location in field assigning financial costs unto them. From an existing model-algorithm developed to create paths on irregular surfaces, impacts of soil loss are obtained and assigned to their respective track-segments. Additionally, procedures were embedded to the model to calculate costs of manoeuvring, overlap and proper use of the reservoir regarding the track length. Two case studies of different field geometries and crop growing properties were submitted to processing by the algorithm. Spatial cost distribution due to path definition was obtained along with studies of varying financial balances over the field. In a sugarcane study, the model obtained that for the average of five harvests, 2.69% of the area presented negative turnover due to the path-planning costs; however, this area increases tenfold when financial balance is calculated for the last two harvests of the crop. In a cotton case study, a high input cost was calculated for overlap of applied products in headland; with the adoption of a section control boom for the spraying operation, a significant reduction of costs up to US$ 50.00 per hectare was obtained. Given the costs regarding path planning, they cannot be ignored in financial spatial studies.

Keywords: Path planning; Unproductivity of operations; Soil loss costs; Spatial distribution of costs; Land use; Modelling

4.1 Introduction

Diversity of agricultural practices (crop nutrition, pest control and irrigation) and crop cycles (annual or perennial) has attracted focus for site-specific management in agricultural fields. Some of these studies approached the financial aspects of the field's natural variability and, when it is the case, the respective intervention on them. (BULLOCK et al., 2002; BONGIOVANNI; LOWENBERG-DEBOER, 2004; BOYER et al., 2010).

Among agricultural cost components, mechanization costs and machine traffic impacts are often considered as fixed cost in a production system, being often considered for the total area. In such analysis, the unproductive impacts of machines and their traffic and coverage impacts are rounded up in broad percentages of inefficiency.

However, a trend of increasing adoption of automatic pilot systems (SILVA et al., 2011; HOLLAND et al, 2013) and of controlled traffic farming (CTF) practice (LOADSMAN, 2002; TULLBERG, 2007; DERPSCH, 2010) pushed the efforts to plan in advance the machine traffic on fields (BOCHTIS et al., 2010). This planning aimed to identify and quantify impacts like manoeuvres or coverage overlap, and minimize them by computational path planning.

Observing the advance in GNSS guided machines, Stoll (2003) listed some aspects to be considered for computational path planning: operation strategy, neighbouring area, field geometry, field specific data, machine specific data and field slope.

Field geometry and machine width have been accounted in most of these studies about path planning works (PALMER et al., 2003; JIN; TANG, 2006; TAIX et al., 2006; HOFSTEE et al., 2009). Advances included optimized logistics of reloading machine reservoir for applying agricultural inputs or collecting harvested product (BUSATO et al., 2007; OKSANEN; VISALA, 2007). Furthermore, turning radius was considered a machine parameter for optimizing the manoeuvre types (BOCHTIS; OKSANEN, 2009; JIN; TANG, 2010). More comprehensive approaches embodied these issues in a more global path planning optimization (BOCHTIS et al., 2010; SPEKKEN; DE BRUIN, 2013).

Still, despite machine and coverage efficiency were approached in the above mentioned works, they were restricted to flat surfaces, and impacts of path establishment in irregular landscape were not accounted for. In these surfaces, crop and machine orientations are suggested to be parallel to the terrain contours to reduce water runoff and erosion, however contours are hardly (if ever) parallel to each other, while machine patterns are always parallel. For the path-planning scope, this poses a challenge to define the least erosive orientation for tracks and if (or where) the orientation should change upon a field. Unavoidably, the decision to set machine paths and/or crop rows following a certain orientation will have implications in soil loss and, in aggravated scenarios, erosion may take form of gullies.

Jin and Tang (2011) created a path-planning approach for rolling terrains. The authors considered manoeuvring and uncropped areas as costs, embedding a soil loss cost calculated by the Revised Universal Soil Loss Equation (RUSLE; RENARD, 1997). The proposed model assigns a weight to the paths oriented off the terrain grade resulting in a round soil loss estimate for the whole field.

Path planning efforts focused in obtaining and minimizing the total cost of allocating machine tracks for covering the whole field. However, not all crop-tracks created upon a field have the same cost-benefit balance. Manoeuvre and coverage overlap costs do not depend on the length of a track, aggravating the relative cost in short tracks. Spekken et al. (2015) pointed this issue in sugarcane operations, calculating that sugarcane rows shorter than 50 m may have their financial revenue compromised by the manoeuvring costs.

Spekken and Molin (2012) developed a path planning approach that identifies regions covered by short tracks for different track patterns. Results pointed that, depending on the case,

short tracks in corners of the fields can respond to over 15% of the manoeuvres and, in these, overlap of inputs in headland could be over 3 times higher than for the whole field.

In contrast, long tracks may create a logistic problem for operations that depend on reloading of inputs or offloading of harvest produce. This procedure, here known as servicing, requires a machine to load/offload either on the field boundary before reservoir capacity is fully used (SPEKKEN; DE BRUIN, 2013), or demand an auxiliary unit moving within the field to aid in this procedure. An ideal track-length allows a machine to work the field reaching the field boundary with a full use of its reservoir. For crops like sugarcane, the crop-rows are interrupted by logistic roads in every 500 to 700 m intervals (BENEDINI; CONDE, 2008).

As manoeuvres, coverage overlap and servicing have a fixed cost upon a single track, soil loss often varies along this by the changes in altimetry. Calculation of site specific soil loss in dependence to track orientation was obtained by Spekken et al. (2014), who also made use of the RUSLE to quantify erosion in path planning. The authors calculated soil loss for cumulative water runoff along the tracks (and not across them). This proposed algorithm retrieved only the number of tracks (thus manoeuvres) on field, neglecting an accurate machine cost calculation.

The variance in operational costs is explained by different path lengths on fields with irregular geometry, while the variance in soil loss is explained by a path pattern on an irregular surface.

Given the advances of obtaining machine (or crop) planned tracks and its impacts, and that the relative cost of the tracks vary over the field; in this paper a method is suggested to quantify and spatially distribute the cost of a computational path on a field.

4.2 Methodology

The methods here described are modified after Spekken et al. (2014) who proposed an approach for designing curved tracks and retrieving the soil loss along these. The method was enhanced for obtaining the full path planning cost by adding the unproductive operational cost (*UOC*), which includes manoeuvring cost (*MC*), overlap cost (*OvC*), and cost for inadequate length of track (*CILT*).

The cost calculation method for each of the impacts is described in the following chapters, whilst methods that are derived from previous works are presented by summarized description.

4.2.1 Creating tracks and calculating soil loss costs

The creation of tracks on field and soil loss calculations follow the methodology proposed by Spekken et al. (2014) to create geometric virtual tracks on field-polygons in computational algorithms. Tracks are polylines composed by shorter straight line segments linked in a curved pattern, which can represent a machine path or a crop row. Terrain contours are a common data source used as reference for creating parallel tracks.

In the methodology used, tracks have to be reshaped in curved with a degree of smoothness that allows a machine to steer along. Thus, tracks are submitted to a three-step process of:

- Line simplification, which removes small oscillations in its shape;
- Decrease in concavity, which reduces the degree of curvature of the polyline, reducing or eliminating convergence of parallel passes (i.e. avoids rough turns);
- Smoothness, which makes use of parametric cubic splines to interpolate new edges in between the existing ones, creating a round steerable track.

By overlaying created tracks with a DTM (Digital Terrain Model), altimetry can be retrieved for existing and created features.

The reference-tracks are then designed in parallel replications in an offset distance user-defined, while the altimetry is assigned to the edges of the segments making possible for RUSLE to be applied. The method calculates a soil loss quantity for cumulative water runoff along the tracks (FOSTER; WISHMEYER, 1974), resulting in soil loss estimates in units of Mg ha^{-1} $year^{-1}$ for each segment. The soil loss is adjusted to Mg^{-1} $year^{-1}$ for its respective area of coverage.

The financial soil loss cost is calculated in proportion to quantity of eroded soil. De Andrade et al. (2011) made use of the RUSLE to quantify the loss of nutrients in the arable layer, multiplying this by the cost of replenishing the nutrient content. The study obtained a cost of US$ 1.19 Mg^{-1} of soil eroded. Still, such calculation does not account for loss of yield and/or possible concentration of water within the field, soil re-development of arable layer and formation of gullies.

A more comprehensive study was carried by Telles et al. (2011), who reviewed many approaches for soil loss costs considering impacts of in-field (loss of nutrients, organic matter and yield) and off-field (soil sedimentation on rivers and eutrophication of water) suggesting

US$ 5.00 per Mg of soil eroded. The latter value was used as the final parameter for soil loss cost in the cases to be studied in this work.

4.2.2 Costs from headland manoeuvre and coverage overlap

Manoeuvring costs in headland were calculated considering its time, space and length costs. The methods used for obtaining these are given after Spekken et al. (2015). The main variables that compose the manoeuvring costs are: manoeuvring type, machine turning radius (r), machine width (w) and angle of machine orientation towards the border (θ). The types of manoeuvres considered and its participant variables are shown in Figure 4.1.

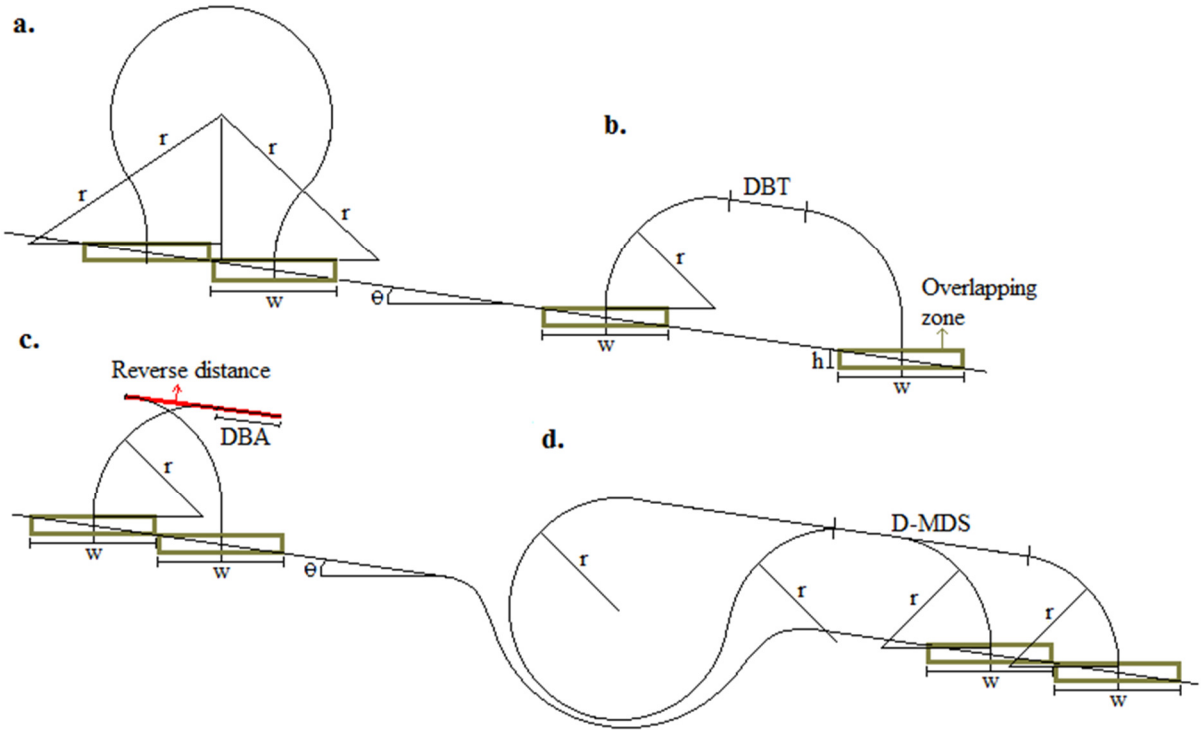

Figure 4.1 - Composition of the types of manoeuvres: Ω-turn (a), U-turn (b), T-turn (c) and P-turn (d)

In Figure 4.1, the variables shown *DBT*, *DBA* and *D-MDS* are respectively distance between steering in a U-turn, distance between rear and steering axles of the machine, and distance to a manoeuvring dedicated space.

The time for the manoeuvre is given by distinct machine working speeds along it. These velocities, along with the other variables mentioned, are given as external model parameters. The parameters must be provided upon definition of the manoeuvring type and kept constant for all manoeuvres in an operation. Only two parameters are derived from the model for each track: the track length and the angle θ. The latter is retrieved for the first and last segments of a

curved track when these reach the field boundary. The final manoeuvre cost is thus obtained by:

$$TMC = MT * MC + MS * {w^2}/{\cos(\theta)} * OCA + MD * Tw * CR \quad (4.1)$$

Where:

TMC is the total manoeuvring cost (in US$);

MT is the manoeuvring time (in s);

MC is the machine cost (in US$ s^{-1});

MS is the manoeuvring space (in m);

OCA is the opportunity cost of the land (in US$ m^2);

MD is the manoeuvring distance;

Tw is the width of the area under the machine's tires (in m);

CR is the crop revenue or costs for compacted surface per area (in US$ m^2);

Owing that the manoeuvre may happen in any of the extremities of a track, the final impact cost is an average of the values calculated for both extremities.

The coverage overlap is calculated only for the headland and it is dependent on two of the variables listed, *w* and θ. Usually, in agricultural operations, the overlap exceeds the exact need for overlap length in order to achieve safe area coverage, this is shown in Figure 4.2 by the variable *ASL*, which must be given as an input parameter in the model.

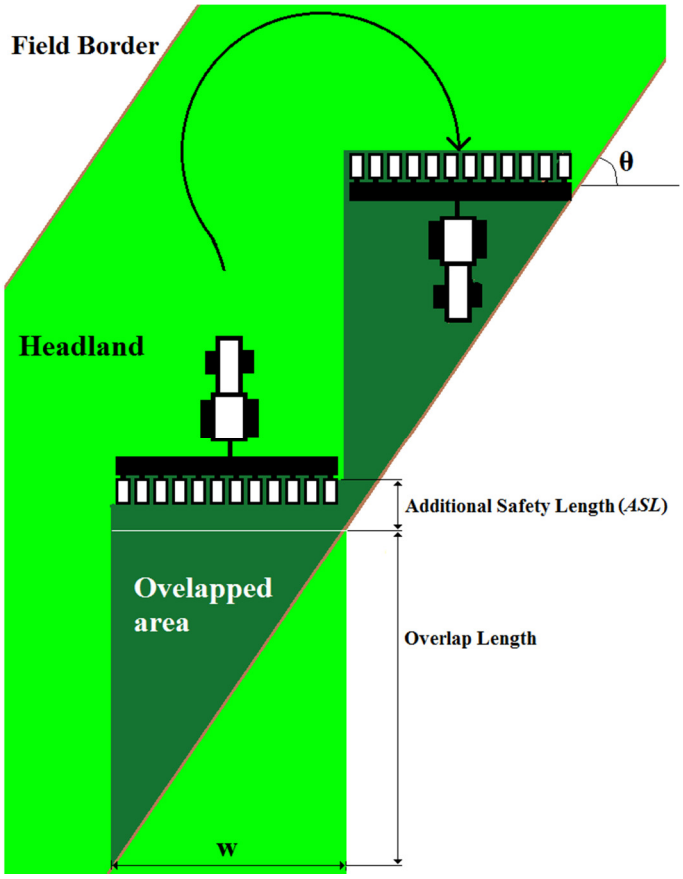

Figure 4.2 - View of headland overlap and its related variables

As shown in Figure 4.2, the overlapped area (OvA, in m^2) at the extremity of a track is calculated by Equation 4.2 and the overlapped cost (OvC, in US$) is given in Equation 4.3:

$$OvA = w * ASL + \frac{w^2}{\tan(\pi/2 - \theta)} \tag{4.2}$$

$$OvC = OvA * APC \tag{4.3}$$

Where APC is the product value applied per area (in US$ m^{-2}).

The final OvC is summed for both extremities of a created track.

4.2.3 Cost of servicing

Machine loading or offloading of agricultural goods can happen by two means: servicing with aid of auxiliary units within the field, or servicing restricted to the field boundary (headlands or roads). The first is more related to harvesting procedures, where high quantities of product must be constantly offloaded in a narrow time-window operation; while the latter is

related to application of inputs (seeds, fertilizer, pesticides), in which auxiliary units on field would be either unaffordable financially or soil/crop damaging.

The ideal length to attend the capacity of a machine (*IdL*, in m) is given by:

$$IdL = \frac{Tank}{Rate * w} \tag{4.4}$$

Where *Rate* is the application rate or product harvested along the followed track (units m^{-2}); and *Tank* is the capacity the reservoir (units).

When a track presents the same length as *IdL*, the *CILT* is nil, meaning that it has no impact to the servicing procedure. In the same way, when auxiliary units can follow the primary unit without stopping the latter for offloading (like for grain discharge of harvesters unto wagons in motion), unproductive time is inexistent and the *CILT* is also nil.

Unproductive use of a machine is found in harvesting operations when there is need of constant presence of an auxiliary unit, like for silage or sugarcane harvesting as in Figure 4.3a.

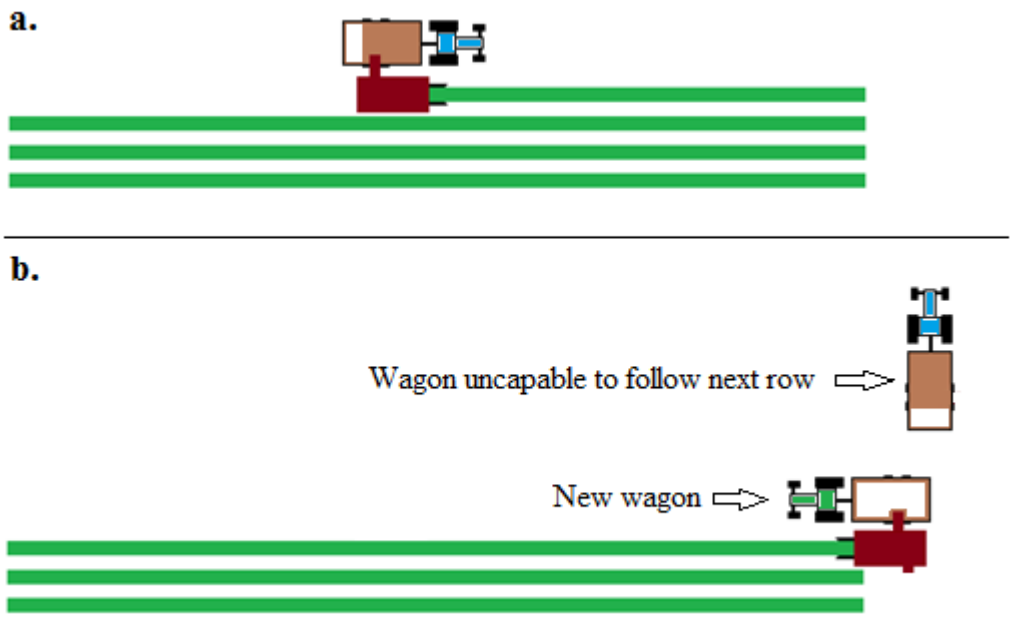

Figure 4.3 - Harvesting operation with primary and secondary units (in 'a'), and switch of wagon carriers at the edge of a row-track (in 'b')

The replaced wagon in Figure 4.3b is leaving the field with underused capacity. Therefore, the transportation cost for the incomplete cargo is added to the track, which is the proportional fraction to the transport of a full wagon.

For harvested product, a tolerance value (*Slack*, in %) is considered to transport an additional weight for tracks a minimally longer than *IdL*. The real length of a track (*RLen*, in m) is given by the created tracks on the field by the model. *RLen* is obtained by the number of passes (*NP*) capable to approximate to *IdL*, i.e. when more passes of a certain track are needed to complete the ideal length. *NP* and *RLen* are given by equations 4.5 and 4.6 respectively;

$$NP = int\,[(IdL+IdL*Slack) / TrackL] \tag{4.5}$$

$$RLen = NP*TrackL \tag{4.6}$$

The lacking load of the reservoir at the edge of a track (*LLoad*, in units) is given by:

$$LLoad = Tank - \left(\frac{Tank * RLen}{IdL} \right) \tag{4.7}$$

If *LLoad* is negative, meaning that the carrier is using the tolerance capacity to finish the track, and the machine managed to fully use the track length and *LLoad* is then equalled to zero.

The cost of the lacking cargo is calculated by multiplying *LLoad* by the cost of unit-weight transported, which is based in an hourly auxiliary-unit time cost (*ATC*, in US$ s^{-1}) and an average trip time (*ATT*, in s) to offload the cargo. The final *CILT* for this operation is obtained by equation 4.8:

$$CILT = \frac{ATC * Load}{ATT * Tank * NP} \tag{4.8}$$

When the *Lload* is excessively high, the carrier may continue with the harvester and be replaced in the middle of the field to complete its loading, and an empty carrier will replace it when the cargo becomes critical. In this case, the replacing time interruption is for the whole operation (primary and auxiliary units) and for a fixed time-cost value (in US$). When this cost

is lower than the *CILT*, as calculated by equation 4.8, it overrules the equation and becomes the new *CILT* (i.e. cost of in-field swap of carriers is lower than cost for transporting incomplete cargo).

In other field operations, where application of product on field is involved, auxiliary units are absent or attending the primary units only on the boundaries of the fields. These operations have no additional tolerance for its capacity (no *Slack*), and when tracks do not meet the *IdL* criteria, a machine-time cost is computed to refill the reservoir. *CILT* is then proportional to the length that is not covered by the remaining capacity, calculated by equation 4.9.

$$CILT = \frac{(IdL - RLen) * TCM}{IdL * NP} \tag{4.9}$$

The values of *MC*, *OvC* and *CILT* compose the unproductive operational cost (*OUC*), and are unique for each track. When this cost is divided by the track-length, it becomes a relative cost per distance (US$ m^{-1}). This relative cost is assigned to each of the segments composing the track.

4.2.4 Model implementation

The methods were applied on the model developed by Spekken et al. (2014). An algorithm was embedded to the existing model within the Lazarus free-pascal environment. Figure 4.4 provides a view of the developed model with a practical case being evaluated.

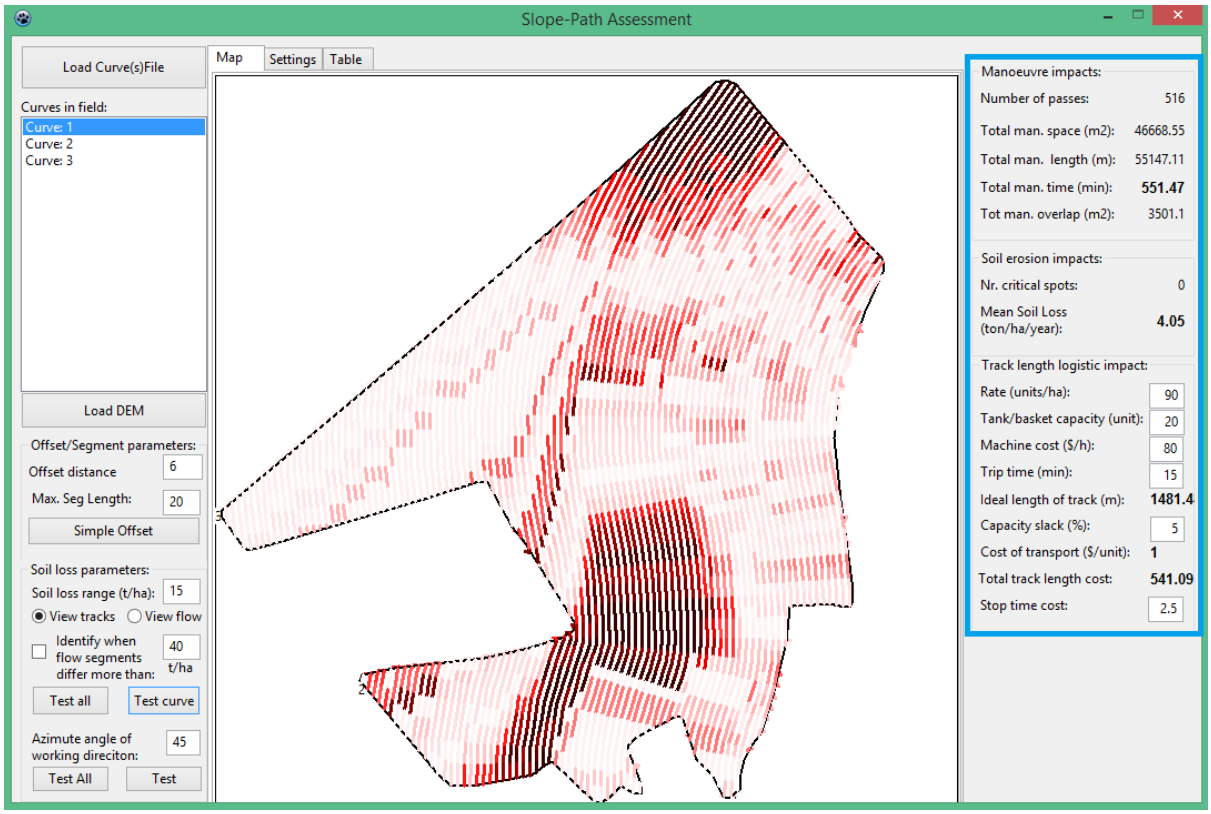

Figure 4.4 - View of the implemented model showing an output of track coverage where red coloured intensity in the field-map is proportional to the local soil loss intensity

The input parameters are given to the model as setting variables that can be altered for each simulation and/or case study. The blue square in the right side of the window shows the overall calculated impacts for the chosen pattern.

The algorithm calculates soil loss and operational parameters in real time, storing the coordinates of the segments in the form of an array-list along with the relative cost per distance of the calculated soil loss, *MC*, *OvC* and *CILT* for each segment. The list can be exported in comma separated value (.CSV) files for analysis.

4.3 Case studies

Two case studies were applied as scenarios into the model-algorithm to assess its performance and outputs on distinct environments and crops. The crops analysed were sugarcane (*Saccharum spp.*) and cotton (*Gossypium hirsutum*) grown in Brazilian representative regions (São Paulo and Mato Grosso states respectively); both crops are established as row crops with prohibitive traffic across them. Sugarcane has an intense mechanization cost concentrated in its harvest operation, which can encompass up to 30% of the total production costs (COELHO, 2009) and over 80% the total mechanization costs

(SPEKKEN et al., 2015); thus the operational cost calculation and its distribution for this case study is confined to harvesting. Cotton crop, on the other hand, has an intense cost related to use of inputs (seeds, fertilizer and pesticides), which makes overlap a higher issue among unproductive costs. In the latter case, four field operations (sowing, fertilizer spreading, spraying and harvesting) were considered to calculate the path planning cost. The field study areas are displayed in Figure 4.5 identifying the case study I (sugarcane) and II (cotton), their respective properties are displayed in Table 4.1.

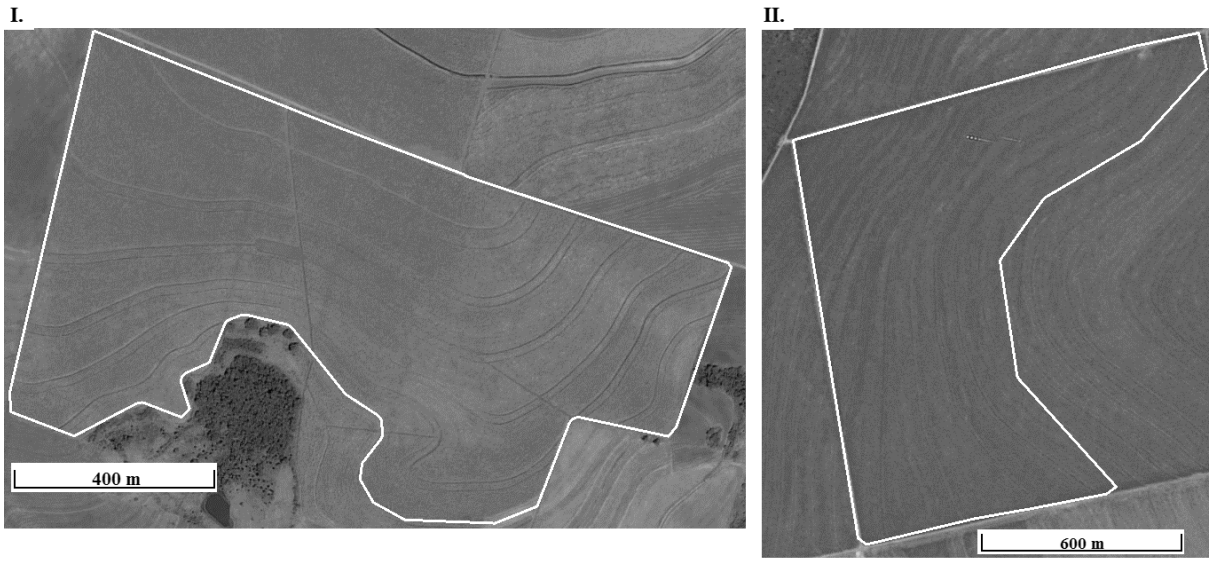

Figure 4.5 - View of the two case study areas (I and II)

For case study I, altimetry data was available from logged RTK (Real Time Kinematic) measurements, retrieved from the auto-guidance system during the planting operation. A cotton harvest operation logging data (GNSS L1 receiver) was the altimetry source for case study II. The data was interpolated to a 5 m regular-grid by ordinary kriging using VESPER 1.6 (MINASNY et al., 2006). The extraction of the surface contours was done in the GIS software Quantum GIS 2.4.0 Chugiak (QUANTUM GIS DEVELOPMENT TEAM, 2014), which was also used for sorting and viewing the data of the spatial cost distribution.

In case study I, the average slope steepness is 6.6%, varying from 2.7 to 12.7%, and the surface contours were used as reference to find the least erosive option (model obtained). For case study II, the slope steepness average is 2.9%, varying from 0.4 to 5.6%; the lower steepness of this case study is counter balanced by a higher erosion susceptibility of the soil (factor K in Table 4.1). The least erosive option in case study II was a hybrid line obtained from two surface contours. The source references used for creating parallel tracks are identified by a green line within the field-maps in Figure 4.6.

Table 4.1 displays the environmental properties for the fields analyzed with the calculated soil loss value from the model output.

Table 4.1 - Description of the case study environmental properties

	Case study I	Case study II
Location	Latitude 21° 27'42'' Longitude 47°59'03''	Latitude: 14°56'56'' Longitude: 54°56'25''
Land use	Agriculture - Sugarcane	Agriculture – Cotton
Area size (ha)	77.56	91.65
Soil classification (ISRIC[a])	Ferrasol Udox	Ferrasol Udox
Soil type	Sandy clay	Sandy loam
RUSLE R factor [b]	1785.0	1087.4
RUSLE K factor [c]	0.012	0.057
RUSLE C factor [d]	0.307	0.58
RUSLE P factor [e]	1	1
Average soil loss for the whole surface using the least erosive reference (Mg ha^{-1} year^{-1})	7.93	6.35

[a] ISRIC - International Soil Reference and Information Centre, 1998.
[b] R factor calculated after Lombardi Neto & Moldenhauer (1992), for monthly and annual rainfall of 250 and 1350 for 'i'; and of 200 and 1500 for 'ii'.
[c] K factor calculated after Lobardi Neto & Bertoni (1975), for a clay-silt-sand particle fraction of 45-10-45 for 'i'; and 15-12-73 for 'ii'.
[d] C factor obtained after Machado et al. (1982) for 'i' and Murphree & Mutchler (1980) for 'ii'.
[e] P factor suggested after Spekken et al. (2014) for water running along crop row without obstacle.

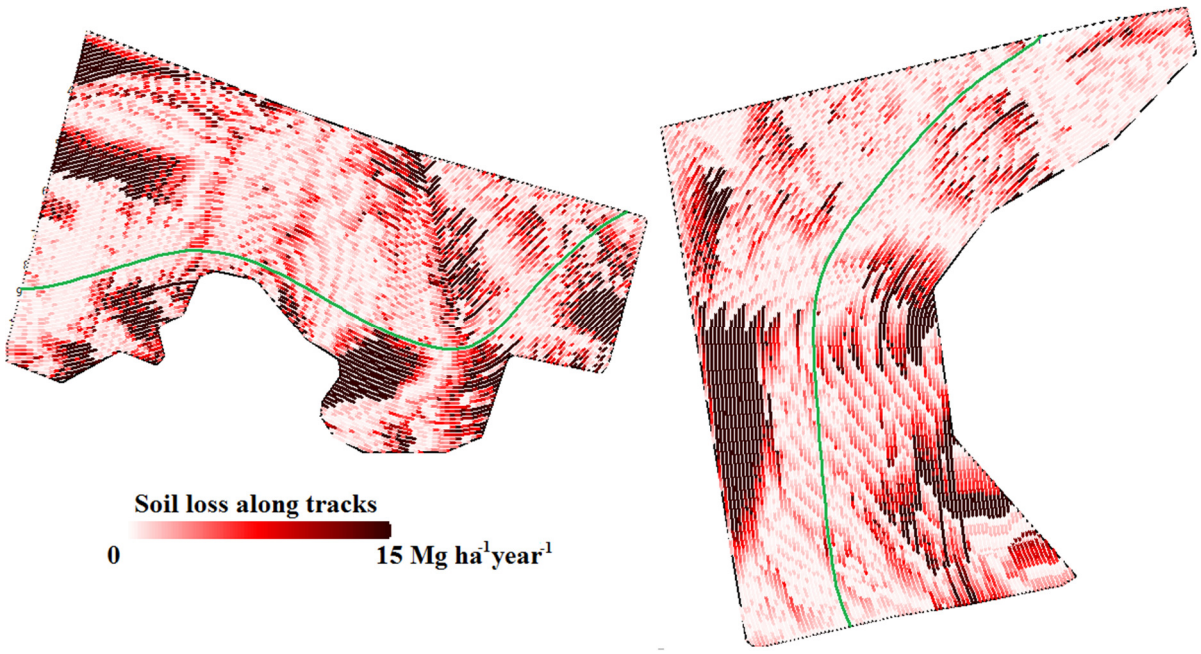

Figure 4.6 - Algorithm-suggested pattern for field coverage for the least soil loss impact

The tracks created by the algorithm were fractured (if necessary) in shorter line segments of 15 m. Figure 4.6 displays parallel tracks offset in 9 m for the purpose of viewing the orientation, yet the studied data was processed to create offsets of 3 m for sugarcane (2 sugarcane rows) and 4.5m for cotton (5 cotton rows, to match harvester width). A total of 24204 and 19181 segments were generated for the cases I and II respectively.

The segments carrying its relative soil loss and unproductive operational costs had the coordinates of the edges averaged to a point-location, and exported for analysis.

4.3.1 Case study I

The parameters used for the harvesting operation are described as follows: turning radius (r) of 10.5 m (for wagon-carriers); operation width (w) of 1.5 m; manoeuvring type as P-turn; distance to manoeuvring dedicated space (D-MDS) of 20 m; turning speed of 1.5 $m.s^{-1}$ and road speed of 2.5 m s^{-1}. In sugarcane operations headland is inexistent, and all the manoeuvres are done in roads around the fields; therefore, no costs apply for crop overrunning, soil compaction or overlap. Hence, the cost for manoeuvring is limited to space (road width) and time. The time cost of the harvest operation was US$ 170.00 h^{-1} and the area lease cost (to calculate manoeuvring area) was US$ 410 ha^{-1}. The *CILT* was calculated for a harvesting rate of 78 Mg ha^{-1}, basket capacity of 17 Mg, slack capacity of 10%, time cost for carrier of US$ 30.00 and a round-trip time for offloading of 15 min.

The algorithm retrieved a total manoeuvring time and space of 20.36 h and 3.18 ha with respective costs of US$ 3481.15 and US$ 1313.34. The *CILT* cost was of US$ 500.99. The final *UOC* regarding the working orientation is US$ 5295.48 or US$ 68.27 ha^{-1}. The total soil loss cost was of US$ 3075.25 or US$ 39.65 ha^{-1}.

A financial balance of the crop was calculated using the total costs of each segment-location subtracted from a revenue per length. The average revenue of five harvests (US$ 400.00 ha^{-1}) has its value adjusted to US$ 0.12 m^{-1} (for a width of 3 m between tracks). Also the balance for the last two harvests was studied (revenue of US$ 107.00 ha^{-1} or US$ 0.032 m^{-1}). The revenue values were obtained from FNP consultoria e comércio (2012).

The spatial distribution for the operational unproductive cost and soil loss cost are given in Figure 4.7.

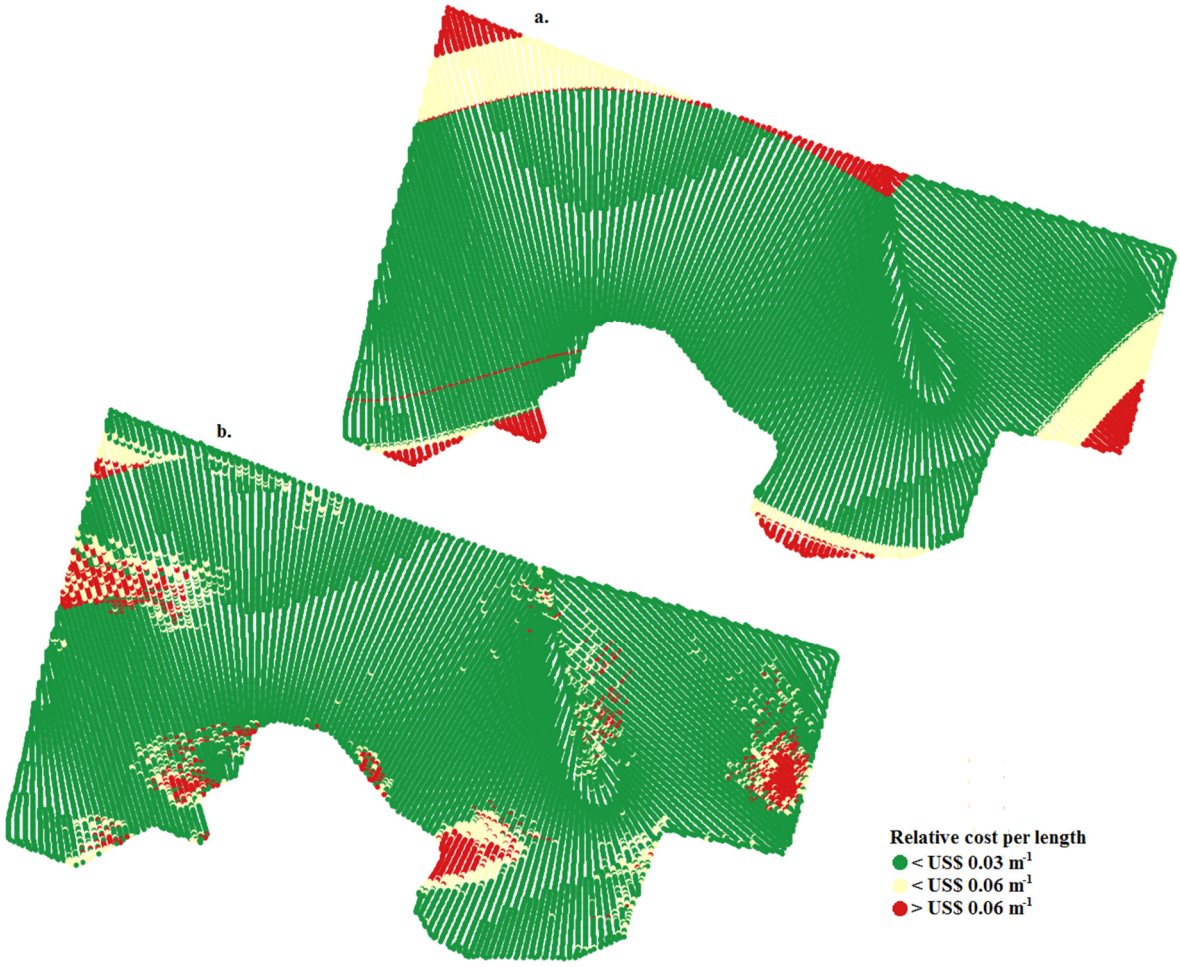

Figure 4.7 - Spatial distribution of the unproductive operational costs in 'a' and soil loss cost in 'b'

In Figure 4.7, the range of the three cost categories (green, yellow and red) was defined in steps of US$ 0.03 m^{-1}, which represent a quarter of an expected crop revenue (US$ 0.12 m^{-1}). This implies that the cost in the regions covered by red dots consumes over 50% of the expected profit. Also, the total *UOC* for the red area in 'a' (13.7 ha) was of US$ 1604.35, which represents 30.3% of the *UOC* of the whole field.

As expected, the distributed *UOC* were higher for segments of short tracks, with manoeuvring as the leading cost. Soil loss costs are more scattered, with some major clusters concentrated in regions where tracks are in higher off-grade.

The spatial financial balances calculated for the two proposed revenues are shown in Figure 4.8.

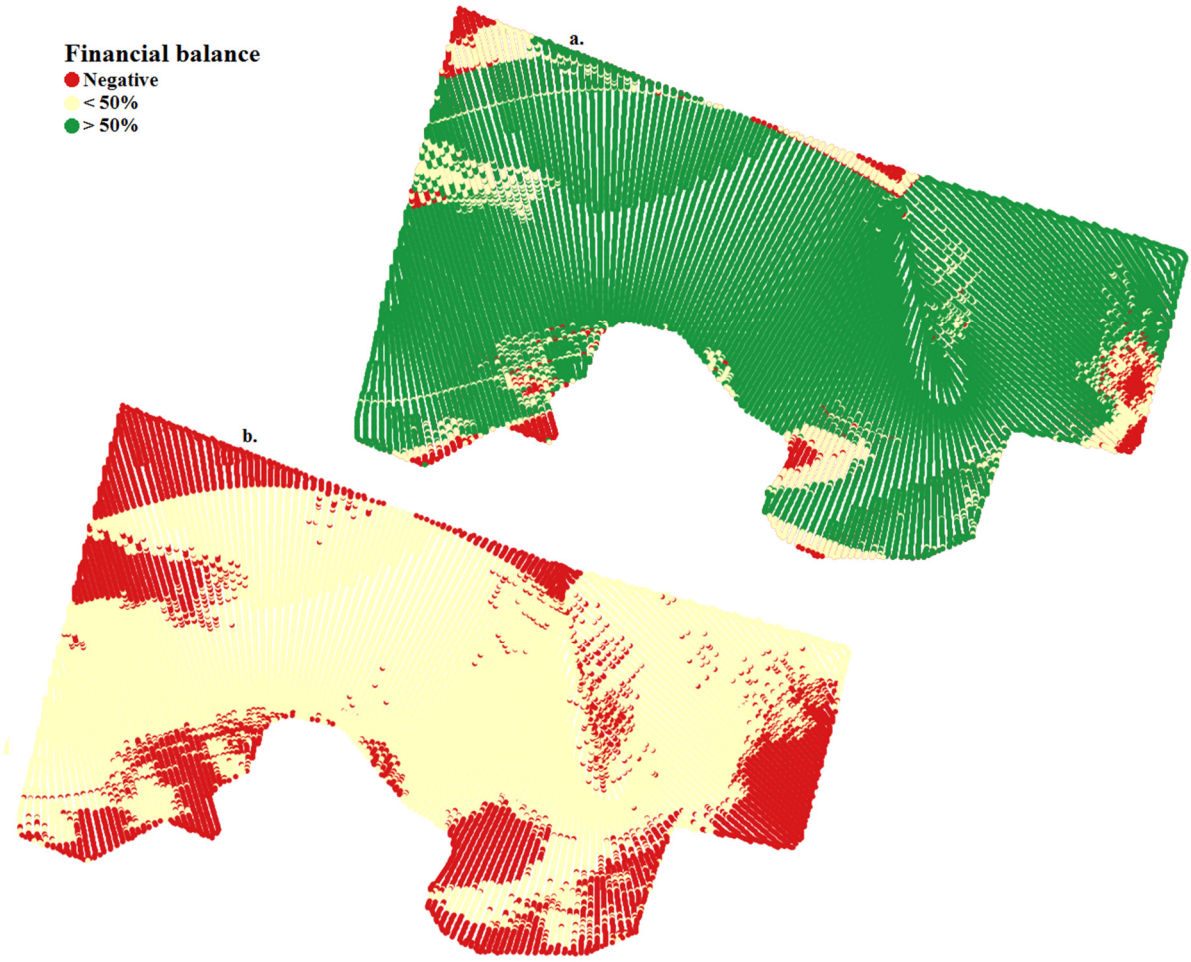

Figure 4.8 - Localized financial balance in sugarcane for the path planning impact for a fixed income expected per meter. In ‘a’ the balance considers an income averaged by all five harvests and in ‘b’ the balance considers the average of the last two harvests

The area of negative turnover in Figure 4.8a is 2.08 ha (2.69% of the field) and the area with financial margins below 50% is 7.04 ha (9.07% of the field); these areas increase to 20.36 ha and 57.23 ha respectively, in Figure 4.8b. Tracks with length shorter than 50 m showed no revenue.

4.3.2 Case study II

In this case study, four operations were simulated by the algorithm using width multiple of the cotton harvester (4.5 m). The highest costs among *UOC* is the overlap of fertilizer and pesticides (over 50% of *UOC*), for which the latter counts over 20 spraying applications during the growing of the crop for the local conditions. Table 4.2 displays the operational properties used as parameters and the total costs retrieved by the algorithm.

Table 4.2 - Operational and machine cost values used as parameters in the model

	Sowing	Fertilizer spreading	Spraying	Harvesting
	Operational parameters			
Operation width (m)	9	27	27 [a]	4.5
Machine turning radius (m)	6	6	5	6
Composition of manoeuvring cost	Time	Time + Length [b]	Time + Length [b]	Time
Manoeuvre type	Ω-turn	U-turn	U-turn	T-turn
Application overlap	Yes	Yes	Yes	No
Rate of product loaded/offloaded (units ha^{-1})	400 kg Fertilizer [c]	200 kg Fertilizer	100 L water + prod.	3750 kg cotton
Reservoir/basket capacity (units)	2700 kg	5000 kg	2700 l	2700 kg
Sum of the value of products applied (US$ ha^{-1})	153	321	695.5	0
Machine cost (US$ h^{-1})	191	131.66	41.01	272.25
Replenishment time of reservoir/basket (min)	15	60	10	4
	Operational cost of the path planning calculated by the algorithm			
Total manoeuvring costs (US$)	146.73	163.53	524.83	855.06
Total overlap costs (US$)	239.64	1439.9	3119.78	0
Total *CILT* costs (US$)	60.00	24.87	33.08	262.13
Total unproductive operational costs (US$)	446.38	1628.30	3678.50	1117.20

a. Sprayer boom without section-control.
b. Length of the manoeuvre calculated for crop overrun in the after-implanted crop in the headland. The calculated length was multiplied by a track width of 1 m and the overrun area was multiplied by an expected crop revenue of US$ 400 ha^{-1}.
c. Fertilization and seeding are simultaneous operations in the local sowing procedures. However, fertilizer reservoir has higher frequency of replenishment, and the re-loading of seeds happens during these events.

The calculated *UOC* summed US$ 6870.38 (US$ 75.96 ha^{-1}), and the soil loss cost was US$ 2909.88 (US$ 31.75ha^{-1}). Figure 4.9 displays the spatial distribution of these costs where the *UOC* (in 'a') of the red spots sums US$ 4372.73 (US$ 259.29 ha^{-1}) and the soil loss cost (in 'b') of the red spots sums US$ 1614.51 (US$ 213.04 ha^{-1}). Similarly to case study I, the three categories of costs in Figure 4.9 are separated in ranges (of US$ 0.045 in this case), identifying the local *UOC* or soil loss costs when these surpassed 25% (yellow dots) or 50% (red dots) of a suggested revenue. This revenue was set on US$ 400.00 ha^{-1} (or US$ 0.18m^{-1} for tracks offset in 4.5m).

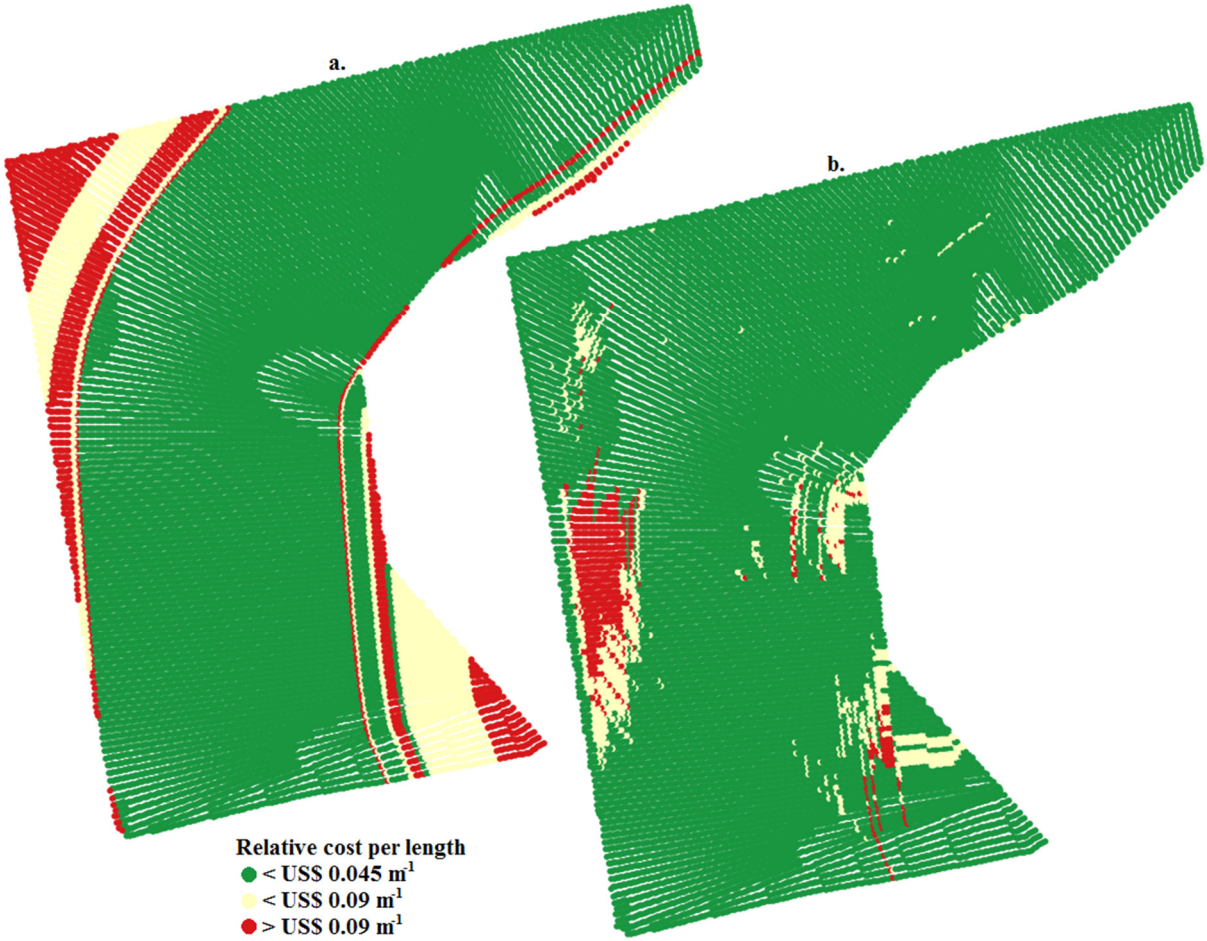

Figure 4.9 - Spatial distribution of the unproductive operational costs in ‘a’ and soil loss cost in ‘b’

The high overlap cost in Table 4.2 can also be seen in the maps of Figure 4.9a, where tracks reaching borders with a large angle θ increases overlap and the relative cost per length. Such costs make the use of sprayer with section control along the boom a suitable acquisition. The standard financial balance of the crop for the path planning costs was thus compared to a similar setting yet dividing the sprayer boom in four equidistant sections. Figure 4.10 shows the spatial distribution of the balance for both scenarios.

The overlap area of the spraying coverage decreased from 9.1 ha (9.9% of the field area) to 2.43 ha (2.65% of the field area) with the section control, proposing an expense savings of US$ 4638.98 (US$ 50.61 ha^{-1}) of product that would be previously applied twofold. Similar results were found in path planning for one case study in Bochtis et al. (2010), where the overlapped area of the sprayer was the key-factor for defining a more financially affordable working orientation on the field.

The area correspondent to a negative turnover in Figure 4.10a is 2.82 ha (3.08 % of field area), and the area with revenue below 50% than expected because of path planning costs was

of 12.5 ha (13.67% of field area). These areas decrease respectively to 1.53 ha and 7.12 ha (1.67% and 7.77% of the field area) with adoption of the section control in the sprayer boom as shown in Figure 4.10b.

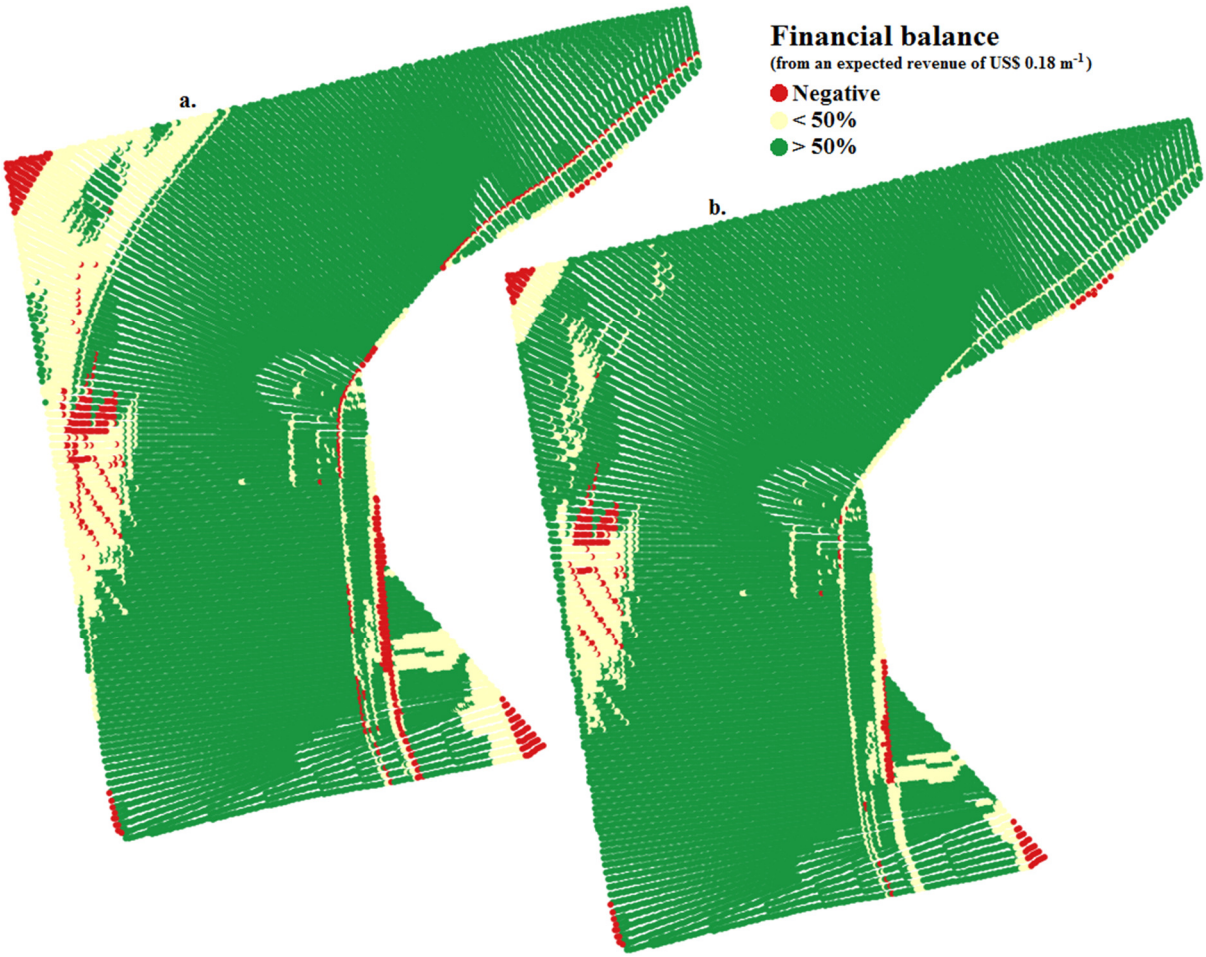

Figure 4.10 - Localized financial balance for the path planning impact for a fixed income expected per meter. In 'a' the balance with a standard operational setting and in 'b' the balance for a modified sprayer

4.4 Discussion

The case studies already searched for optimized track establishment with minimal soil loss. Still, the parallel behaviour of machines is limited by the non-parallel conditions of the slope. This will unavoidably result in off-grade condition of the rows and machine paths in varying intensities. An alternative for more reduction of soil loss through path planning would then require divisions in the pattern of orientation of the tracks within the field to increase perpendicularity to slope; yet such option would likely increase the unproductive operational costs. Other alternatives like establishment of wide base ridges (in which machines can move

across) following the surface contours can reduce runoff within the tracks; also, to adopt minimal soil mobilization would also be an option.

The simplified assumption of assigning a fixed cost-value for a quantity of soil eroded is not fully accurate. Aspects like re-sedimentation has to be taken into account (which is not computed in the RUSLE), and calculation for across-track runoff must be considered. Other aspects of soil erosion cost should be studied further, especially to consider the concentration of water on spots within the field, which may lead to the formation of gullies. Such drastic outcomes have no specific way to calculate its costs, because its consequences can harm from the soil morphology to the very traffic of machines across the field.

Nevertheless, the approximation for assigning costs to soil loss (drawing back from JIN; TANG, 2011) can direct decision makers to search for long-term sustainable soil use.

Land use issues arise for areas in field corners, where operational costs are unprofitable. Such areas must also require attention from the decision makers that may find alternatives, like compliance with legislation for establishment of natural reserves (Brazilian Federal Law 4771/1965), or assigning these for transhipment areas (offload from sugarcane carriers onto trucks in case study I) for logistic purposes.

4.5 Summary and Conclusion

In the current agricultural context, machine unproductivity on fields and their impacts on soil along pathways are unavoidable. The development of path planning algorithms for these machines in fields searched for means to decrease their impacts, however these impacts are not uniform over agricultural areas.

This work makes use of an existing model-algorithm for simulating virtual tracks and retrieving their respective soil erosion impact. In this model, methods were embedded for obtaining machine unproductive operational impacts like manoeuvring, overlap of inputs applied in headlands, and cost of inadequate length of tracks due to underutilization of the machine's reservoir-capacity.

The model-algorithm was subject to assessment by case studies applied for covering a field with an erosion-minimized set of tracks. These tracks had soil loss and unproductive operational costs assigned to each of the track-segments. In a sugarcane case study, the top cost issue was manoeuvring, which identified a range of unprofitable short tracks and showed that 17.65% of the inefficient area comprises for almost a third of the unproductive operational costs. Also the results suggest that, for the last two years of harvest, the low revenue margins

increase significantly the financial prohibitive area. For the cotton case study, overlap of applied inputs were the top cost issue for which the angle between field boundary and machine orientation is the most costly factor. The *UOC* of the high cost areas were 3.4 times higher than the field average; and the adoption of a section controlled sprayer boom decreased the overlap area in 3.74 times and halved the non-profitable and low profitable areas.

In conclusion, in irregular shaped fields the operational costs are not equally distributed; likewise for soil loss costs in irregular surfaces. These issues need to be accounted as an in-field variability because of its potential to compromise the income of certain regions, particularly when studies of robust financial balance are aimed. Also suggests better planning and destination for the areas with limited operability.

References

BENEDINI, M.S; CONDE, A.J. Sistematização da área para a colheita mecanizada de cana-de-açúcar. **Revista Coplana,** Jaboticabal, v. 25, nov. 2008. Disponível em: <http://www.coplana.com/gxpfiles/ws001/design/RevistaCoplana /2008/Novembro/pag23-24-25.pdf>. Acesso em: 03 mar. 2015.

BOCHTIS, D.D.; SØRENSEN, C.G.; BUSATO, P.; HAMEED, I.A.; RODIAS, E.; GREEN, O.; PAPADAKIS, G. Tramline establishment in controlled traffic farming based on operational machinery cost. **Biosystems Engineering,** London, v. 107, n. 3, p. 221-231, 2010.

BONGIOVANNI, R.; LOWENBERG-DEBOER, J. Precision agriculture and sustainability. **Precision Agriculture,** Dordrecht, v. 5, n. 4, p. 359-387, 2004.

BOYER, C.N.; BRORSEN, B.W.; SOLIE, J.B.; RAUN, W.R. Profitability of variable rate nitrogen application in wheat production. **Precision Agriculture,** Dordrecht, v. 12, n. 4, p. 473-487, 2011.

BRASIL. Leis, decretos, etc. **Código florestal brasileiro:** Lei nº 12.651, de 25 de maio de 2012. Brasília, 2012. Disponível em: <http://www.planalto.gov.br/ccivil_03/_ato2011-2014/2012/lei/L12651compilado.htm>. Acesso em: 03 jun. 2015.

BULLOCK, D.S.; LOWENBERG-DEBOER, J.; SWINTON, S.M. Adding value to spatially managed inputs by understanding site-specific yield response. **Agricultural Economics,** Hoboken, v. 27, n. 3, p. 233-245, 2002.

BUSATO, P.; BERRUTO, R.; SAUNDERS, C. Modelling of grain harvesting: interaction between working pattern and field bin locations. **Agricultural Engineering International**, Gainesville, v. 7, n. 1, 2007.

COELHO, M.F. **Planejamento da qualidade no processo de colheita mecanizada da cana-de-açúcar.** 2009. 74 p. Tese (Mestrado em Máquinas Agrícolas) – Escola Superior de Agricultura “Luiz de Queiroz”, Universidade de São Paulo, Piracicaba, 2009.

DE ANDRADE, N.S.; MARTINS FILHO, M.V.; TORRES, J.L.; PEREIRA, G.T.; MARQUES JÚNIOR, J. Impacto técnico e econômico das perdas de solo e nutrientes por erosão no cultivo da cana-de-açúcar. **Engenharia Agrícola,** Jaboticabal, v. 31, n. 3, p. 539-550, 2011.

DERPSCH, R.; FRIEDRICH, T.; KASSAM, A.; LI, H. Current status of adoption of no-till farming in the world and some of its main benefits. **International Journal of Agricultural and Biological Engineering,** Beijing, v. 3, n. 1, p. 1-25, 2010.

FNP CONSULTORIA E COMÉRCIO. AGRIANUAL 2012: anuário da agricultura brasileira. São Paulo, 2012. 482 p.

FOSTER, G.R.; WISCHMEIER, W.H. Evaluating irregular slopes for soil loss prediction. **Transactions of the ASAE,** St Joseph, v. 17, n. 1, p. 305–309, 1974.

HOFSTEE, J.W.; SPÄTJENS, L.E.E.M.; IJKEN, H. Optimal path planning for field operations. In: EUROPEAN CONFERENCE ON PRECISION AGRICULTURE, 7., 2009, Wageningen. **Proceedings…** Wageningen: Wageningen Academic, 2009. p. 511-519.

HOLLAND, J.K.; ERICKSON, B.; WIDMAR, D.A. **Precision agricultural services dealership survey results.** West Lafayette: Purdue University, Dept. of Agricultural Economics, 2013. 68 p.

JIN, J.; TANG, L. Optimal path planning for arable farming. In: ASABE ANNUAL INTERNATIONAL MEETING, 2006, Portland. **Proceedings…** St. Joseph: American Society of Agricultural Engineers, 2006. p. 304-312.

_____. Optimal coverage path planning for arable farming on 2D surfaces. **Transactions of the ASABE,** St. Joseph, v. 53, n. 1, p. 283, 2010.

_____. Coverage path planning on three-dimensional terrain for arable farming. **Journal of Field Robotics,** Hoboken, v. 28, n. 3, p. 424-440, 2011.

LOADSMAN, R.; LOTZ, G.; YULE, D.; STEVENS, S.; ROHDE, K.; CARROLL, C.; CHAPMAN, W. **Adoption of controlled traffic farming across central Queensland:** final project report. Canberra: Natural Heritage Trust, 2002. 45 p.

LOMBARDI-NETO, F.; BERTONI, J. **Tolerância de perdas de terra para solos do Estado de São Paulo.** Capinas: Instituto Agronômico de Campinas, 1975. 12 p. (Boletim Técnico, 28).

LOMBARDI-NETO, F.; MOLDENHAUER, W.C. Erosividade da chuva: sua distribuição e relação com perdas de solo em Campinas, SP. **Bragantia,** Campinas, v. 51, n. 2, p. 189-196, 1992.

MACHADO, E.C.; PEREIRA, A.R.; FAHL, J.I.; ARRUDA, H.V.; CIONE, J. Índices biométricos de duas variedades de cana-de-açúcar. **Pesquisa Agropecuária Brasileira,** Brasília, v. 17, n. 9, p. 1323-1329, 1982.

MINASNY, B.; MCBRATNEY, A.B.; WHELAN, B.M. **Vesper:** version 1.6. Sidney: The University of Sidney; Australian Centre for Precision Agriculture, 2002. Disponível em: <http://sydney.edu.au/agriculture/pal/software/download_vesper.shtml>. Acesso em: 03 jun. 2015.

MURPHREE, C.E.; MUTCHLER, C.K. Cover and management factors for cotton. **Transactions of the ASAE,** St Joseph, v. 23, n. 3, p. 585-595, 1980.

OKSANEN, T.; VISALA, A. **Path planning algorithms for agricultural machines.** 2007. 112 p. Thesis (PhD) - Automation Technology Laboratory, Helsinki University of Technology, Helsinki, 2007. (Series A: Research Reports, 31).

PALMER, R.J.; WILD, D.; RUNTZ, K. Improving the efficiency of field operations. **Biosystems Engineering,** London, v. 84, n. 3, p. 283-288, 2003.

RENARD, K.G.; FOSTER, G.R.; WEESIES, D.K.; TODER, D.C. (Coord.). **Predicting soil erosion by water**: a guide to conservation planning with the revised universal soil loss equation (RUSLE). Washington: USDA, 1997. 407 p. (Agriculture Handbook, 703).

SILVA, C.B.; DE MORAES, M.A.F.D.; MOLIN, J.P. Adoption and use of precision agriculture technologies in the sugarcane industry of São Paulo state, Brazil. **Precision Agriculture,** Dordrecht, v. 12, n. 1, p. 67-81, 2011.

SPEKKEN, M.; DE BRUIN, S. Optimized routing on agricultural fields by minimizing manoeuvring and servicing time. **Precision Agriculture,** Dordrecht, v. 14, n. 2, p. 224-244, 2013.

SPEKKEN, M.; MOLIN, J.P. Optimizing path planning by avoiding short corner tracks. **In: Proceedings of the International conference on precision agriculture. International Society in Precision Agriculture**, 11, p. 314-328 2012, Monticello.

SPEKKEN, M.; DE BRUIN, S.; MOLIN J.P. Ferramentas para sistematização de percursos de máquinas agrícolas sobre relevo declivoso. **Anais do congresso brasileiro de agricultura de precisão, Jaboticabal: Sociedade Brasileira de Engenharia Agrícola**, 2014. Disponível em: <http://www.sbea.org.br/conbap/2014/trabalhos/R0077-1.PDF>. Acesso em: 03 jun. 2015.

SPEKKEN, M.; MOLIN, J.P.; ROMANELLI, T.L. Cost of boundary manoeuvres in sugarcane production. **Biosystems Engineering,** London, v. 129, p. 112-126, 2015.

STOLL, A.; STAFFORD, J.; WERNER. A. Automatic operation planning for GPS-guided machinery. **Proceedings of the european conference on precision agriculture, 4, 2003, Berlin: Wageningen Academic Publishers**. Wageningen, p. 657-664, 2003.

TAÏX, M.; SOUÈRES, P.; FRAYSSINET, H.; CORDESSES. Path planning for complete coverage with agricultural machines. In: ZELINSKY, A. **Field and service robotics.** Berlin; Heidelberg: Springer, 2006. p. 549-558.

TELLES, T.S.; GUIMARÃES, M.F.; DECHEN, S.C.F. The costs of soil erosion. **Revista Brasileira de Ciência do Solo,** Viçosa, v. 35, n. 2, p. 287-298, 2011.

TULLBERG, J.N.; YULE, D.F.; MCGARRY, D. Controlled traffic farming: from research to adoption in Australia. **Soil and Tillage Research,** Amsterdam, v. 97, n. 2, p. 272-281, 2007.

5 SUMMARY AND FINAL REMARKS

The focus of this thesis was to propose (and adapt) methods to develop the agricultural path planning science. This methods are described along three main chapter-manuscripts along with some case-studies applied for method-assessment.

In the first chapter, geometric equations are presented to calculate space, time and length of machines manoeuvring near boundaries of field. Four geometry-types were considered: Ω-manoeuvre, U-manoeuvre, T-manoeuvre and P-manoeuvre. The latter manoeuvre is newly introduced in this field of science, and it models a common procedure of manoeuvring done by trailed units in sugarcane operations. The chapter also introduces a different approach for observing the impact of machine paths, by translating them into an equivalent cost of crop-length. This approach already suggests how operational costs can compromise the financial turnover by field geometry aspects (short paths/rows in field corners). Further quantitative findings belong to sugarcane production scope and can provide inputs for decision makers involved.

The second chapter initially addresses methods for creating curved tracks and references capable to be properly steered by machines. This is followed by a newly proposed method to obtain an adequate single reference for track patterns on irregular surfaces, named curve hybridization. In order to make an appropriate evaluation of the water-erosion resilience of a certain pattern, the Universal Soil Loss Equation was used, in a new approach, to quantify the soil capable to be displaced along the fluctuation of altimetry of a track. A qualitative procedure was also added to help identify spatially the locations for water concentration along tracks and over the field. These methods were implemented in computer algorithms capable to propose and simulate machine tracks on fields and spatially quantify the erosion intensity by the choice of a path pattern. Real field data was applied into the algorithm drawing discussions on distinct path planning aspects, and showing results not obvious for an observer (or decision maker). Further works for path planning in steep surfaces should be addressed regarding the water flow and concentration, suggesting the development of computational procedures that shape the tracks to gently deviate the water from the field into non-risk zones (grassed waterways), instead of relying exclusively on infiltration.

Methods of the first and second chapters are merged in a third chapter, which proposes a comprehensive gathering of impacts due to establishment of path patterns. A total of four undesirable impacts are calculated: soil loss, manoeuvring time, headland coverage overlap and inadequate length of tracks for use of the machine's reservoir. In a distinct approach, the

financial cost of these impacts were calculated per track created, and a relative cost (cost per length/distance followed) was assigned to each segments composing this track. Such approach permits the path pattern impacts to be accordingly distributed over field, which was observed in two case studies submitted to the model created by the combined methods.

A few remarks can be derived from the case studies processed by the models:

- Sugarcane rows of short length have compromised revenue, studies herein point the financial break-even threshold to be in 50 m.
- Decreased manoeuvring time has linear relation to manoeuvring costs, while continuous increase in track length shows decreasing benefits in cost savings. Minimizing manoeuvring time by increasing track length is applicable until a certain limit, afterwards, more investments could be oriented to speed the manoeuvre.
- Choice of appropriate agricultural equipment can achieve operational savings of some impact, like wagon-carrier with smaller turning radius or control section in the boom of sprayers.
- The use of human intuition to define machine and crop-row patterns on steep irregular surfaces is limited and might lead to poor choices.
- The operational cost is not constant over the field, and its variance may identify regions in field that might be dedicated to other uses.

Steps for further development of methods are appointed in the chapters, and the actual development of the algorithm finds itself in the form of a prototype application prepared to be tested, improved and run assessment for new cases.

APPENDIX

APPENDIX A. PSEUDO-CODES

The two code boxes that follows summarize the tool for creating tracks and calculating the soil loss along these (text preceded by "*" is works as a documentation guide of the code).

1. Pseudo-code algorithm for creating parallel tracks and extracting altimetry along these.

```
*     This following procedure creates parallel tracks along a field, assigns
      altimetry to the vertices and prepares the list of vertices with same
      facet for which erosion is going to be calculated.
*     It requires the variables: DEM (matrix of elevation values), NSegPLine
      (Number of vertices in the reference to be replicated), ODist (Offset
      Distance),

Procedure Replicate_PLines_Extract_Soil_Loss(NSegPLine,ODist)

      * Creating a new offset line

      Create_Matrix_List(OLine)
      For i=1 to NSegPLine
            Ang=Extract_Vertex_Bisector(PLine[i])
            IfConvex=IfAngConvex(PLine[i],Ang)
            If IfConvex Then
                  Compose_Arc_Around_Vertex(PLine[i],OLine,ODist)
            Else
                  Insert_Offset_Vertex(Ang,OLine,ODist)
            End If
      Next

      * Extracting altimetry to new sequence of vertices

      For i=1 to Count(OLine)
            Extract_Point_Altitude(DEM,OLine[i].Z)
      Next

      * Get seq. of vertices of same facet and call soil loss procedure

      IniDif=OLine[1].Z-OLine[2].Z
      NP=0
      Initiate(List_LS)
      For i=2 to Count(OLine)
            Dif=OLine[i].Z-OLine[i+1].Z
            NP=NP+1
            List_LS[1]=Dist_Points(OLine[i]-OLine[i+1])
            List_LS[2]=Slope(OLine[i]-OLine[i+1])
            If (IniDif<0 And Dif>0) Or (IniDif>0 And Dif<0) Then
                  RUSLE_Foster_Wischmeyer(NSeg,AvSlope,RKCP)
                  IniDif=Dif
                  NP=0
            End If
      Next
End Procedure
```

2. Pseudo-code algorithm for calculating the distinct soil losses within a list of segments following a same slope facet.

```
*     This following procedure makes the calculation of soil loss from a list
      of vertices.
*     It requires a list-matrix containing 3 columns, being 2 input columns
      (Length of the segment, Slope-steepness of the segment) and a third
      column to save the RUSLE estimated soil loss.
*     AvSlope is the average slope within the full facet.
*     NSeg is the number of segments within the list.
*     RKCP is the Rainfall, Soil, Coverage and conservation Practice
      given/calculated for the whole field.

Procedure RUSLE_Foster_Wischmeyer(NSeg,AvSlope,RKCP)

      m=10*AvSlope
      If AvSlope<0.03 then m=0.3
      If AvSlope>=0.05 then m=0.5
      For i=1 to NSeg
         Li=(List_LS[i,1]/22.13)^m
         W=i^(m+1)+(i-1)^(m-1)
         S=List_LS[i,2]
         Si:=65.41*S^2/(1+S^2)+4.56*S/SQRT(1+S^2)+0.065
         LS:=Si*W*Li;
         List_LS[i,3]:=LS*RKCP;
     Next

End Procedure
```

APPENDIX B. APPLICATION VIEWS

A sequence of images display examples of case studies being worked by the proposed methods as they are retrieved from the applications.

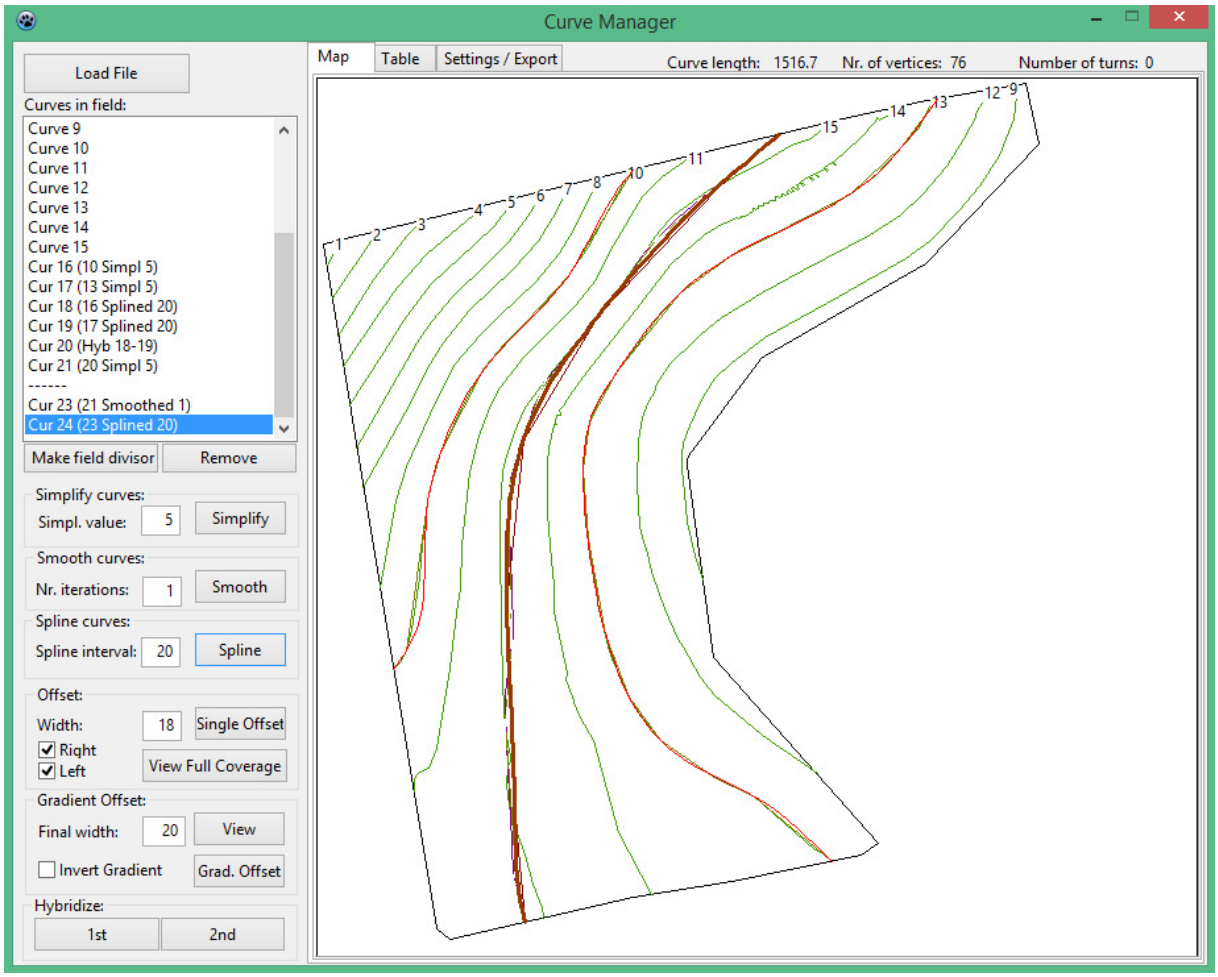

Figure 1. View of the “Curve Manager” application in which two reference lines where hybridized into a single curve. The origin lines where submitted to simplification (to remove ondulation) and spline (to increase smoothnes). The hybridized line was additionally submitted to a reduction on concavity by one iteration of coordinate averaging before being splined.

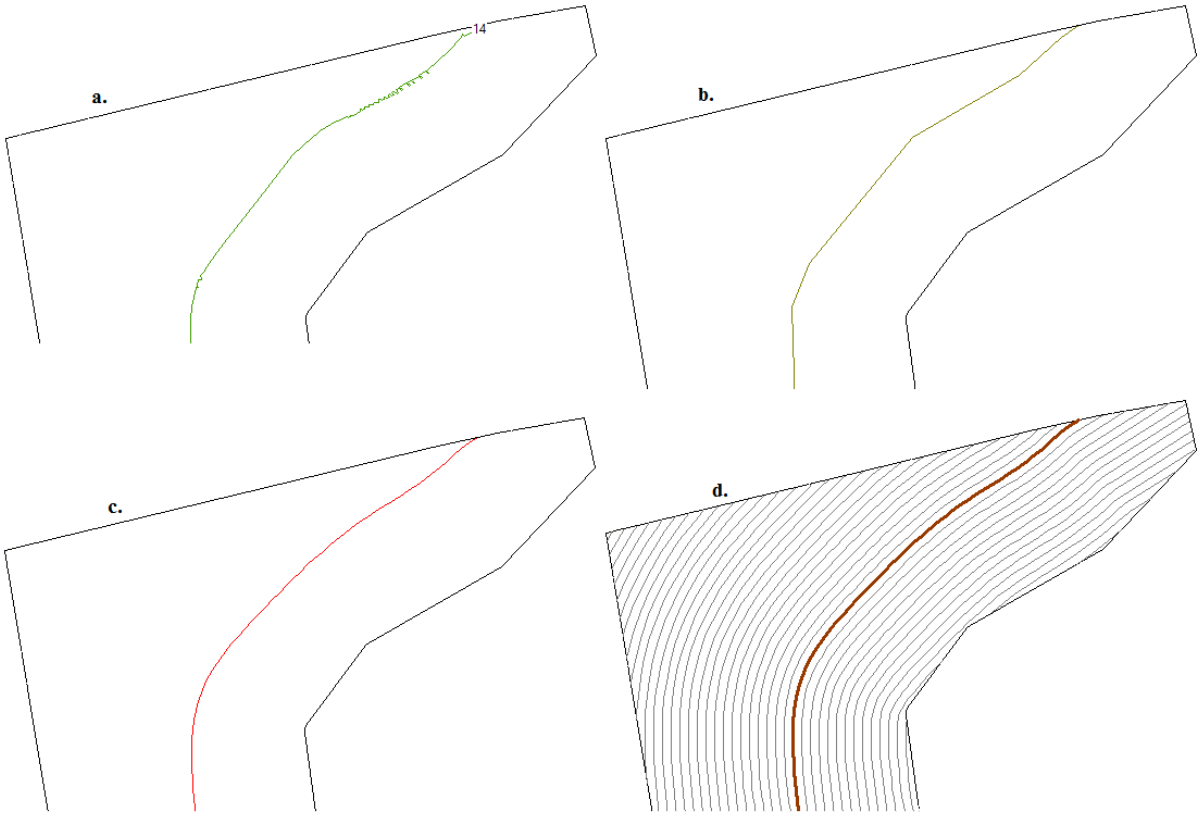

Figure 2. Sequence of curve re-shaping procedures available in the “Curve Manager” application, where one original reference extracted among the contours (in “a”) presents small undulations along its shape. The undulations are removed by simplification (in “b”), and a spline interpolation (in “c”) gives smoothness. In “d” the final smooth curve is replicated in parallel passes for full field coverage showing no steering issues for a machine to follow it.

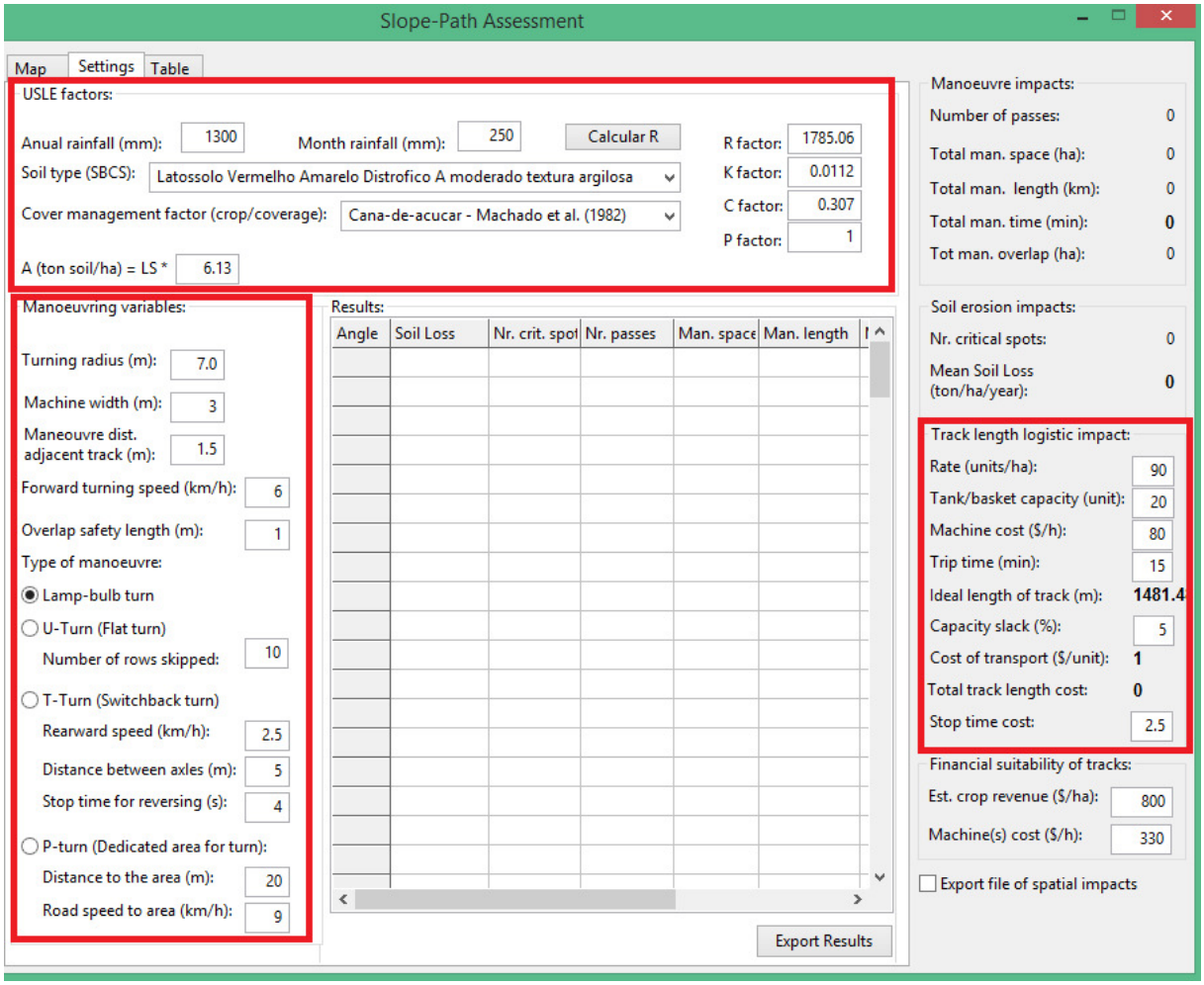

Figure 3. View of the input parameters within the "Slope-Path Assessment" used for the calculation of soil loss (in "USLE factors"), manoeuvres (in "Manoeuvring variables") and inadequate length of track (in "Track length logistic impact").

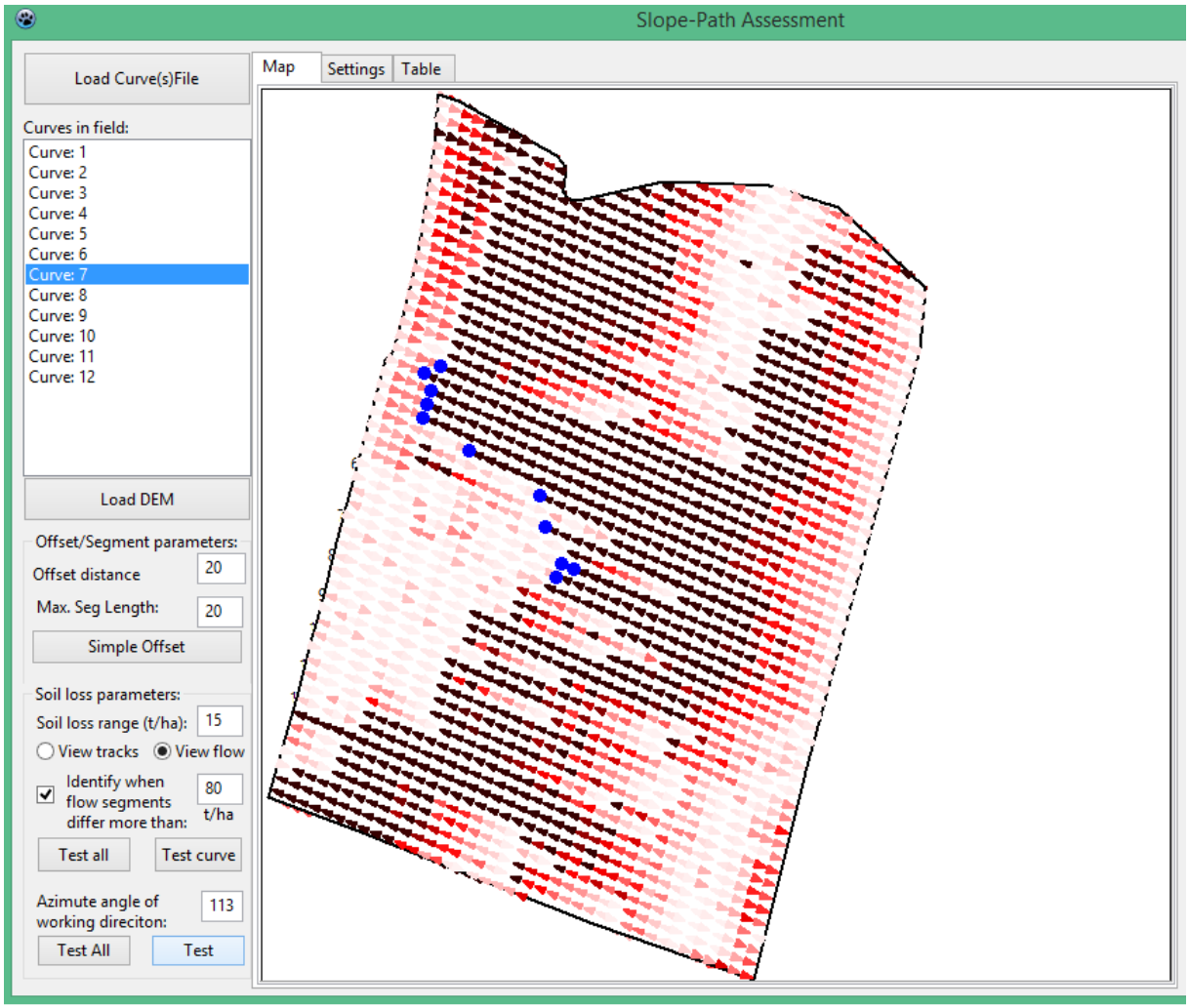

Figure 4. View of the algorithm showing the soil loss intensity and water flow direction for a straight pattern simulated on the field. The image shows the critical points (blue dots) in which the soil loss becomes critical, these spots are always located in the end of an intense water flow sequence.

Manoeuvre impacts:	
Number of passes:	800
Total man. space (ha):	6.96
Total man. length (km):	97.24
Total man. time (min):	**972.4**
Tot man. overlap (ha):	0.5

a

Manoeuvre impacts:	
Number of passes:	800
Total man. space (ha):	3.57
Total man. length (km):	178.27
Total man. time (min):	**1517.54**
Tot man. overlap (ha):	0.5

b

Manoeuvre impacts:	
Number of passes:	800
Total man. space (ha):	4.57
Total man. length (km):	74.16
Total man. time (min):	**1299.09**
Tot man. overlap (ha):	0.5

c

Figure 5. Real-time manoeuvre calculated impacts retrieved for three distinct turning types: Ω-Turn (in “a”), P-Turn (in “b”) and T-Turn (in “c”) for the case study in Figure 4 and using the settings displayed in Figure 3 (for sugarcane harvest).